Atrophy of basal forebrain and abnormal Functional Connectivity of the basal forebrain in Subjective Cognitive Decline

Dissertation

zur Erlangung des Doktorgrades (PhD)

der Medizinischen Fakultät

der Rheinischen Friedrich-Wilhelms-Universität

Bonn

Shumei Li
aus Henan, China
2021

Angefertigt mit der Genehmigung
der Medizinischen Fakultät der Universität Bonn

1. Gutachter: Prof. Dr. Lukas Scheef

2. Gutachter: Prof. Dr. Michael T. Heneka

Tag der Mündlichen Prüfung: 18.02.2021

Aus der Klinik und Poliklinik für Neurologie
Direktor: Prof. Dr. Thomas Klockgether

Table of Contents

List of abbreviations:

AAL	Automated Anatomical Labelling
AChE	Acetylcholinesterase
AD	Alzheimer's disease
ADAS-Cog	Alzheimer's Disease Assessment Scale-Cognitive
ADRDA	Alzheimer's Disease and Related Disorders Association
ANCOVA	Univariate analyses of covariance
APOE	Apolipoprotein E
APP	Amyloid precursor protein
Aβ	Amyloid beta
Aβ+/Aβ-	Beta-amyloid positive/ negative
BF	Basal Forebrain
BOLD	Blood oxygen level–dependent
CDR	Clinical Dementia Rating
CDR-SOB	Clinical Dementia Rating-Sum of Box
CERAD	Consortium to Establish a Registry for Alzheimer's Disease
Ch1	Medial septal nucleus
Ch2	Vertical nucleus of the diagonal band of Broca
Ch3	Horizontal limb of Broca
Ch4	Nucleus basalis Meynert
Ch4ai	Intermediate and medial of Nucleus basalis Meynert
Ch4al	Anterior lateral of Nucleus basalis Meynert
Ch4p	Posterior of Nucleus basalis Meynert
ChAT	Choline acetyltransferase
CSF	Cerebrospinal fluid
DAD	Dementia due to Alzheimer's Type
DARTEL	Diffeomorphic Anatomical Registration Through Exponentiated Lie Algebra
DELCODE	German Center for Neurodegenerative Diseases Longitudinal Cognitive Impairment and Dementia Study
DMN	Default mode network
DPABI	Data Processing & Analysis for Brain Imaging
EPI	Echo-planar Imaging

EXEC	Executive functions and mental processing speed
FBB	[18F]-Florbetaben
FC	Functional Connectivity
FDG	Fluoro-deoxy-D-glucose
fMRI	Functional Magnetic Resonance Imaging
FOV	Field of View
FWE	Family-wise Error
FWHM	Full width at half maximum
GM	Grey Matter
GRAPPA	Generalized Autocalibrating Partial Parallel Acquisition
HC	Healthy Control
LANG	Language abilities
MCI	Mild Cognitive Impairment
MEM	Memory
MMSE	Mini Mental State Examination
MNI	Montreal Neurological Institute
MPRAGE	Magnetization-Prepared Rapid Acquisition with Gradient Echo
MRI	Magnetic Resonance Imaging
MTL	Medial temporal lobe
N	Neurodegeneration
NBM	Nucleus basalis Meynert
NFT	Neurofibrillary tangles
NIA-AA	National Institute of Aging-Alzheimer's Association
NINCDS	National Institute of Neurological and Communicative Disorders and Stroke
NPT	Neuropsychological test
PCC	Posterior Cingulate Cortex
PET	Positron emission tomography
PiB	Pittsburgh Compound B
PSEN1	Presenilin-1
PSEN2	Presenilin-2
Ptau	Phosphorylated tau

ReHo	Regional Homogeneity
ROI	Regional of Interest
rs-fMRI	Resting state functional MRI
SCD	Subjective Cognitive Decline
$SCD_{A\beta+}$	Amyloid-positive Subjective Cognitive Decline
$SCD_{A\beta-}$	Amyloid-negative Subjective Cognitive Decline
SUVR	Standard uptake values ratio
TE	Echo time
TI	Inversion Time
TIV	Total Intracranial Volume
TR	Repetition time
ttau	Total tau
VBM	Voxel based Morphometry
VIS	Visual spatial ability
WM	White Matter
WME	Working Memory

1 Introduction

Alzheimer's Disease (AD), which is a progressive neurodegenerative disorder that affects millions of people worldwide, is currently incurable. With the advent of in vivo neuroimaging- and cerebrospinal fluid (CSF) biomarkers for its neuropathological hallmarks, beta-amyloid and tau depositions, and neurodegenerative consequences, considerable evidence has accumulated which indicates that disease progression begins many years before clinically relevant cognitive impairments show up. Thus, one possible reason for the recent failures of high-profile clinical studies is that the selected dementia patients are too advanced in AD progression, and the pathology and neurodegeneration for these patients are already irreversible. Therefore, the research focus of disease-modifying treatment for AD has shifted from dementia to populations at earlier stages of AD pathogenesis. Mild cognitive impairment (MCI), where performance of individual on objective neuropsychological tests is below average age-, gender- and education-adjusted performance, has been considered as the first clinical manifestation before converting to AD dementia. However, subjective loss of cognitive function may occur before lower performance on objective cognitive assessments becomes detectable, and is currently discussed as the earliest clinical symptoms of AD (Jessen *et al.*, 2014a). Several nomenclatures were used to describe these subjective complaints, such as 'subjective memory impairment' (SMI) (Jessen *et al.*, 2010), 'subjective memory complaints' (SMC) (Schmand *et al.*, 1997)', 'subjective cognitive impairment (SCI) (Stewart, 2012)', or 'subjective cognitive complaints/concerns' (SCC) (Dufouil *et al.*, 2005; Donovan *et al.*, 2014)'. The lack of a consistent concept makes it difficult to compare findings across studies. To address this need, the term Subjective Cognitive Decline (SCD) and operational criteria for a research framework were conceived and standardized in 2014 by an international working group of researchers and clinicians to describe this condition (Jessen *et al.*, 2014a). The proposed criteria of SCD include 'self-report persistent decline in cognitive abilities compared to his/her earlier performance level, despite the objective cognitive performance level still being within normal range'. Moreover, the subjective cognitive decline is not associated with physical or psychiatric conditions. Previous studies have shown that individuals with SCD are at higher risk of developing MCI and AD compared to cognitive normal healthy older individuals (Reisberg *et al.*, 2010; Jessen *et al.*, 2014a). Especially, SCD in combination with proven AD pathology may

reflect the progression from stage 1 (asymptomatic) to stage 2 (transitional cognitive impairment) of the Alzheimer's continuum, as defined in the 2018 National Institute on Aging and the Alzheimer's Association (NIA-AA) research criteria for AD (Jack *et al.*, 2018). Therefore, to identify the earliest intervention stage in clinical trials and accelerate the development of new therapies, studies focusing on the characterization of early brain structural and functional profiles in SCD with AD amyloid pathology are highly needed.

There are two interesting brain structures to investigate in the SCD stage. The first one is the basal forebrain (BF) since it is the main source of acetylcholine production, and its neurodegeneration is a consistent feature of clinical AD (Grothe *et al.*, 2010; Kilimann *et al.*, 2014). Three out of 4 currently approved medication (Donepezil, Rivastigmine, Galantamine) to slow down the cognitive deterioration in AD are acetylcholine esterase inhibitors (Ellis, 2005). Recent evidence suggests that atrophy of of the posterior Nucleus Basalis of Meynert, a subnucleus of the BF, is already detectable and even precedes the volume loss of the entorhinal cortex in individuals with preclinical Alzheimer's pathology (Schmitz *et al.*, 2016a). Thus, the cholinergic BF might be one of the earliest brain structures affected in AD. The second brain structure we will be interested in is the precuneus. Dysfunctions of the so-called default mode network (DMN), especially in its posterior core regions precuneus and posterior cingulate cortex (PCC), were consistently found in both AD and MCI patients and considered to be a key feature in AD (Greicius *et al.*, 2004; Zhang *et al.*, 2012; Long *et al.*, 2016; Marchitelli *et al.*, 2018). Interestingly, the precuneus, as an important hub region of the DMN, is one of the brain regions showing vulnerability for early amyloid deposition (Palmqvist *et al.*, 2017; Mattsson *et al.*, 2019). Therefore, previous studies suggest that there are causal relationships between the dysfunctions of DMN and earliest amyloid deposition in these brain regions, although the direction is not clear (Sheline *et al.*, 2010b; Mormino *et al.*, 2011; Palmqvist *et al.*, 2017). Therefore, the aims of the three studies presented in this thesis were to investigate the structural and functional changes of these brain structures in SCD patients as an at-risk population for dementia of the Alzheimer's type (DAD), especially in those with proven preclinical amyloid pathology. Study 1 include structural analyses of BF cholinergic system across the whole AD spectrum, including SCD and Healthy controls (HC). Moreover,

functional connectivity (FC) measures of the cholinergic BF and precuneus were also investigated in SCD (study 2 and study 3).

The thesis is structured as follows: After a brief introduction on the clinical background and key concepts within the AD continuum, the general material and methods used for all experiments will be given in Chapter 2. The different studies are described in Chapter 3. Each subsection belonging to one study will contain a study-specific 'Material and Method' section as well as its own 'Discussion' section. An overall 'Discussion' is presented in Chapter 4.

1.1 Alzheimer's disease (AD): Definition and overview

1.1.1 History and definition of AD

AD was first reported as "A peculiar severe disease process of the cerebral cortex" by Dr. Alois Alzheimer, a German psychiatrist and neuropathologist, in 1906 (Hippius and Neundorfer, 2003). The patient was a 51-year-old woman, who already began to show memory impairment, poor language skills and behavioral deficits. Dr. Alzheimer performed an autopsy on the patient's brain after she died, and observed extensive cortex atrophy (Alzheimer *et al.*, 1995), along with distinctive plaques and neurofibrillary tangles in brain histology. The first academic paper about AD was published in 1907, and Kraepelin named this disease AD some years later (Moller and Graeber, 1998). The most common early symptoms of AD are memory problems of which short term memory impairments are most pronounced (Burns and Iliffe, 2009). As the disease develops, more and more cognitive domains become affected, including problems with language, spatial navigation. Step by step the personality changes, and patients lose ability to manage their daily life. Gradually, loss of motor ability appears such as difficulty in speaking, swallowing and walking, ultimately leading to death. Even though the speed of disease progression can vary, the typical life expectancy after dementia diagnosis is three to nine years (Querfurth and LaFerla, 2010; Todd *et al.*, 2013).

In 1984, the National Institute of Neurological and Communicative Disorders and Stroke (NINCDS) and the Alzheimer's Disease and Related Disorders Association (ADRDA) established the criteria of the clinical diagnosis of AD (McKhann *et al.*, 1984). These criteria, commonly referred to as NINCDS-ADRDA criteria, suggest that AD is a clinical-pathological construct, and it is assumed that individuals with typical

amnestic symptoms would show AD neuropathological changes at autopsy. Specifically, AD dementia patients diagnosis criteria are quoted as follows (McKhann *et al.*, 2011): “ AD dementia patients are diagnosed when there are cognitive or behavioral (neuropsychiatric) symptoms that: (1) Interfere with the ability to function at work or at usual activities; and (2) Represent a decline from previous levels of functioning and performing; and (3) Are not explained by delirium or major psychiatric disorder; (4) Cognitive impairment is detected and diagnosed through a combination of (1) history-taking from the patient and a knowledgeable informant and (2) an objective cognitive assessment, either a mental status examination or neuropsychological testing. Neuropsychological testing should be performed when the routine history and mental status examination cannot provide a confident diagnosis. (5) The cognitive or behavioral impairment involves a minimum of two of the following domains:

a. Impaired ability to acquire and remember new information-symptoms include […].

b. Impaired reasoning and handling of complex tasks, poor judgment symptom, inability to manage finances, poor decision-making ability–symptoms include […].

c. Impaired visuospatial abilities–symptoms include […].

d. Impaired language functions (speaking, reading, writing)–symptoms include […].

e. Changes in personality, behavior, or comportment–symptoms include […].

After meeting criteria for cognitive or behavioral symptoms described above, it has the following characteristics:

(1) Insidious onset: Symptoms have a gradual onset over months to years, not sudden over hours or days; (2) Clear-cut history of worsening of cognition by report or observation; and (3) The initial and most prominent cognitive deficits are evident on history and examination in one of the following categories:

a. Amnestic presentation: It is the most common syndromic presentation of AD dementia. The deficits should include impairment in learning and recall of recently learned information. There should also be evidence of cognitive dysfunction in at least one other cognitive domain, as defined earlier in the text.

b. Non-amnestic presentations:

Language presentation: The most prominent deficits are in word-finding, but deficits in other cognitive domains should be present as well.

Visuospatial presentation: The most prominent deficits are in spatial cognition, including object agnosia, impaired face recognition, simultanagnosia (inability to perceive more than one object at a time), and alexia. Deficits in other cognitive domains should be present.

Executive dysfunction: The most prominent deficits are impaired reasoning, judgment, and problem solving. Deficits in other cognitive domains should be present.

(4) The diagnosis of probable AD dementia should not be applied when there is evidence of one of the following aspects: (a) substantial concomitant cerebrovascular disease; (b) core features of Dementia with Lewy bodies other than dementia itself; (c) prominent features of behavioral variant frontotemporal dementia; (d) prominent features of semantic variant primary progressive aphasia or nonfluent/agrammatic variant primary progressive aphasia; or (e) evidence for another concurrent, active neurological disease, or a non-neurological medical comorbidity or use of medication that could have a substantial effect on cognition''.

However, these criteria were revised by the NIA-AA in 2009 and published in 2011 (McKhann *et al.*, 2011). There was cumulative evidence that the cognitive decline in AD occurs continuously over a long period (Resnick *et al.*, 2010; Wilson *et al.*, 2010; Monsell *et al.*, 2014), and that the pathological changes start many years before the first clinical symptoms occur (Villemagne *et al.*, 2011; Bateman *et al.*, 2012; Benzinger *et al.*, 2013; Villemagne *et al.*, 2013; Fleisher *et al.*, 2015). Accordingly, the updated NIA-AA criteria proposed that AD is a clinical-biomarker construct, where biomarkers are used to support a diagnosis of AD in symptomatic individuals, and that AD should be conceptualized as a progressive disease with three different stages (Jack *et al.*, 2011): This included a preclinical stage of AD (Sperling *et al.*, 2011), MCI due to AD (Albert *et al.*, 2011) and dementia due to AD (McKhann *et al.*, 2011). In 2018, a NIA-AA work group unified and updated the 2011 criteria for the different clinical stages, to consider AD as continuum in both biomarker and symptom aspects rather than defining three separate stages (Jack *et al.*, 2018). Specifically, they developed a 'numeric clinical staging scheme' that is applicable for individuals in the AD continuum, as defined by proven biomarker evidence for AD neuropathology (see chapter 1.1.3).

According to this scheme, the symptomatology of AD is classified into six stages that reflect the increasing severity of the disease, starting from asymptomatic individuals to MCI, mild dementia, moderate dementia, and finally to severe dementia **(Table 1.1)**.

Table 1.1: Six numeric clinical staging of AD continuum according the NIA-AA research framework.

Stage 1	Performance within normal range on objective tests; No evidence of recent cognitive decline or neurobehavior symptoms by report of an observer; Dose not report recent decline in cognition or neurobehavioral symptoms of concern.
Stage 2	Performance within normal range on objective tests; Subjective report of cognitive decline that is concern to the individual or Subtle objective cognitive decline (or both), but not meeting criteria for cognitive impairment. Recent onset of mild neurobehavioral changes-for example, changes in mood, anxiety, or motivation- may coexist or could be the primary symptom.
Stage 3	Objective cognitive decline to the level of impairment; Performs daily life activities independently, but cognitive difficulty may result in detectable but mild functional impact on the more complex activities of daily life.
Stage 4	Mild Dementia; Clearly evident functional impact on daily life; No longer fully independent/requires occasional assistance with daily life activities.
Stage 5	Moderate Dementia; Extensive functional impact on daily life; No longer independent and requires frequent assistance with daily life activities
Stage 6	Severe Dementia; Clinical interview not be possible; Complete dependency due to severe functional impact on daily life, including basic self-care

This table is modified from Jack et al., (2018)

1.1.2 Etiology and epidemiology of AD

It is still not completely clear what causes AD, although various factors, including genetics, age along with environmental and lifestyle factors, may affect the prevalence of AD. There are two forms of AD: familial and sporadic AD (Piaceri *et al.*, 2013). Familial AD is inherited, and it accounts for less than 5 % of all cases of AD. Three familial AD related genes have been discovered: the presenilin-1 (PSEN1), presenilin-2 (PSEN2), and amyloid precursor protein (APP) genes (Papassotiropoulos *et al.*, 2006). The mutation in any one of these three genes will almost certainly cause familial AD. As compared to the sporadic form, its age of onset is lower roughly from 30 years to 65 years) (Bird, 1993), and will become manifest well below an age of 65 (Goldman *et al.*, 2011). However, the most common form of AD is so-called sporadic AD. However, the most important risk factor is increasing age. The general age of onset of sporadic AD is above 65. The percentage of AD dramatically increase with age: 3 % of people age 65-74,17 % of people age 75-84 (Hebert *et al.*, 2013). Above an age of

85 years, the percentage reaches nearly one-third (Alzheimer's Association, 2020). It is worthy to note that AD is not a part of normal aging (Nelson *et al.*, 2011), and old age alone is not a direct cause of AD. The known genetic risk factors do not increase the risk as much as age does. So far, no single genetic cause for sporadic AD is known, even though the number of discovered genetic risk factors is steadily increasing. The largest genetic risk for AD is associated with alleles of the apolipoprotein E (APOE) gene. The APOE gene exists in three isoforms, APOE2, APOE3, and APOE4. The coded proteins differ only in two of 299 amino acids of the APOE, at positions 112 and 158 (Mahley and Rall, 2000). APOE plays a role in the transportation of cholesterol in the bloodstream (Huang and Mahley, 2014) and synapse formation (Mauch *et al.*, 2001). It was first reported by Strittmatter and Roses, who showed that the frequency of APOE4 carriers is 0.16 in healthy control people, while it is 0.4 in AD patients (Strittmatter and Roses, 1996). While the frequency of APOE4 carriers estimates vary across studies and ethnic backgrounds, APOE4 is typically present in more than 50 % of AD patients, but is found only in about 15 % of healthy older controls (Ward *et al.*, 2012). Interestingly, APOE2 is protective: Only about 10 % of the patients with AD are APOE2 carriers vs. a twofold higher occurrence in the normal population (Rebeck *et al.*, 2002). Several previous studies have further proven that the risk for AD is 2-3-fold higher in people with one APOE4 allele and about 12-fold higher in those with two APOE4 alleles (Corder *et al.*, 1993; Roses, 1996). Moreover, APOE4 carriers have an earlier average age of AD onset by 10–15 years compared to non-carriers (Jansen *et al.*, 2015). However, several studies in Europe suggest that the effect of the APOE4 on dementia and mortality disappears in very old age (Sulkava *et al.*, 1996; Juva *et al.*, 2000). Even though the mechanisms underlying APOE4's influence on AD risk are not fully understood, the roles of APOE4 in exacerbating brain changes related to AD, increasing greater deposition of amyloid-β, and resulting in increased aggregation of this pathological hallmark of AD, have been proposed (Huang *et al.*, 2004; Caselli *et al.*, 2009; Tai *et al.*, 2013; Villemagne *et al.*, 2013). As APOE may function as an Aβ binding protein, it has been hypothesized that the interaction between APOE and Aβ contributes to AD pathogenesis (Kim *et al.*, 2009).

Except for the two main risk factors, age and genetics, Recent evidence has shown that cardiometabolic related factors, including hypertension, obesity, and diabetes,

may contribute to the development to AD dementia (Alzheimer's Association, 2020). Several previous studies have shown that the hypertension in midlife had increased the prevalence of AD (Kivipelto *et al.*, 2001; Kivipelto *et al.*, 2002; Wu *et al.*, 2003). A prospective longitudinal study based on 10276 individuals in their middle age evaluated the association between obesity and risk of dementia and found that obesity had a 74 % increase in the risk of developing dementia compared to individuals with normal weight (Whitmer *et al.*, 2005). A meta-analysis with 15 prospective studies including more than 72000 subjects reported that obese people are associated with an increased risk of AD in mid-life (Anstey *et al.*, 2011). A longitudinal study followed 824 older subjects (age > 55 years) up to 9 years and found that compared to those without diabetes mellitus, individuals with diabetes mellitus had a 65 % increased risk of developing AD (hazard ratio, 1.65; 95 % confidence interval, 1.10-2.47) based on a proportional hazards model. The last but not least, it is gradually considered that higher education is a protective factor for developing of AD (Bickel and Kurz, 2009; Meng and D'Arcy, 2012). People with less years of education are reported to have a higher risk of AD than those with more years of education (Sando *et al.*, 2008; Stern, 2012).

1.1.3 Neuropathology of AD

As already noted, the two pathological hallmarks of AD, extracellular Aβ plaques and intracellular neurofibrillary tangles (NFT) in brain histology, were first described by Alois Alzheimer in 1907 (Braak and Braak, 1991). Aβ is the main component of amyloid plaques (Glenner and Wong, 1984; Masters *et al.*, 1985). NFTs are composed of aggregates of microtubule-associated tau protein, which then becomes abnormally hyperphosphorylated tau (Kosik *et al.*, 1986; Goedert *et al.*, 1988). The neuropathology, including amyloid plaques and tau accumulation, could induce neuronal loss and synaptic dysfunction in the brain. The brains of AD dementia patients at the time of death weigh one-third less than the brain of age-matched, non-demented individuals (LaFerla *et al.*, 2007). Even though it appears that the key players, i.e. amyloid and tau, are known, the neuropathological mechanism is still largely unknown. In addition, neuroinflammation, activated by amyloid plaques and tau tangles, has also been considered to play a significant role in pathogenesis of AD (Zhang *et al.*, 2013; Heneka *et al.*, 2015).

The amyloid cascade hypothesis

Over past 20 years, combining observations from neuropathology, genetics and biochemistry, a hypothesis known as the amyloid cascade hypothesis was formulated which is still dominating AD related research (Hardy and Higgins, 1992; Selkoe, 2000; Hardy and Selkoe, 2002; Citron, 2010). The core of this hypothesis is that the deposition of Aβ peptides in the brain triggers a cascade of disease-causing processes including induction of tau-tangle formation, synapse dysfunction and cell death as well as neurodegeneration which ultimately leads to AD.

Aβ denotes peptides of 36 to 43 amino acids and it is the product of sequential cleavage of the APP. Previous studies have shown that Aβ peptide is released in its monomeric form, and monomeric Aβ peptides are able to assemble into progressively more aggregated forms, ranging from dimers and oligomers to fibrils (Hardy and Selkoe, 2002). Aβ oligomers are soluble and may exist throughout the brain, while Aβ fibrils accumulated as deposits in the extracellular space of the brain and its microvasculature (Chen *et al.*, 2017). APP is an integral membrane protein related to neurite outgrowth, neuronal development and axonal transport (Kang *et al.*, 1987). APP can be cleaved in two different ways. The so-called non-amyloidogenic pathway is the 'normal' pathway. Its end-product is soluble Aβ. The endpoint of the 'amyloidogenic' cleavage is the deposition of insoluble amyloid.

In the non-amyloidogenic pathway (**Figure 1.1**), APP is cleaved first by α-secretase which lies within the Aβ sequence and thus precludes Aβ formation. This cleavage yields secreted APP alpha (sAPPα) from the cell membrane and leaves the C-terminal fragment alpha (CTFα) in the plasma membrane. Subsequent cleavage of CTFα by γ-secretase releases a soluble extracellular peptide (p3) and the APP intracellular domain (AICD). In the amyloidogenic pathway **(Figure 1.1)**, APP is cleaved first by β-secretase 1 (BACE-1) and produces soluble secreted APP beta (sAPPβ) and leaves C-terminal fragment beta CTFβ in the membrane. Then, the CTFβ was cleaved by γ-secretase which yields AICD and Aβ monomers. The majority of Aβ peptides are secreted to the extra-cellular space, although a small amount can aggregate in-side neurons(Bu, 2009). Moreover, γ-secretase cleaves CTFβ at different sites and in multiple sequential steps, which ultimately produces mainly two species of Aβ, namely Aβ40 and Aβ42 (Zheng and Koo, 2011). The only difference between Aβ42 and Aβ40 is the two additional C-terminal residues on Aβ42. Aβ40 comprises 90 % of all Aβ

produced species and Aβ42 comprises 10 %. Although the Aβ40 comprises the majority of the Aβ species, Aβ42 is found to be the major component of amyloid plaques in AD brains (Iwatsubo *et al.*, 1994; Mak *et al.*, 1994; Gravina *et al.*, 1995), while Aβ40 is only shown in a subset of amyloid plaques (Mak *et al.*, 1994). These findings suggest that the Aβ42 deposition precedes Aβ40 deposition, however, the underlying mechanism that led to the preferential deposition of the Aβ42 is still not clear (Gu and Guo, 2013).

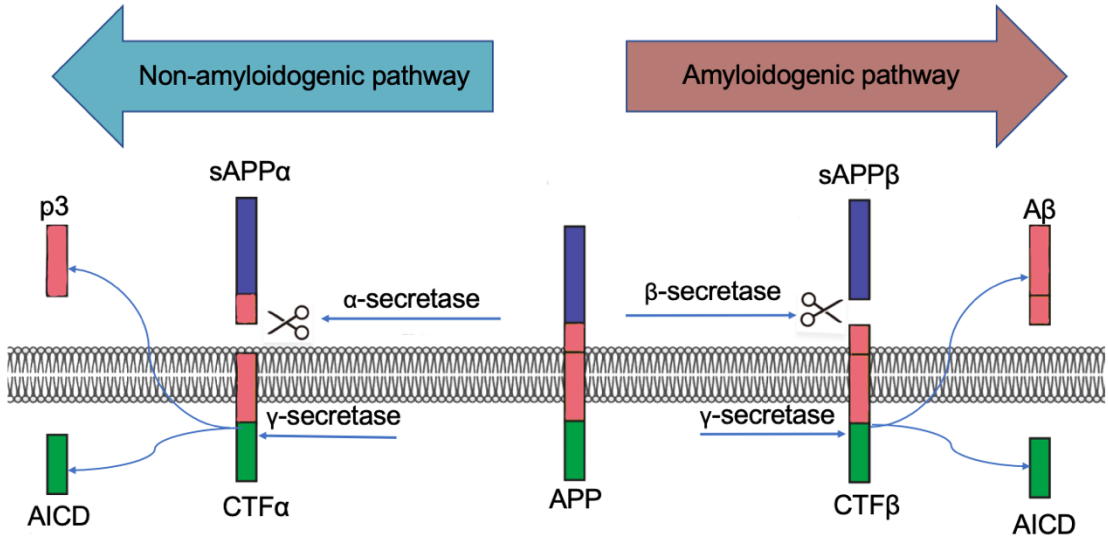

Figure 1.1: Non-amyloidogenic and amyloidogenic pathway of APP processing (*modified from* Zhou et al., (2018))**.** The left side is the non-amyloidogenic pathway and the right side is the amyloidogenic pathway; Abbreviations： APP = Amyloid precursor protein; sAPPα = secreted APP alpha; sAPPβ = secreted APP beta; CTFα = C-terminal fragment alpha; CTFβ = C-terminal fragment beta; AICD = APP intracellular domain; p3 = Extracellular peptide.

The main support for the amyloid hypothesis formed after the discovery of the dominantly inherited mutations that are responsible for the familial AD. Mutations in three genes, including APP, PSEN1 and PSEN2, are known to cause autosomal dominant AD, which generally manifests with an early-onset AD (St George-Hyslop and Petit, 2005). The commonality of the mutations in these genes is that they all affect the metabolism or stability of Aβ. In one common mutation of APP, the so-called Swedish mutation (APP_{swe}), a double amino-acid change leads to increased cleavage of APP by the β-secretase (Haass *et al.*, 1995). In addition, Down syndrome, in which triplication of chromosome 21 (on which APP resides) occurs, leads to Aβ accumulation early in life (Gyure *et al.*, 2001). Moreover, two additional AD mutations

identified on PSEN1 and PSEN2 affect the location at which γ-secretase cuts APP (Levy-Lahad *et al.*, 1995; Sherrington *et al.*, 1995; Scheuner *et al.*, 1996). The mutations lead to the production of longer variants of Aβ that clump together more readily, which induces the accumulation of Aβ into larger structures called oligomers. Further oligomers accumulation produces insoluble fibrils, which then aggregate into the amyloid plaques characteristic of AD. These mutations in APP and PSEN are closely correlated with the Aβ production process, providing rational evidence for the idea that Aβ production or Aβ amyloid fibril formation is one of the key steps in the genesis of AD. However, the formation of Aβ plaques is a necessary but not sufficient for the development of AD. Without amyloid deposition AD will not evolve – however, amyloid depositions not necessarily lead to AD, suggesting that additional factors have to be considered. Amyloid deposition is only weekly correlated with cognitive impairment and the degree of dementia (Murphy and LeVine, 2010; Nelson *et al.*, 2012). In addition, genetic mice studies have shown that the Aβ is deposited in the brain without NFT formation and neuronal loss (Bryan *et al.*, 2009). Even though the amyloid cascade hypothesis is reviewed and challenged (Kepp, 2017), it is generally considered that Aβ only initiates the onset and progression of AD, and that a cascade of events, including tau aggregation and neuronal dysfunction, is the proximal trigger for the clinically significant cognitive impairments that characterize AD-related dementia.

Temporal modelling of AD biomarkers

A temporal biomarker model of AD which follows the amyloid cascade hypothesis of AD was proposed by Jack and colleagues (Jack *et al.*, 2010). A key concept of this model is the temporal ordering of different biomarkers of AD across development from cognitively normal to AD (**Figure 1.2**). The biomarkers used in this model are several well-established measures of AD neuropathological and neurodegenerative alterations. The first biomarker in this model that is typically rising to abnormal levels is amyloid deposition, which can be measured e.g. by CSF levels of Aβ42 and by brain Aβ- positron emission tomography (PET) imaging. The next abnormal biomarker in this model is neuronal injury and dysfunction which can be measured by CSF tau (and, more recently, Tau PET) or fluorodeoxyglucose (FDG) PET. Compared to CSF total tau, CSF phosphorylated tau (ptau) seems to be more specific to AD (Buerger *et al.*, 2006). FDG-PET is used for measuring brain metabolism, which is considered to

indicate synaptic activity (Schwartz *et al.*, 1979). Decreased brain metabolism in posterior cingulate, precuneus and lateral temporal-parietal pattern is commonly reported in FDG PET studies with AD dementia (Jagust *et al.*, 2007). Interestingly, disruption of functional connectivity (FC) in similar brain regions as those showing reduced glucose metabolism was found in resting-state functional MRI (rs-fMRI) studies with AD patients (Greicius *et al.*, 2004; Wu *et al.*, 2011). Rs-fMRI, as a non-invasive imaging technique, is also increasingly used in AD studies as an indirect measure of neuronal activity. The final biomarker becoming abnormal before the clinical symptoms show up is brain atrophy, which can be measured by structural magnetic resonance imaging (MRI). In general, the cognitive symptoms are directly correlated with neuronal injury or brain atrophy rather than the biomarkers of Aβ deposition (Jack *et al.*, 2010).

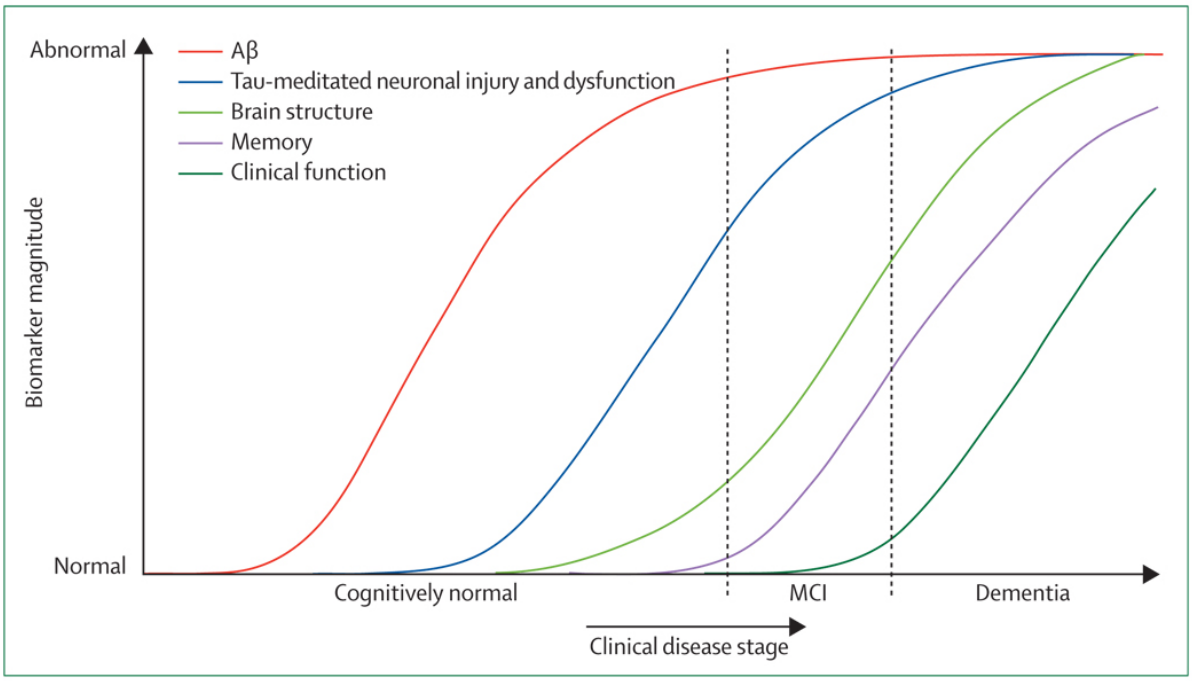

Figure 1.2: Dynamic biomarkers of the Alzheimer's pathological cascade. The figure is taken from Jack et al.,(2010). The permission to be used this figure in this thesis was granted by Elsevier (RightsLink License number: 201027-000228)

Although this biomarker model received a great attention in the field of AD research, and cumulative studies have been implemented according to the model, it doesn't cover all temporal patterns of biomarker-based changes, as exemplified by the phenomenon of suspected non-Alzheimer disease pathophysiology (SNAP). SNAP

refers to individuals with normal Aβ biomarker, however, the biomarkers related to neuronal injury or neurodegeneration are abnormal (Jack *et al.*, 2016). About 23 % of clinically normal individuals with age older than 65 years present SNAP, and this proportion is about 25 % in mildly cognitively impaired individuals (Jack *et al.*, 2016). Therefore, it is important to have a biomarker-based structure to classify SNAP as a non-AD form of pathological biomarker change. According to the 2018 NIA-AA research framework (Jack *et al.*, 2018), AD is defined using a three-biomarker construct: Aβ (A), tau (T) and neurodegeneration (N). The scheme is called AT(N)-scheme. 'A' refers to amyloid biomarkers (A) obtained CSF (i.e. Aβ42 or Aβ42/Aβ40-ratio) or cortical-Aβ deposition accessed by PET, 'T' refers to tau pathology. The relevant markers are either the phosphorylated tau (ptau) derived from CSF or tau deposition as measured by tau-PET. Neurodegeneration (N) is defined either by elevated total tau (ttau) in the CSF, brain atrophy revealed by MRI, or proven hypometabolism in an ^{18}F-fluorodeoxyglucose-PET scan. The addition of a normal/abnormal cut point for each AT(N) biomarker results in eight different AT(N) biomarker profiles **(Table 1.2)**. According to this scheme, A positive (A+) and T negative (T-) are considered to indicate AD-associated pathological change. A+T-(N)+ may indicate additional SNAP; Both A+ and T+ together mark the progression along the AD continuum.

Table1.2: AT(N) biomarkers and categories

AT(N) Profile	Biomarker Category
A-T-(N)-	Normal AD biomarkers
A+T-(N)-	AD Continuum-Alzheimer's pathologic change
A+T+(N)-	AD Continuum-Alzheimer's Disease
A+T+(N)+	AD Continuum-Alzheimer's Disease
A+T-(N)+	AD Continuum-Alzheimer's and concomitant suspected non-Alzheimer's pathologic change
A-T+(N)-	Non-AD pathologic change
A-T-(N)+	
A-T+(N)+	

This table is modified from Jack et al., (2018).

1.2 Imaging findings in AD

Complementary to *postmortem* and histopathological method, brain imaging has played an important role in understanding the characteristic brain changes in AD in vivo. MRI is a powerful and non-invasive technique for imaging of the human brain structure and provides functional brain responses with functional MRI (fMRI). More recently, Amyloid PET imaging has allowed the in vivo detection brain Aβ plaques in AD. These imaging modalities and related approaches offer opportunities to investigate structural decline (e.g. brain volume loss, cortical thinning), functional alterations (e.g. fMRI hyperactivity/ hypoactivity, altered network connectivity) and the underlying neuropathology related to amyloid aggregation in AD.

1.2.1 Amyloid PET Imaging

Amyloid-PET imaging can measure the cerebral Aβ deposition in the brain in vivo. Since cerebral amyloid deposition has been considered as a critical neuropathology biomarker to be detected even in an early stage of AD progression, PET scans with radiolabeled tracers that bind specifically to Aβ have been widely used in the AD studies. Amyloid PET imaging was first explored with [11C] carbon-based tracers such as Pittsburgh Compound B (PiB) (Klunk *et al.*, 2004). However, the half-life for [11C] tracers is only about 20 minutes which makes radiopharmaceutical production and distribution demanding. The development of [18F] fluorine-based tracers, including [18F]-flutemetamol (Nelissen *et al.*, 2009), [18F]-florbetapir (Wong *et al.*, 2010), and [18F]-florbetaben (Barthel *et al.*, 2011a) with an extended half-life of about 110 minutes facilitated the wide use of amyloid PET imaging in AD-related studies (Marquez and Yassa, 2019). These ^{18}F-labeled tracers are approved for “visualization of intracerebral amyloid β plaques in patients with cognitive impairment suspected of AD” (Matsuda *et al.*, 2019).

Considering that we used [18F]-florbetaben (FBB) PET imaging in one of the presented studies in this thesis, the studies introduced below focus on FBB-PET imaging. Compared with healthy controls, the uptake of FBB was higher in frontal, temporal, parietal, occipital and cingulate cortices in AD patients, with the posterior cingulate cortex representing the best region for discrimination (Barthel *et al.*, 2011a). Sensitivity and specificity of FBB for the distinction of AD from healthy controls were 80 % and 91 % based on visual analysis, respectively (Barthel *et al.*, 2011a; Barthel *et al.*, 2011b). The uptake pattern of FBB has been reported to associate with

histopathologic distribution of Aβ, with sensitivity and specificity of 97.9 and 88.9 %, respectively (Sabri *et al.*, 2015). One substantial advantage of amyloid imaging may come in the setting of the cognitively normal elderly. In accordance with previous autopsy findings, several [11C]-PiB PET studies have consistently found increased [11C]-PiB binding in normal older volunteers, with the proportion of these "amyloid-positive" cases ranging from 10 to 30 %, depending on the age of the cohort and the threshold used to define [11C]-PiB positivity (Mintun *et al.*, 2006; Pike *et al.*, 2007; Aizenstein *et al.*, 2008; Klunk *et al.*, 2015). Therefore, detection of underlying cerebral Aβ deposition at this clinically "invisible" stage may give us the greatest insights into the very beginnings of AD.

1.2.2 Structural brain imaging, with a special focus on basal forebrain

Structural MR imaging provides clear anatomical detail and provides a good grey and white matter contrast. Brain atrophy can be easily visualized and quantified with structural MRI images. Because it is widely available, non-invasive, and part of the standard diagnostic routine in neurology and psychiatry, it has been extensively used to investigate neurodegenerative processes in AD on a macroscopic level. Previous studies have shown that the typical atrophy pattern in AD locates in the structures of medial temporal lobe, including the hippocampus, entorhinal cortex and parahippocampal gyrus (Henneman *et al.*, 2009; Ledig *et al.*, 2018). The entorhinal cortex is typically the earliest brain region showing atrophy, closely followed by the hippocampus and parahippocampus in the early stages of AD (Dickerson *et al.*, 2001; Killiany *et al.*, 2002). Meanwhile, a recent study suggests that volume loss of the NBM, a subnucleus of the cholinergic BF, already shows atrophy in preclinical AD and even precedes volume loss of the entorhinal cortex (Schmitz *et al.*, 2016b).

Apart from cerebral Aβ deposition, cholinergic BF neurodegeneration is also considered as an early event in the progression of AD (Whitehouse *et al.*, 1981; Mann *et al.*, 1984; Sassin *et al.*, 2000). Acetylcholine, as neurotransmitter and neuromodulator in the brain, is widely distributed in the central nervous system and plays a critical role in modulating cognitive performance, learning and memory process (Schliebs and Arendt, 2006). The BF brain region is important in the production of acetylcholine and is then distributed widely to the cortical and limbic structures (Mesulam *et al.*, 1983). Previous studies have shown that cholinergic synaptic conductance plays an important role in learning and memory (Deutsch, 1971).

Pharmacological studies have demonstrated that anticholinergic drugs impaired cognitive performance in young healthy patients to a level detectable in dementia, while enhancement of cholinergic function improved the cognitive performance of aged patients (Drachman and Leavitt, 1974; Drachman, 1977). The observation of cholinergic innervation of limbic areas, including the hippocampus, provides support to understand the critical role of cholinergic basal forebrain system in memory function. Previous animal studies have found the important role of acetylcholine in hippocampal long-term potentiation which may provide cellular mechanisms underlying the putative relationship of cholinergic pathways to memory (Tanaka *et al.*, 1989; Auerbach and Segal, 1994). However, the findings of the exact relationship between the cholinergic system and memory are not consistent in previous studies, and the exact nature of this relationship continues to elude a clear description. For example, the selective lesion of cholinergic neurons in the BF leads learning and memory impairments in some experiments, but not in all rodent studies (Berger-Sweeney *et al.*, 1994; Wenk *et al.*, 1994; Galani *et al.*, 2002). Even non-selective destructive lesions that include the cholinergic as well as noncholinergic components of the BF cause memory deficits in some primate experiments (Ridley *et al.*, 1986), but not in others (Voytko *et al.*, 1994). Despite the inconsistent findings regarding relationships between the cholinergic system and cognition in animal studies, BF cholinergic cell loss is a consistent feature of AD. The BF cholinergic neurodegeneration has been suggested to cause, at least partly, the observed cognitive deficits, and has led to the formulation of the cholinergic hypotheses of cognitive dysfunction (Whitehouse *et al.*, 1982; Vogels *et al.*, 1990). And one type of drugs to slow down the cognitive deterioration in AD, which have been proven clinically useful, is cholinesterase inhibitor (Summers *et al.*, 1986). It increases the availability of acetylcholine at synapses in the brain, validating the BF cholinergic system as an important therapeutic target in AD.

Using histochemical and immunohistochemical labelling for acetylcholinesterase (AChE) and choline acetyltransferase (ChAT) in macaque monkey, Mesulam et al., (1983) identified four overlapping magnocellular groups within the basal forebrain BF and described four cholinergic cell groups Ch1–Ch4. Ch4 is the largest cholinergic cell groups in BF and can be further subdivided into several distinct subnucleis in the macaque monkey (Mesulam *et al.*, 1983). According to findings from previous studies based on tracer experiments in the macaque monkey using the retrograde labeling of

cholinergic perikaryal, Ch1 and Ch2 provide the major cholinergic innervation for the hippocampal, Ch3 for the olfactory bulb, and Ch4 for the rest of the cerebral cortex and the amygdala (Mesulam *et al.*, 1983; Mesulam *et al.*, 1986). Accumulating evidence suggest that cholinergic BF dysfunction or degeneration have tight interactions with Aβ. Perry et al. found correlations between diminishing activity of the ChAT and increasing numbers of amyloid plaques in the post-mortem brains of patients with AD (Perry *et al.*, 1978). It has been reported that AChE accelerates the assembly of Aβ into insoluble amyloid fibrils (Inestrosa *et al.*, 1996). In amyloid precursor protein transgenic (APP23) aged mice, modest decreased cholinergic enzyme activity was reported compared to age-matched wild-type mice. Unilateral NBM lesions in adult APP23 mice after several months lead to a 38% reduction in ChAT activity and significant cholinergic fiber loss in the ipsilateral frontal cortex. Histopathologic studies on the relationship between amyloid deposition and cholinergic decline in AD brain specimens found increased cortical amyloid load to be associated with degeneration of cholinergic BF neurons (Arendt *et al.*, 1985; Beach and McGeer, 1992) and reduced cortical ChAT activity (Perry *et al.*, 1978; Ikonomovic *et al.*, 2011). These findings could also be reproduced in nondemented elderly that showed AD pathology at autopsy (Beach *et al.*, 1997; Potter *et al.*, 2011). Therefore, the tight association between amyloid formation and dysfunction of cholinergic may reflect the vulnerability of cholinergic BF neurons to cerebral amyloidosis. This first cytoarchitectonic atlas of basal forebrain follows Mesulam's nomenclature divides the BF into cholinergic nuclei the medial septal nucleus (Ch1), the vertical nucleus of the diagonal band of Broca (Ch2), its horizontal limb (Ch3), and the nucleus basalis Meynert (NBM, Ch4) with anterior lateral (Ch4al), medial (Ch4am), intermediate (Ch4i) and posterior (Ch4p) subregions. Due to their small sizes, Ch1 and Ch2 were combined into one ROI (Ch1/2), Ch4am and Ch4i into Ch4ai (**Figure 1.3**). Whitehouse et al first reported 90 % NBM cell loss in a familial AD case compared to controls based on the autopsy findings (Whitehouse *et al.*, 1981). Further histological studies have reported different magnitude of cell loss in the anterior, intermediate and posterior subdivisions of NBM in AD relative to controls, most prominently in the NBM (Whitehouse *et al.*, 1982; Vogels *et al.*, 1990). The underlying mechanism may be Ch4p providing cholinergic innervation to the temporal pole and superior temporal cortex (Mesulam *et al.*, 1983), this correlates well with memory loss and language impairment in AD. Moreover, a severe loss of cholinergic innervation in the cerebral

cortex, especially temporal lobes including the entorhinal cortex, is considered to reflect the main characteristics of AD (Geula and Mesulam, 1989, 1996). Perry et al reported that the cholinergic denervation of the temporal lobe was present even in patients at the early stages of AD neuropathology (Perry *et al.*, 1981). A progression of abnormalities has been observed in the cholinergic neurons of the BF of non-demented younger adults, non-demented elderly people, and people with mild or severe AD (Geula *et al.*, 2008). These findings suggest that BF neuronal pathology emerges very early in the course of aging and AD.

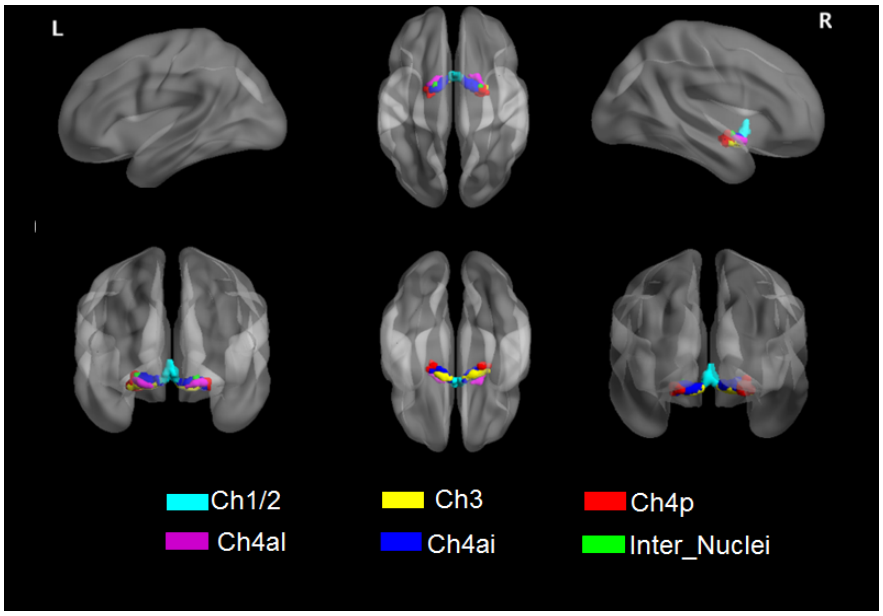

Figure 1.3: Illustration of the subregions of the cholinergic basal forebrain in 3D. 3D view of BF from the sagittal, coronal and axial view: L = left; R=right

Since histological approaches do not allow for longitudinal observations, and post mortem studies are mainly suitable for advanced stage of AD, in vivo MRI studies of BF cholinergic system focused on high-risk AD individuals have significant practical implications in early detection of AD. Combined the cytoarchitectonic atlas of the BF, high-resolution structural MRI-based BF volumetry has been particularly used to study cholinergic BF degeneration in high-risk AD individuals. MRI-based in vivo studies have confirmed severe BF gray matter atrophy in patients with AD and revealed BF atrophy in MCI (Grothe *et al.*, 2010; Kilimann *et al.*, 2014). Using amyloid PET imaging, it was also shown that BF atrophy on MRI was linked with cortical amyloid deposition during pre-dementia phases of AD (Grothe *et al.*, 2014). Moreover, BF volume, especially the volume of posterior NBM, was significantly more accurate on distinguishing amyloid positive and amyloid negative in cognitively unimpaired and

mildly impaired subjects (Teipel *et al.*, 2014). A recent longitudinal study found that NBM volume, but not entorhinal cortex, showed progressive atrophy over a two year period in healthy individuals showing abnormal CSF biomarkers of amyloid-β accumulation (Schmitz *et al.*, 2016a).

1.2.3 Resting-state functional MRI

fMRI is a noninvasive imaging technique to investigate brain activity. It provides an indirect measure of neuronal activity by measuring changes of the magnetic properties of the blood. The derived signals depend on local oxygenation - and perfusion – changes caused by regional brain activity changes. The contrast is called blood oxygen level–dependent (BOLD) contrast (Ogawa *et al.*, 1990; Kwong *et al.*, 1992). There is a growing interest to use rsfMRI to examine the neurophysiological mechanisms associated with AD owing to its noninvasive and task-free nature. Resting-state refers to spontaneous BOLD signal during a non-active state when the participant is lying quietly in the MRI scanner with the eyes closed or passively viewing a stimulus. The spontaneous BOLD signal in the resting brain had initially been thought to represent noise. In 1995, Biswal et al. (1995) found that BOLD signal in low-frequency (.01 to .08 Hz) fluctuations in resting brain were highly correlated across the hemispheres in the bilateral motor cortices. Subsequently, low-frequency fluctuations were shown to be of neural origin and specific to gray matter (Li *et al.*, 2000). FC analyses, using rs-fMRI to measure synchronous low-frequency brain activity fluctuations in spatially distinct brain areas, can be used to identify the spatial extent of temporally correlated brain networks within the brain (Damoiseaux *et al.*, 2006). The most straightforward method to investigate the FC of a particular brain region is to correlate the time-series of the prior defined brain region against the time-series of all other remaining voxels in the brain, resulting in a voxel-based FC-Map (Biswal *et al.*, 1997). This prior defined brain region is typically called seed and the method is called seed-based FC. Previous studies have identified a set of regions, including precuneus, PCC, anterior cingulate cortex, parietal cortex, and the medial temporal lobe, which is known as DMN and shows the highest level of spontaneous activity during resting-state brain (Raichle, 2015). The DMN network is also active during directed tasks that require participants to remember past events or imagine upcoming events. Converging data have confirmed impaired intrinsic FC in the DMN during the resting state in AD (Greicius *et al.*, 2004; Rombouts *et al.*, 2005; Sorg *et al.*,

2007; Rombouts *et al.*, 2009; Koch *et al.*, 2012). A meta-analysis about resting-state network dysfunction in AD found a strong tendency in the literature toward specific examination of the DMN (Badhwar *et al.*, 2017). Interestingly, the brain regions in the DMN network, especially precuneus and posterior cingulate, overlap with those brain regions that show the highest amyloid burden (Klunk *et al.*, 2004; Buckner *et al.*, 2005; Sperling *et al.*, 2009) (**Figure 1.4**) and hypometabolism (Foster *et al.*, 1983; Reiman *et al.*, 1996; Minoshima *et al.*, 1997; De Santi *et al.*, 2001) in AD patients. Moreover, there is growing evidence that FC alterations already emerge during the preclinical stages of AD, and are linked with brain amyloid accumulation (Sheline and Raichle, 2013; Palmqvist *et al.*, 2017): The involvement of DMN structures is of special interest here, as its hub regions like the PCC/ precuneus appear particularly vulnerable to amyloid accumulation, and are among the first brain structures that show increasing amyloid tracer uptake in early amyloidosis (Mattsson *et al.*, 2019).

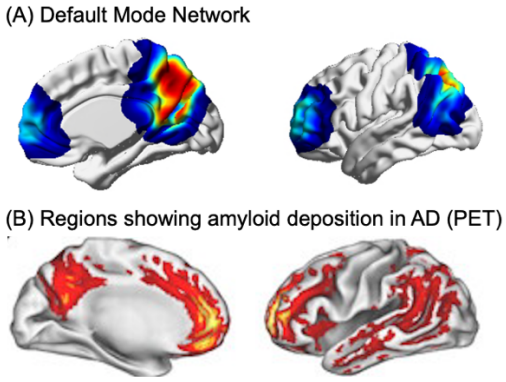

Figure 1.4: Convergence between default mode network and amyloid load (modified from Buckner *et al.* (2005)). The upper panel: brain regions of default mode network; The bottom panel: brain regions showing amyloid deposition in AD

Regional Homogeneity (ReHo) is a local FC measure that measures the functional coherence of resting-state series between one given voxel and its neighbor voxels (Zang *et al.*, 2004). ReHo has been widely used in explore alterations of regional brain coherence in patients with AD and MCI. He and his colleagues found that the PCC/precuneus region showed decreased ReHo in AD patients compared to healthy controls, while increased ReHo was shown in the occipital lobule, including bilateral cuneus, left lingual gyrus and right fusiform gyrus (He *et al.*, 2007). Several studies also consistently reported ReHo decreases in DMN regions in AD patients, especially in PCC/precuneus (Liu *et al.*, 2008; Zhang *et al.*, 2012; Marchitelli *et al.*, 2018). The majority of previous studies reported decreased ReHo in PCC/precuneus in MCI patients (Bai *et al.*, 2008; Zhang *et al.*, 2012; Long *et al.*, 2016; Ni *et al.*, 2016; Yuan *et al.*, 2016), while only one studies showed increased ReHo in precuneus (Wang *et*

al., 2015b). Parallel increases of ReHo in brain regions located in occipital and frontal lobule were also reported in the MCI patients (Bai *et al.*, 2008; Liu *et al.*, 2014; Yuan *et al.*, 2016). A meta-analysis investigating ReHo alterations in MCI identified significant changes mainly in the DMN, executive control network, visual network and sensorimotor network (Zhen *et al.*, 2018). These local FC changes may indicate the coexistence of functional decline and compensation adaptions in these brain networks in MCI patients.

1.3 AD research framework and subjective cognitive decline (SCD)

1.3.1 Characteristics of SCD

The concept of SCD refers to elderly individuals who self-report persistent decline in cognitive abilities, despite their objective cognitive performance level still being within normal range. The basic concept of SCD came up more than 30 years ago, where Reisberg and colleagues developed the Global Deterioration Scale (GDS) for the clinical staging of dementia (Reisberg *et al.*, 1982): Their scheme includes a stage 2 that is characterized as complains or concerns memory deficit, no objective evident of memory deficits, which is in line with the term 'pre-MCI-SCD' proposed by the SCD-Initiative in 2014 (Jessen *et al.*, 2014a). Several nomenclatures and various forms of approaches to define SCD were used on this topic (Abdulrab and Heun, 2008) in the field, mainly including 'subjective memory impairment (SMI)' (Jessen *et al.*, 2010), subjective memory complaints (SMC)' (Schmand *et al.*, 1997), 'subjective cognitive impairment (SCI)' (Stewart, 2012), 'subjective cognitive complaints/concerns (SCC)' (Dufouil *et al.*, 2005; Donovan *et al.*, 2014). Thus, a consistent concept for terminology and research framework regarding subjective experience of cognitive decline is needed. To address this need, the term SCD and criteria of research framework was standardized by an international working group of researchers and clinicians, known as the SCD-initiative (SCD-I) in 2014 (Jessen *et al.*, 2014a). "Subjective" refers to individual self-experience, regardless of objective performance on neuropsychological tests. The term "cognitive" rather than "memory" was used since the first symptoms of AD are not necessarily restricted only to the memory domain. Yet, subjective decline in the memory of an individual irrespective of decline in other cognitive domains is a "SCD plus" feature which is considered to increase the probability of preclinical AD in individuals with SCD (Jessen *et al.*, 2014a). "Decline" refers to the idea of progressive deterioration or a change from the previous level of functioning and not just an isolated

complaint. Currently, there are two main criteria for SCD based on the standardized definition by SCD-I. First, a self-experienced persistent decline in cognitive capacity in comparison with a previously normal status and unrelated to an acute event. Second, normal age-, gender-, and education-adjusted performance on standardized cognitive tests. In addition, the subjective cognitive complains should be not explicable by a psychiatric or neurologic disease, medical disorder, medication, or substance use.

1.3.2 Association of SCD with risk of cognitive decline and increased AD biomarker positivity

Longitudinal studies have shown that SCD is a risk factor for future cognitive decline, and for the conversion into MCI and AD. Reisberg et al followed 213 subjects for a mean period of 6.8 years and found 14.9 % cognitive normal elderly and 54.2% SCD subjects declined to MCI or AD (Reisberg *et al.*, 2010). Another study found that 3.7% of cognitive normal elderly converted to AD during four follow-up visits with 18-month intervals, while 6.2 % in in the SMI group (Jessen *et al.*, 2014b). A meta-analysis including twenty-eight longitudinal epidemiological studies found that the overall annual conversion rate (ACR) was 2.33 % in those with SMC at baseline compared with 1% in those without SMC (Mitchell *et al.*, 2014). This represents a twofold increased risk of developing dementia compared with non SCD healthy controls to SCD (Mitchell *et al.*, 2014). Moreover, they found that the overall proportion of SMC conversion to AD was 10.99 % over the follow-up period of about 5 years (Mitchell *et al.*, 2014). In a recent multicenter study on 2987 SCD individuals and 1391 cognitive normal controls, they found an overall dementia incidence rate in individuals with SCD of 17.7 per 1000 person-years, compared to 14.2 in controls (Slot *et al.*, 2019). In a study focusing on the trajectories of cognition and daily functioning in SCD, Verlinden et al found that dementia cases first reported memory complaints 16 years before diagnosis followed by the decline of overall cognition ability and daily function (Verlinden *et al.*, 2016).

In line with the increased conversion risk for SCD,a CSF AD profile was more often observed in patients with SCD (52 %), than in healthy controls (31 %) (Visser *et al.*, 2009). Further support of the role of SCD within the clinical trajectory of AD is provided by imaging data. The subjective memory complaints were suggested to be an early indicator of AD pathology, since a significant relationship between cortical PiB binding and a subjective memory complaints composite score instead of objective cognitive

measures of memory and executive functions was found (Amariglio *et al.*, 2012). Moreover, a significant APOE by SCD status interaction was found, showing that the APOE4/SCD exhibited the lowest cerebral metabolic rates for glucose of parahippocampal gyrus and the highest CSF ptau, and ptau/ Aβ42 levels as compared with all other subgroups (Mosconi *et al.*, 2008). A longitudinal study investigated the relationships between [18F] florbetapir PET and concurrent/longitudinal cognitive performance in 107 SCD and found higher Aβ load in SCD from a memory clinic was associated with lower concurrent global cognition and faster rate of decline in a variety of cognitive domains (Timmers *et al.*, 2019). Low Aβ42 was found to be the strongest predictor of clinical progression in patients with subjective complaints relative to total tau, and ptau (van Harten *et al.*, 2013). It was also reported in the literature that SCD atrophy in established brain regions can be found including, the medial temporal lobe, hippocampus or entorhinal cortex (van der Flier *et al.*, 2004; Jessen *et al.*, 2006; Scheef *et al.*, 2012; Perrotin *et al.*, 2015; Hu *et al.*, 2019; Scheef *et al.*, 2019). One longitudinal study found an association between longitudinal changes in hippocampal volume in nondemented individuals with subjective reports of memory impairment in a population-based sample (Stewart *et al.*, 2011). A recent study found initial evidence that cholinergic BF atrophy was already detectable in cohorts with subjective cognitive complaints (Scheef *et al.*, 2019) and may be associated with a lower cognitive performance trajectory (Teipel *et al.*, 2018b). In summary, converging findings found that SCD is associated with AD biomarkers across a range of modalities and represents a higher risk to develop MCI or AD (Ronnlund *et al.*, 2015; van Harten *et al.*, 2018; Slot *et al.*, 2019). Therefore, SCD patients are increasingly considered as at-risk for cognitive decline and eventual progression to AD, and SCD in preclinical AD may be a promising target population for AD prevention trials.

Importantly, SCD or subtle cognitive decline in combined with proven AD pathology corresponds to stage 2 of the Alzheimer's continuum according to NIA-AA Alzheimer's research framework (Jack *et al.*, 2018). There is a growing research interest to determine and provide evidence that SCD with additional AD-related biomarkers represents the late preclinical phase of AD compared to asymptomatic elderly with AD biomarker positivity. A longitudinal study found that SCD with Aβ positivity assessed by PET imaging showed deeper objective cognitive decline than individuals with either Aβ or SCD alone (Vogel *et al.*, 2017). This finding suggests that the presence of both

SCD and Aβ contributes to the cognitive decline. Another longitudinal study also found that SCD with higher brain amyloid load showed cognitive decline at a higher rate (Timmers *et al.*, 2019). This notion that SCD in combination with proven AD pathology may reflect a late preclinical stage of AD is also supported by a study which found higher hippocampal atrophy and lower cognitive performance in SCD with ApoE4, even though ApoE4 carriers is a risk factor for AD rather than a direct biomarker for amyloid pathology (Striepens *et al.*, 2011).

1.3.3 Functional connectivity findings based on resting-state functional MRI in SCD

As a potential imaging biomarker in AD, FC alterations (especially in DMN areas) in individuals with SCD have also been investigated in a variety of studies (Hafkemeijer *et al.*, 2013; Wang *et al.*, 2013; Dillen *et al.*, 2017). However, the FC of DMN findings in SCD are ambiguity. Hafkemeijer et al (2013) first reported that SCD individuals exhibited increased FC in the DMN and the medial visual network compared to the HC. In contrast, decreased FC within the DMN is also reported in individuals with SCD in comparison to HC (Wang *et al.*, 2013). One study also found that decreased FC between the DMN and hippocampus in individuals with SCD (Dillen *et al.*, 2017). Precuneus (or more generally: posterior DMN) based FC studies also showed both increased (Verfaillie *et al.*, 2018; Viviano *et al.*, 2019) or decreased FC (Yasuno *et al.*, 2015) patterns in SCD individuals compared to HC. Currently, no previous study has examined the ReHo alterations in SCD patients.

1.4 Objectives

As outlined above SCD is increasingly recognized as a concept to identify people who are at high risk of developing MCI or AD (Reisberg and Gauthier, 2008; Gifford *et al.*, 2014; Jessen *et al.*, 2014b; Buckley *et al.*, 2016). Even though SCD is not specific for AD, it might be one of the earliest warning signs of AD-related neurodegeneration within the AD trajectory. Following the NIA-AA research framework (Jack *et al.*, 2018), SCD symptoms might reflect a progression from stage 1 (asymptomatic) to stage 2 (transitional cognitive impairment) of the Alzheimer's continuum. However, there are very limited data available so far to test this hypothesis. The main goal of this thesis is to provide neuroimaging evidence to support this assumption.

For this purpose, data will be analyzed that are derived from the German Center for Neurodegenerative Diseases Longitudinal Cognitive Impairment and Dementia (DELCODE) Study, which focuses on the characterization of SCD individuals recruited from memory clinics. The first aim of this thesis is to investigate whether BF volume reductions might not only be detectable in the MCI and AD, but also in SCD, and examined its relationship with cognitive performance and CSF-Aβ pathology. In order to access the functional consequences of an early disturbance of the cholinergic system, functional connectivity of the NBM was accessed in SCD individuals in the second study. Considering that the precuneus is an important hub region of the DMN showing a high vulnerability for amyloid depositions, the third aim was to investigate how cerebral amyloid pathology relates to FC of the precuneus in SCD patients.

2 Material and methods

2.1 DELCODE project design

The analyses presented in this thesis are based on cross-sectional data from the DELCODE project (Jessen *et al.*, 2018). It is an ongoing observational longitudinal memory clinic-based multicenter study focusing on SCD in the context of AD. The participating DZNE sites include Bonn, Magdeburg, Berlin, Munich, Göttingen, Tübingen, Cologne, and Rostock/Greifswald. Apart from a SCD patient group, the DELCODE cohort includes individuals with MCI and AD, relatives of AD, as well as healthy control (HC) subjects. The examination items in the DELCODE project include extensive clinical and neuropsychological questionnaires, MRI and optional amyloid PET scans, as well as CSF biomarker collection through lumbar puncture. The clinical and neuropsychological tests are harmonized across all the DELCODE participating sites (Jessen *et al.*, 2018). Each experimenter at all sites underwent training in order to guarantee high image and data quality based on the standard operation procedures (SOPs) *(Jessen et al., 2018)*. The standard protocol was established at each site in an identical manner and underwent continuous quality control by the DZNE site Magdeburg.

The DELCODE study protocol was approved by the institutional review boards of all participating sites. The PET sub-study was also approved by the national radiation authority (Bundesamt für Strahlenschutz [BfS]). All investigations were performed in

accordance with the relevant guidelines and regulations. All participants provided written informed consent in accordance with the Declaration of Helsinki.

2.2 Clinical assessments and group definition of SCD, MCI and AD

The clinical patient groups were recruited from the memory clinics of the participating sites. The grouping of SCD, MCI and AD patients was based on the clinical and neuropsychological test (NPT) assessments at the memory clinics. These clinical assessments used to define levels of cognitive impairment included the Mini-Mental State Examination (MMSE), Clinical Dementia Rating (CDR) as well as the Consortium to Establish a Registry for Alzheimer's Disease (CERAD) neuropsychological test battery.

The SCD group was defined if individuals caused concern but showed normal performance in the CERAD test battery, along with MMSE scores ≥ 26. MCI individuals were defined by MMSE score ≥ 24 and cognitive performance level being 1.5 standard deviations (SD) below the normal range in the delayed recall trial of the CERAD word list. While a delayed recall deficit was mandatory, however, the performance of MCI individuals in other CERAD tests could equally fall below -1.5 SD. Accordingly, MCI participants enrolled in DELCODE included single and multiple-domain amnestic MCI, but no non-amnestic MCI patients. Thus, the term 'MCI' within the presented studies of the thesis refers to amnestic MCI patients. DAD patients fulfilled the clinical NINDCS/ADRDA criteria of probable Alzheimer's disease (McKhann *et al.*, 2011). HC were recruited *via* public advertisement, and included if individuals showed cognitive performance in the normal range, and reported no, or only subtle subjective decline that caused no concerns.

The general inclusion criteria for all groups were as follows: individuals 1) gave informed consent; 2) presence of an informant, who is willing to provide information on the participant throughout the study; 3) presence of an informant, who is not participating in the study and willing to provide information on the healthy control throughout the study; 4) fluent German language abilities; 5) age >/= 60 years. The exclusion criteria for all groups were as follows: individuals had 1) any condition that clearly interferes with participation in the study and interferes with the clinical and neuropsychological study procedures; 2) contraindications for MRI; 3) severe or unstable medical condition and current major depressive episode as well as psychotic disorder, bipolar disorder, substance abuse at present or in the past; 4)

neurodegenerative disorder other than AD and vascular dementia; 5) history of stroke with residual symptoms and current or past unstable malignant disease within the last two years; 6) chronic use of psychoactive drugs with sedative or anticholinergic effects and use of antidementia drugs in SCD, MCI and in control subjects; 7) investigational agents for treatment of dementia or cognitive impairment one month prior to study entry; 8) participation in a study using investigational medicinal products.

2.3 Neuropsychological tests

In addition to clinical standard measures like MMSE, CDR scale, and a modified version of the Alzheimer's Disease Assessment Scale-Cognitive-Plus (ADAS-Cog-13), the yearly study visits included an extensive NPT battery that was applied for all of the study participants to capture early and subtle cognitive changes (Jessen *et al.*, 2018). Confirmatory factor analysis was used to derive 5 cognitive factors from the various NPT dependent variables to reduce measurement error for each test and improve sensitivity to early AD-related changes: (1) *learning and memory* (MEM), comprising test scores from the Alzheimer's Disease Assessment Scale, Cognitive part (ADAS-Cog) Word List, The Free and Cued Selective Reminding Test (FCSRT) Free Recall, FCSRT Cue Efficiency, The Wechsler Memory Scale (WMS) Logic Memory, Figure savings, Incidental learning (SDMT), and Face Name Test; (2) *language abilities* (LANG), comprising tests of Verbal Fluency Groceries, Verbal Fluency Animals, Boston Naming Test (20 item version), and FCSRT Naming Part; (3) *executive functions and mental processing speed* (EXEC), comprising speed-dependent executive functioning tests such as the Trail-Making-Test A and B and and Number Cancellation, Flanker Test; (4) *working memory* (WME), comprising tests such as Digit Span Forward and Backward, and FCSRT interference task; (5) *visuo-spatial abilities* (VIS), comprising tests of figure copying, clock copying and clock drawing. For a detailed description of the tests, and the procedure to derive the 5 factors, please refer to Wolfsgruber et al. (2020).The extracted factor score estimates were scaled as z-scores for the performance of the complete sample. Lower scores represented worse performance.

2.4 CSF biomarkers assessment

About 50% of the participants underwent lumbar puncture. CSF biomarkers were analyzed according to vendor specifications: V-PLEXAβ Peptide Panel 1 (6E10) Kit (K15200E) and V-PLEX Human Total Tau Kit (K151LAE) (Mesoscale Diagnostics LLC,

Rockville, USA), and Innotest Phospho-Tau(181P) (81581; Fujirebio Germany GmbH, Hannover, Germany) (Jessen *et al.*, 2014a). As recent studies suggested that CSF Aβ42/40 is a more accurate and sensitive biomarker for MCI and clinical AD compared to Aβ42 alone (Hansson *et al.*, 2007; Janelidze *et al.*, 2016; Lewczuk *et al.*, 2017), we used the cutoff ratio (Aβ+: Aβ42/Aβ40 ratio < 0.09) or amyloid-negative (Aβ-: Aβ42/Aβ40 ratio ≥ 0.09) to group participants as amyloid-positive (Aβ+: Aβ42/Aβ40 ratio < 0.09) or amyloid-negative (Aβ-: Aβ42/Aβ40 ratio ≥ 0.09) (Janelidze *et al.*, 2016).

2.5 APOE genotyping

APOE genotyping was performed using a commercially available TaqMan® SNP Genotyping Assay (ThermoFisher Scientific) (Jessen *et al.*, 2018). The analytical variable used in the thesis based on APOE genotyping is APOE4 carriers vs. non-carriers.

2.6 PET Methods

2.6.1 [18F]-Florbetaben PET data acquisition

DELCODE-PET is a substudy of DELCODE that only focused on the SCD population of the study, i.e. did not include healthy controls or clinically impaired patients, due to regulatory restrictions. PET data acquisition followed established standard procedures for FBB (Neuraceq^{TM}: Life Radiopharma Berlin GmbH) scanning. In addition, to calculate attenuation correction maps, low-dose CT were collected. The acquired PET data were reconstructed iteratively according to the established PET brain protocols of the participating nuclear medicine sites. This included decay, random, scatter, dead time, normalization, and attenuation correction.

2.6.2 [18F]-Florbetaben PET data analysis

Qualitative visual analysis of PET scans: The clinical gold standard for interpreting FBB PET scans is visual reading, and it was used to classify the subjects in the third study as amyloid-positive ($SCD_{Aβ+}$) or -negative ($SCD_{Aβ-}$). According to manufacturer guidelines (Seibyl *et al.*, 2016), visual readings of the FBB scans were conducted by two experienced readers. Specifically, four predefined ROIs, including frontal lobe, lateral temporal lobe, parietal lobe, and posterior cingulate/precuneus, were used by the readers to evaluate the cortical tracer binding. Across the majority of slices within any of the four predefined ROIs, the readers rated if significant cortical tracer binding

was found for each subject. If cortical tracer binding was observed in at least one of these four predefined ROIs, the subject was grouped as amyloid positive.

Quantitative analysis of PET scans: PMOD 4.004 (PMOD Technologies LLC, Zurich, Switzerland) was used to derive additional quantitative measures for the severity of amyloidosis, as indicated by cortical tracer binding. The motion-corrected of PET images and co-registered with a T1-weighted image of the participant were performed using the PNEURO Maximum Probability Atlas pipeline. The T1-weighted image of the participant was segmented using Unified Segmentation (Ashburner and Friston, 2005). The AAL atlas template (Tzourio-Mazoyer *et al.*, 2002) was warped into participants' native PET space using the normalization parameters from above segmentation step. The transformed AAL regions of interest (ROI) were additionally binary masked by thresholded individual GM and CSF probability maps. A voxel was considered to belong to the GM fraction if a probability threshold of p=0.5 was exceeded, while additionally excluding voxels showing p>.5 for CSF. SUVR were calculated by averaging across voxels and time frames within each ROI in AAL. A global SUV ratio ($SUVR_{FBB}$) for measuring global Aβ load was derived followed procedures suggested by Barthel et al (2011a) . In brief, a volume-weighted average of bilateral frontal, lateral temporal, parietal, and occipital and cingulate SUV was calculated. Then, the SUV was scaled by tracer uptake in the cerebellar cortex as a reference region with low tracer binding to derive the SUVR score. The regional $SUVR_{FBB}$ for the bilateral precuneus was calculated by the same procedure.

2.7 MRI methods

The main neuroimaging approaches that were used for the presented studies are morphometry of the cholinergic basal forebrain system, seed-based FC and ReHo analysis

2.7.1 MRI data acquisition

MRI data were acquired at nine scanning sites using identical acquisition parameters and harmonized instructions. Every site operated Siemens scanner, including three TIM Trio systems, four Verio systems, one Skyra system, and one Prisma system. The standard DELCODE protocol included a structural T1-weighted image and a resting state fMRI. As harmonization of imaging methods across participating sites in a multi-center study is a very important issue, we tried to eliminate several sources of

variance between sites even before starting the project. For quality assurance and assessment of MRI datasets, several steps were taken (Jessen *et al.*, 2018). First, each DZNE site was qualified with a traveling head measurement by the DZNE imaging network (iNET). Second, the detailed SOPs for the implementation of project protocols were provided and instructed by DZNE iNET. Third, all technicians who were responsible for scanning MRIs in the project underwent centralized training according to the SOPs. The training included several aspects: 1) positioning subjects correctly in the MRI scanner; 2) preparing sequence steps of MRI scanning; 3) setting image angulation for the MRI scanning 4) Instructing participating for the MRI scanning; 5) testing the MRI sequences. Finally, to guarantee the MRI imaging quality during the whole project, an MRI-phantom was used to examine the performance of the MR systems in each site every week.

High-resolution T1-weighted images were acquired using a magnetization-prepared rapid gradient echo sequence (MPRAGE) which was empirically optimized for optimal gray-white contrast, and standardized across scanners (TR: 2500 ms, TE: 4.37 ms, flip angle: 7°, IT: 1100 ms, 256 × 256 matrix, FOV: 256 x 256 mm^2, slice thickness: 1 mm, 192 sagittal sections without gap covering the whole brain; GRAPPA = 2).

The resting state functional MRI (rs-fMRI) data were acquired axially using an echo-planar imaging (EPI) sequence with the following sequence parameters: TR = 2580 ms; TE = 30 ms, field of view = 224 × 224 mm^2, matrix = 64 × 64 mm, flip angle: 80°, slices number = 47, slice thickness = 3.5 mm. The total 180 volumes were acquired in approximately 8 min. During the examination, subjects were instructed to hold still, keep their eyes closed, not to fall asleep, and not to think of anything in particular.

2.7.2 Morphometry of the cholinergic basal forebrain system

Considering the small size of the BF nuclei and the limited spatial resolution and image contrast on the MRI scans, the different cell groups of the BF lack clear anatomical borders and are thus not accurately delineable. Recent studies have developed cytoarchitectonic maps of BF in human brain, based on combined post-mortem MRI and histological sections of post mortem brains, which provides new possibilities for in vivo automated morphometric analyses of the BF cholinergic system (Teipel *et al.*, 2005; Zaborszky *et al.*, 2008). The availability of a detailed cytoarchitectonic maps of the BF combined with the automatic structural MRI processing stream allows for in

vivo volumetry of the cholinergic BF. The structural MRI processing steps followed the procedures (**Figure 2.1**) suggested by Kilimann et al. (2014) and processed using the Computational Anatomy Toolbox (CAT12) toolbox based on SPM12. Specifically, MRI scans were first automatically segmented into gray matter (GM), white matter and CSF partitions. The principle of this BF volumetry approach is to normalize the individual native space MRI scan into the Montreal Neurological Institute (MNI) space where the BF atlas is defined, and use this transform to calculate individual BF volumes. Thus, the next step after segmentation is to normalize GM partitions to the CAT12 default template (IXI555-MNI152), applying modulation for both linear and non-linear normalization. Considering the relatively small spatial extent of the BF and its nuclei, the BF morphometry critically depends on the accuracy of the spatial normalization procedure, aiming for a perfect fit of the native space scan to the normalization template. Best normalisation can be achieved by using high-dimensional nonlinear spatial registration algorithms, such as Diffeomorphic Anatomical Registration through Exponentiated Lie Algebra (DARTEL) algorithm. Non-linear normalization in this thesis was performed using the SPM12 DARTEL algorithm (Ashburner, 2007). The modulation refers to scale by how much a voxel was stretched during normalization step. The purpose of the modulation during normalization is to make the voxel intensity in modulated GM-images represent the volume of grey matter within the given voxel (Good *et al.*, 2001). Finally, the volumes of BF and its subnuclei were obtained by summing up the values of modulated GM voxel within the cytoarchitectonic BF atlas. To adjust for head size differences between subjects, corrected BF volumes were calculated from the residuals of a least-square derived linear regression between raw volumes and total intracranial volume (TIV) (Voevodskaya *et al.*, 2014). The TIV was obtained by summing up the volumes of GM, white matter, and CSF compartments (Malone *et al.*, 2015).

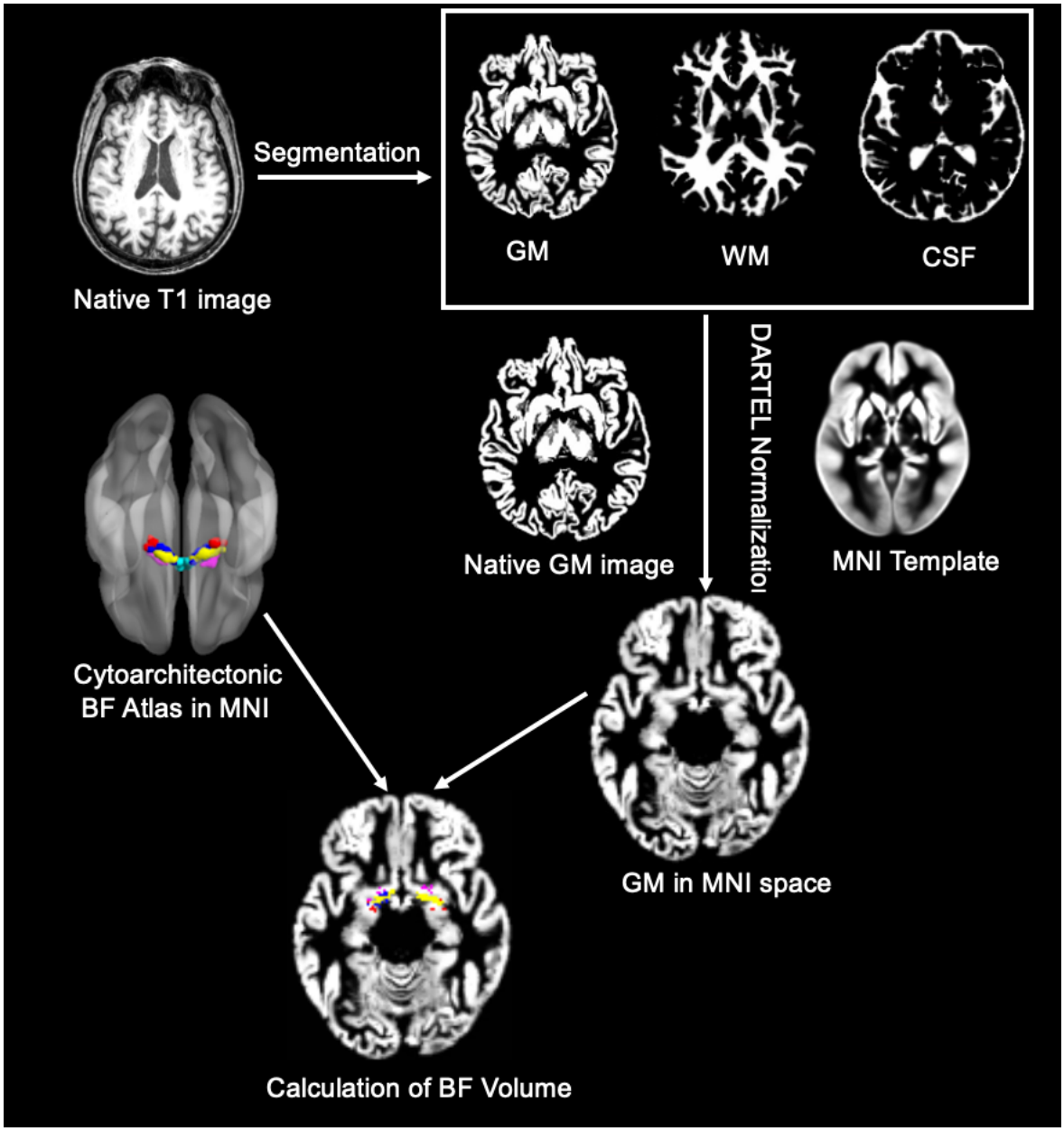

Figure 2.1: Standard processing steps for morphometry of basal forebrain. BF: Basal Forebrain; GM: Grey Matter; WM: White Matter; CSF: cerebrospinal fluid; MNI: Montreal Neurological Institute; FWE: Family-wise error

2.7.3 Seed-based functional connectivity and regional homogeneity

BOLD signal changes at rest are sensitive to artifacts and measures of FC and ReHo highly depend on BOLD signal data processing. Therefore, the preprocessing steps for resting-state fMRI data is very important.

Preprocessing steps for rs-fMRI data

The general preprocessing steps for study 2 and study 3 of this thesis were as follows. Before the preprocessing, the first 5 volumes were discarded to avoid transient signal

changes and keep signal stability of the remaining fMRI time series. The remaining 175 volumes were corrected for the intra-volume acquisition time delay (slice timing) and head motion (realign). Then, spatial normalization was conducted to the aligned functional data to a common stereotaxic space (MNI space). To improve the precision and accuracy of normalization, DARTEL algorithm was used. After normalization, temporal band-pass filtering (0.01–0.08 Hz) was adopted to reduce the effect of low-frequency drifts and high-frequency physiological noise. To reduce effects of confounding factors on BOLD signal in GM, the signal of WM and CSF as well as the 24-parameter head motion profiles (Friston *et al.*, 1996) were regressed out. Adopting 24 head-motion parameters is considered as an efficiency strategy to control for head motion effects since it regresses out 6 head motion parameters, 6 head motion parameters one time point before, and the 12 corresponding squared items (Yan *et al.*, 2013). Global signal regression was not performed considering that it is still a controversial preprocessing option in rs-fMRI studies (Murphy and Fox, 2017) and BF is proven to regulate the global signal (Turchi *et al.*, 2018). To further minimize head motion effects on FC analyses in study 2, 4 individuals in each group were excluded because of excessive head motion (> 2.0 mm or > 2.0° in any direction), resulting in a final sample of 194 individuals in HC and SCD group (Zhang *et al.*, 2016; Kang *et al.*, 2017b; Li *et al.*, 2017). After these strategies, we consider that head motion effects were mitigated as much as possible for study 2. Considering that the sample size in study 3 is relatively small, a motion scrubbing regressor method (Power *et al.*, 2012) was used for each bad time point (frame-wise displacement > 0.2 mm included as covariate) instead of excluding participants with excessive head motion. To ensure the data fulfill Gaussianity (Mikl *et al.*, 2008), increase signal-to-noise ratio (SNR), and decrease remaining inter-subject anatomical variability (Triantafyllou *et al.*, 2006; Pajula and Tohka, 2014), spatial smoothing step is conducted. Spatial smoothing is the averaging of signals from adjacent voxels. The standard method is to convolve the fMRI data with a 3D Gaussian kernel (filter) that averages signals from neighboring voxels with weights that decrease with increasing distance from the target voxel. The optimal Gaussian kernel size is disputed, depending on factors such as slice thickness and in-plane resolution and the need for spatial separation of small activation regions. According to previous studies, spatial smoothing was performed with a Gaussian kernel of 6 mm full-width at FWHM before FC calculation (Zou *et al.*, 2008) in study 3

(Philip *et al.*, 2013). The above preprocessing steps of the resting-state fMRI data for study 2 was performed using GRETNA (Wang *et al.*, 2015a) based on SPM12 (www.fil.ion.ucl.ac.uk/spm). The rs-fMRI data preprocessing steps for study 3 were conducted using the Data Processing & Analysis for Brain Imaging (DPABI) toolbox (Yan *et al.*, 2016). Both toolboxes were run in Matlab 2015a (MathWorks, Inc., Natick, MA).

Seed-based FC calculation

The seed regions selected in study 2 were *Ch4 and Ch1-3*, respectively**.** A recent study revealed that BF is functionally organized into two subdivisions that largely follow anatomically defined boundaries of Ch1-3 and Ch4 (Fritz *et al.*, 2019). To keep comp arable with previous studies and improve the reliability of our fMRI data analysis (Li *et al.*, 2017; Zaborszky *et al.*, 2018; Fritz *et al.*, 2019), we used the BF map from the ten human post mortem brains instead of from one human post mortem brains (Teipel *et al.*, 2005; Kilimann *et al.*, 2014). Therefore, the two seed brain regions in study 2, Ch4 and Ch1-3, were derived from a stereotaxic map of the BF that contains the magnocellular cholinergic corticopetal projection (Zaborszky *et al.*, 2008). The stereotaxic map of the BF is provided as follows: 1) Ten human post mortem brains underwent T1-weighted imaging and then made into histological serial sections; 2) the histological sections were stained by silver; 3) the positions and the extent of each magnocellular cell group of the BF was delineated microscopically, 3D reconstructed and warped to the reference space of the MNI brain (Zaborszky *et al.*, 2008). The seed region Ch1-3 was defined from the BF map including the septum (Ch1-2) and the horizontal limb of the diagonal band (Ch3). The seed region Ch4 was defined from the BF map. FC analysis of the two seed regions were conducted in voxel-wise manner. The two seed regions were defined and warped to MNI space, in correspondence with the normalized rs-fMRI data. For each seed region, voxel-wise FC map were calculated by correlating voxel-wise the mean time series across a certain BF subnucleous with all time-series across the brain. To assure the normality of FC correlation coefficient maps, the correlation coefficients were converted to z values using Fisher's transformation. The obtained z-maps were smoothed with a 5-mm full width at half maximum (FWHM) isotropic Gaussian kernel.

The seed region in study 3 was the bilateral precuneus. FC analysis of the bilateral precuneus was conducted in voxel-wise manner. The seed region was generated from

the AAL atlas, and restricted to GM voxels by multiplying the ROI with the individual GM mask, derived during the preprocessing steps. A voxel was considered to belong to the GM fraction if a threshold of 0.2 was exceeded. A voxel-wise FC map was calculated using the correlations between the mean time series of the seed region and remaining voxels within the brain. Again, the correlation coefficients were converted to z values using Fisher's transformation. Below is an example of voxel-based FC-map of precuneus showing correlated voxels based on a seed in the precuneus (**Figure 2.2**).

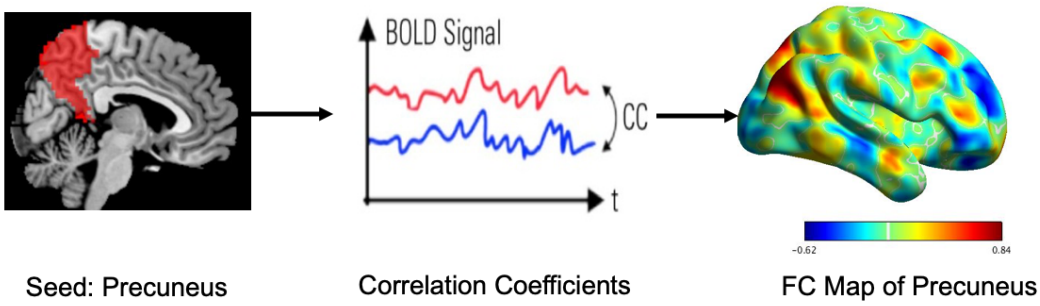

Figure 2.2: Illustration of precuneus-based Functional Connectivity (FC). Warms color in the FC map represents voxels with positive correlation with precuneus, while cold colors represent voxels with negative correlation with precuneus.

ReHo calculation

We used DPABI to obtain each subject's ReHo map by calculating Kendall's coefficient of concordance for a given voxel time series with its nearest 26 neighboring voxels in study 3. This analysis was based on the unsmoothed preprocessed rs-fMRI data (Zang *et al.*, 2004). Following the procedure by Zang and colleagues, the ReHo maps were z transformed and spatially smoothed with a 6 mm FWHM Gaussian kernel (Zang *et al.*, 2004).

3 Results

3.1 Study 1: Basal forebrain atrophy along the Alzheimer's disease spectrum and its relevance for subjective cognitive decline

3.1.1 Introduction

Recent imaging data suggest that individuals with preclinical Alzheimer's pathology already show atrophy of the posterior NBM and that this even precedes the atrophy of the entorhinal cortex (Schmitz *et al.*, 2016a). Even though direct amyloid biomarker evidence is often used to evaluate preclinical AD pathology status, there are also other complementary approaches for identifying at-risk patients for developing to AD dementia. One of these approaches is the clinical examination of individuals with SCD (Jessen *et al.*, 2014a; Studart and Nitrini, 2016). One aim of this study was to investigate the cholinergic BF system across the whole clinical AD spectrum, including SCD as a putative late stage of preclinical AD, and HC. The hypothesis is that the atrophy of the basal forebrain increases with progressing AD stage, starting in the NBM, and spreading until the whole system is affected in later AD stages. It is also hypothesized that BF atrophy is observed even before other well-established regions showing early AD-related neurodegeneration, such as the hippocampus and the entorhinal cortex. Moreover, the interplay between CSF amyloid status and structural changes especially in SCD and HC were further explored, which has not been covered in previous studies. While SCD itself is not an AD stage, SCD combined with AD pathology may reflect a progression from stage 1 (asymptomatic) to stage 2 (transitional cognitive impairment) of the Alzheimer's continuum according to the NIA-AA research framework (Jack *et al.*, 2018), and should therefore present a stronger progression of AD-related BF atrophy. With respect to the HC and SCD groups, it was hypothesized that the amyloid positive subgroups would show a reduced BF volume when compared to the amyloid negative subgroups in SCD, but not in HC. Moreover, BF volume is reduced when comparing amyloid positive SCD with amyloid positive HC. These effects were mainly expected in the posterior part of the BF.

3.1.2 Study-specific materials and methods

To test these hypotheses, we analyzed cross-sectional data of 135 HC, 110 SCD, 60 MCI and 36 DAD from an interim data release of the DELCODE baseline dataset who had undergone structural MR imaging, neuropsychological testing and APOE genotyping. Because the lumbar puncture to obtain the amyloid status was optional,

and not always successful, the amyloid-related analysis was performed only in a subgroup of the study population (**Figure 3.1**).

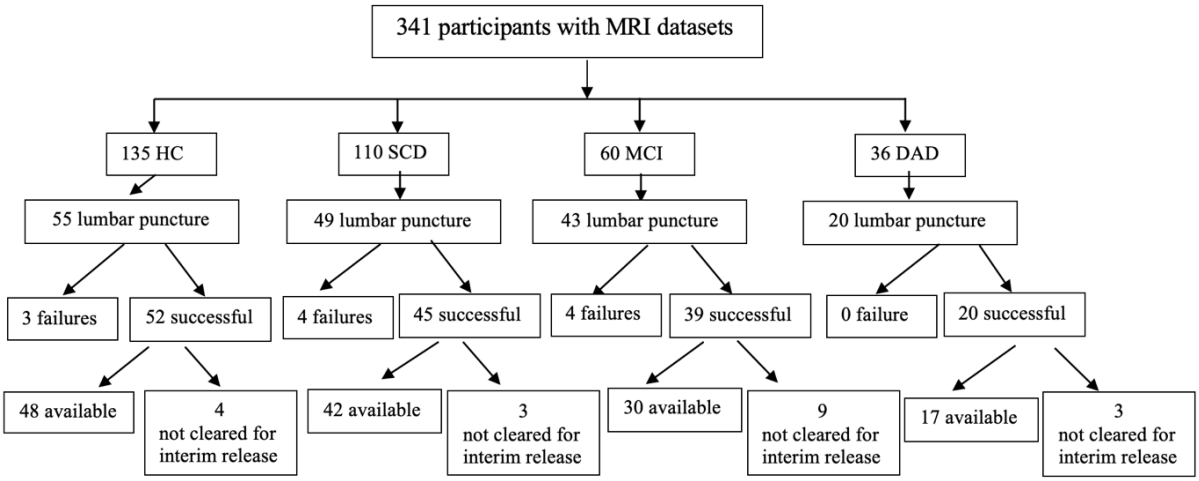

Figure 3.1: Flow chart of number of participants with lumbar puncture in HC, SCD, MCI and AD. HC, Healthy Control; SCD, Subjective Cognitive Decline; MCI, Mild Cognitive Decline; DAD, Dementia due to Alzheimer's Type.

MRI data processing and BF volume calculation

Refer to 2.7.3 in material and methods of the presented studies (page 38).

Confirmatory structural analysis

To test for the regional specificity of observed BF changes, the volumes of two additional structures in direct vicinity of the BF were analyzed: the bilateral caudate nucleus and subgenual cingulate cortex (Brodmann Area 25). The caudate ROIs were taken from the Harvard-Oxford atlas (Makris *et al.*, 2006), and the BA25 from an atlas that is part of the DPABI software package (Yan *et al.*, 2016). Following the same procedure as for the BF, the ROI volumes were obtained by summing up the modulated GM voxel values. All volumes were adjusted for TIV as described in section 2.7.2.

Analysis of 'typical' AD-regions

To explore potential concurrent alterations in established regions showing early AD-related neurodegeneration, additional analyses focused on the hippocampus (total volume, CA1-subfield) (Perrotin *et al.*, 2015; Hu *et al.*, 2019) and the entorhinal cortex (Schmitz *et al.*, 2016a). The ROIs were generated using the 'SPM Anatomy Toolbox'

(Eickhoff *et al.*, 2005) following the same procedure as for the BF and exploratory analysis.

Statistical analysis

All statistical tests were performed two-tailed. The statistical significance levels were set at $p < 0.05$ (Bonferroni-corrected), except for exploratory partial correlation analyses where an uncorrected threshold of $p<0.05$ was chosen. Missing data were treated using pairwise deletion. All statistical analyses were performed using SPSS Statistics v22.0 (IBM, Armonk, NY, USA).

Demographic, clinical and neuropsychological characteristics

Kruskal-Wallis non-parametric tests were used to test group differences in demographic and clinical data for continuous measures, and chi-square tests for dichotomous measures. Univariate analyses of covariance (ANCOVA) was used to test significant differences of the 5 five cognitive factors among the four groups, controlling for age, gender, education in years and APOE status. Pair-wise post hoc t-tests were performed to evaluate cognitive differences between subgroups.

Effects of diagnosis on basal forebrain volumes and relationships with NPT

ANCOVA was used to test for significant differences with respect to the total BF volume and the subnuclei volumes among the four groups, controlling for potential covariates including age, gender, and years of education, APOE4 effects and MRI scanners (dummy-coded). Pair-wise post hoc tests were performed to evaluate volume differences between subgroups.

Controlling for the above covariates, partial correlations were used to explore group-wise relationships between BF total and subnuclei volumes, respectively, and the 5 cognitive factor scores.

Effects of amyloid status on the BF volume in SCD and HC

An ANCOVA was used to investigate the main effect of amyloid-β status factor (Aβ+/Aβ-), diagnostic group factor (HC, SCD) and their interaction on the BF volumes, controlling for covariates described above. Pair-wise follow-up comparisons were evaluated for the four contrasts of interest: SCD+ vs SCD-, HC+ vs HC−, HC+ vs SCD+ and HC− vs SCD-. The within-subgroup relationships between the regional BF volumes, continuous Aß42/40 ratio, and the 5 cognitive factors, respectively, were investigated by partial correlations analysis, controlling for covariates as above.

Confirmatory structural analysis: Effects of amyloid status in SCD and HC on additional regions

ANCOVA, controlling for potential covariates (see above), was used to test the main and interaction effects of amyloid status (Aβ+/Aβ-) and diagnostic group (HC/SCD) on the caudate/BA25, hippocampus (total volume, CA1-subfield) and entorhinal cortex volumes. Follow-up pairwise comparisons included: SCD^{+} vs SCD^{-}, HC^{+} vs HC^{-}, HC^{+} vs SCD^{+} and HC^{-} vs SCD^{-}.

Exploratory analysis: Effects of amyloid status in MCI and HC on BF volume

The main and interaction effects of amyloid status (Aβ+/Aβ-) and diagnostic group (HC/MCI) on the BF volumes was also assessed the using an ANCOVA (covariates as above) to explore the role of amyloid status in the clinical samples. Follow-up pairwise comparisons included: MCI^{+} vs MCI^{-}, HC^{+} vs HC^{-}, HC^{+} vs MCI^{+} and HC^{-} vs MCI^{-}. As expected, the DAD group - except one participant - was amyloid-positive, and therefore a further analysis for the DAD group was not conducted.

3.1.3 Results

Demographic, clinical and neuropsychological test characteristics

Table 3.1 summarizes the demographic characteristics as well as the NPT results for all groups. The four groups showed significantly differences in age, gender, education, and APOE4 genotype. In addition, clinical measures, including MMSE, CDR-global, CDR-SOB, and the five cognitive factors differed significantly among the four groups. Age in HC group was significantly lower than in DAD and MCI groups. Years of education in DAD were significantly lower than in HC. The proportions of male participants in MCI was significantly higher than in HC. APOE4 carriers were significantly less frequent in HC than in MCI and DAD. HC were slightly younger and included significantly fewer APOE4 carriers compared to SCD. MCI and DAD showed significant lower scores on the MMSE and on all five cognitive factors, which corresponds to the inclusion criteria. The scores of CDR-SOB and the CDR-global in HC was significantly lower than in SCD (**Table 3.1**).

Table 3.1: Demographic and neuropsychological sample characteristics

	HC	SCD	MCI	DAD	P value	Post-hoc comparisons
Age [years]	68.7 ± 5.2	71.3 ± 5.7	73.1 ± 5.0	73.3 ± 7.0	< 0.001[a]	HC < AD*** HC < MCI*** HC < SCD**
Gender (M/F)	55/80	53/57	38/22	16/20	0.03[b]	HC < MCI*
Education [years]	14.9 ± 2.8	14.6 ± 3.2	14.1 ± 3.2[A]	13.1 ± 3.2	0.009 [a]	AD < HC*
MMSE	29.4 ± 0.9[A]	29.2 ± 1.0	28.1 ± 1.6	23.6 ± 3.4	< 0.001[a]	AD < MCI*** AD < SCD*** AD < HC*** MCI< SCD*** MCI< HC***
CDR-SOB	0.0 ± 0.1	0.3 ± 0.4	1.5 ± 1.2	4.8 ± 1.4	< 0.001[a]	AD > MCI* AD > SCD*** AD > HC*** MCI > HC*** MCI > SCD*** SCD > HC***
CDR-global	0.0 ± 0.0	0.2 ± 0.3	0.5 ± 0.1	0.9 ± 0.2	< 0.001[a]	AD > SCD*** AD > HC*** MCI > HC*** MCI > SCD*** SCD > HC***
MEM [min/max]	0.6 ± 0.1 [-0.8/1.3]	0.4 ± 0.1[A] [-1.3/1.3]	-0.6 ± 0.1 [-1.9/0.7]	-2.1 ± 0.1 [-3.0/-1.4]	< 0.001[c]	AD < MCI*** AD < SCD*** AD < HC*** MCI< SCD*** MCI< HC***
LANG [min/max]	0.5 ± 0.5 [-0.6/1.9]	0.3 ± 0.6[A] [-1.6/1.6]	-0.6 ± 0.7 [-2.2/0.8]	-1.9 ± 0.7 [-3.6/-0.8]	<0.001[c]	AD < MCI*** AD < SCD*** AD < HC*** MCI< SCD*** MCI< HC***
EXEC [min/max]	0.5 ± 0.5 [-0.9/1.8]	0.3 ± 0.7[A] [-1.6/1.7]	-0.5 ± 0.8 [-2.6/0.8]	-1.9 ± 0.9 [-3.8/-0.3]	<0.001[c]	AD < MCI*** AD < SCD*** AD < HC*** MCI < SCD*** MCI < HC***
WME [min/max]	0.3 ± 0.6 [-0.9/1.9]	0.3 ± 0.7[A] [-1.4/-1.7]	-0.4 ± 0.8 [-2.0/1.1]	-1.5 ± 0.9 [-3.5/0.3]	<0.001[c]	AD < MCI*** AD < SCD*** AD < HC*** MCI < SCD*** MCI < HC***
VIS [min/max]	0.3 ± 0.4 [-1.3/1.1]	0.2 ± 0.5[A] [-1.4/1.1]	-0.3 ± 0.8 [-3.0/0.7]	-1.5 ± 1.5 [-6.7/0.2]	<0.001[c]	AD < MCI*** AD < SCD*** AD < HC*** MCI < SCD*** MCI < HC***
APOE(*ε4/non-4*)	23/109[C] (17.4%)	36/72[B] (33.3%)	21/39 (35.0%)	25/10[1] (71.4%)	<0.001 [b]	HC < SCD* HC < AD*** HC < MCI* HC< SCD* SCD < AD*** MCI < AD**

Values are represented with mean ± standard deviation. Supscripts with capital letters denote number of missing values: A = 1 missing value; B = 2 missing values; C = 3 missing Values. min = minimum; max = maximum; [a] Kruskal-Wallis Non-Parameter Test; [b] Chi-Square Test. [c] ANCOVA Test controlling for age, gender, years in education and APOE4 status. Post hoc Bonferroni-corrected p-value: * p-value < 0.05, ** Bonferroni-corrected p-value < 0.01, *** p-value <0.001.

Effects of diagnosis on basal forebrain volumes and relationships with NPT

The comparison of volumes of the BF and its subnuclei across 4 groups showed significant differences (**Figure 3.2**). Compared to subjects with MCI and SCD as well as HC, all volumes of BF subnucleus in the DAD patients were significantly lower. In the MCI group, the total BF and Ch4p as well as Ch4al regions showed a significant volume reduction compared to SCD and HC. There were no significant differences for total BF volume and any of the subnuclei between SCD and HC. In addition, all subregions of BF in AD showed negative percentage change compared to HC, with the most severe change (-32.01 %) in Ch4p (**Table 3.2**). The most severe change in MCI (-14.88 %) and SCD (-4.55 %) is also Ch4p compared to HC (**Table 3.2**).

Significant correlations between total BF volume and MEM (r=0.433, p=0.002) and LANG (r=0.383, p=0.007) in the MCI group was found in the partial correlation analyses, but not in the DAD group. The same findings emerged with regard to Ch4p and Ch4al. Specifically, significant correlations for Ch4p and Ch4al volumes with MEM (Ch4p, r = 0.443, p = 0.001; Ch4al, r = 0.354, p = 0.013) as well as LANG (Ch4p, r = 0.428, p = 0.002; Ch4al, r = 0.345, p = 0.015) were found only for the MCI group. For SCD, a correlation between Ch4ai and visuo-spatial cognition was observed, but only at a trend level (r = 0.19; p = 0.063).

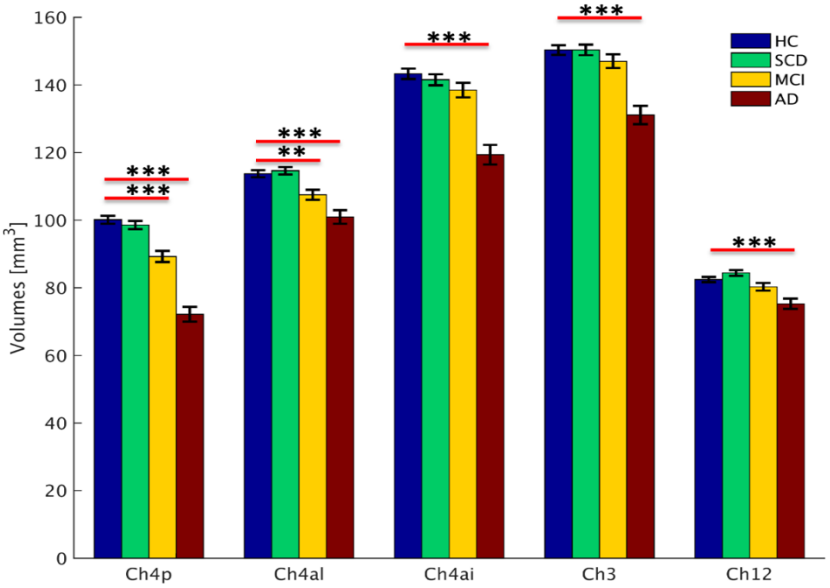

Figure 3.2: Basal forebrain volumes and its subregions across HC, SCD, MCI and DAD. The Volumes of the bar are estimated marginal means ± standard error; *** Bonferroni-corrected p-value < 0.001; ** Bonferroni-corrected p-value < 0.01.

Table 3.2: Percentage changes of basal forebrain volumes and its subregions across in SCD, MCI and AD compared to HC

	HC	SCD [Percentage Change]	MCI [Percentage Change]	AD [Percentage Change]
BF (mm^3)	605.35	590.95 [-2.38%]	558.52 [-7.74%]	496.91 [-17.91%]
Ch1/2 (mm^3)	83.49	83.78 [0.35%]	79.56 [-4.71 %]	73.81 [-11.59%]
Ch3 (mm^3)	152.45	149.08 [-2.21%]	144.11 [-5.47 %]	129.55 [-15.02%]
Ch4ai (mm^3)	146.00	139.91 [-4.17%]	135.55 [-7.16%]	118.08 [-19.12%]
Ch4al (mm^3)	114.83	114.02 [-0.71%]	106.12 [-7.59%]	100.36 [-12.60%]
Ch4p (mm^3)	102.29	97.69 [-4.50%]	87.07 [14.88%]	69.55 [-32.01%]

Values are represented with mean volumes of each BF subregions. Percentage Change = (V2-V1)/V1*100. V1 represents the volumes of BF and its subregions in HC. V2 represents the volumes of BF and its subregions in SCD, MCI and AD.

Effects of amyloid status in SCD and HC on BF volume

Only HC and SCD participants with both structural scans and CSF biomarker were used for this analysis. 38% (16 of 42) participants of SCD and 27% (13 of 48) participants of HC were categorized as Aβ+ (Aβ42/40 < 0.09). As shown in **Figure 3.3,** ANCOVA revealed a main effect of CSF amyloid status (Aβ+/Aβ-: $F_{1,74} = 4.676$, $p = 0.034$) on Ch4p volume and significant interaction effects between amyloid status and SCD status ($F_{1,74} = 4.186$, $p = 0.044$). The Ch4p volume was significantly smaller in amyloid-positive SCD participants in comparison with amyloid-negative SCD ($Ch4p_{SCD^+} = 92.18 \pm 3.04$ mm^3, $Ch4p_{SCD^-} = 103.17 \pm 2.21$ mm^3; $F_{1,74} = 7.964$, $p = 0.006$, partial $\eta^2 = 0.097$). Importantly, the Ch4p volume in the SCD+ group was even significantly smaller than in the amyloid-positive control group ($Ch4p_{,HC^+} = 101.48 \pm 2.95 mm^3$, $F_{1,74} = 4.791$, $p=0.032$, partial $\eta^2 = 0.06$), while no significant difference between amyloid-positive and amyloid-negative HC ($Ch4p_{,HC^-} = 102.25 \pm 1.86$ mm^3; $F_{1,74} = 0.049$, $p = 0.83$, Partial $\eta^2 = 0.001$). No significant main or interaction effects of amyloid status for either total BF volume or the volumes of the other subnuclei of BF were found.

A significant correlation between the Aβ42/40 ratio and the Ch4p volume was shown in the SCD subsample with CSF measures, but not in the HC ($r_{SCD} = 0.365$, $p = 0.044$; $r_{HC} = -0.041$, $p = 0.805$; **Figure 3.4**). There is no significant partial correlation between Ch4p and any of the 5 cognitive factors in SCD subsample (all $p > 0.371$).

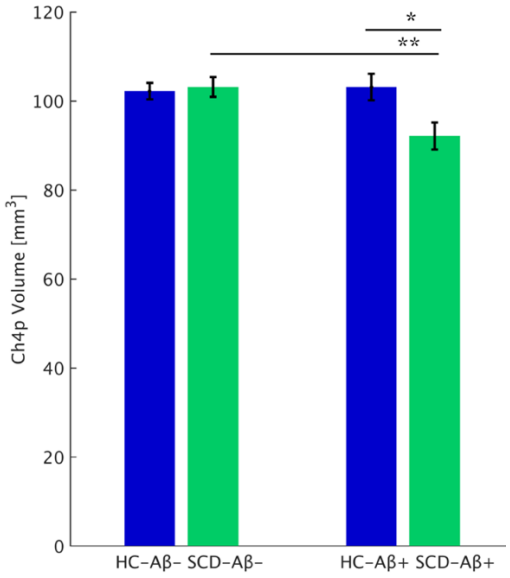

Figure 3.3: Interaction effect of amyloid status factor (Aβ+/Aβ-) and group factor (HC, SCD) on Ch4p volume.

Displayed are the estimated marginal means of the Ch4p volume;
* p-value = 0.032; ** p-value = 0.006
HC-Aβ-: amyloid negative HC;
SCD-Aβ-: amyloid negative SCD;
HC-Aβ+: amyloid positive HC;
SCD-Aβ+: amyloid positive SCD.

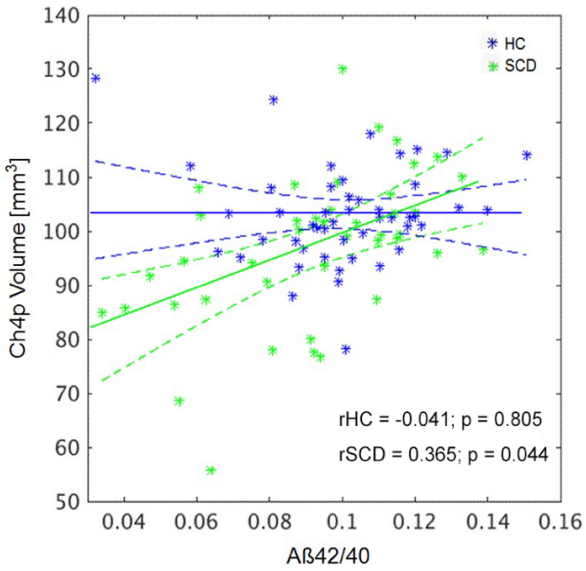

Figure 3.4: Partial correlations between Ch4p volume and Aβ42/40 ratio in HC and SCD group.

The dotted area is the 95% confidential interval. Ch4p volume shown here is after correcting for TIV.

Confirmatory structural analysis: Effects of amyloid status in SCD and HC on additional regions

Explorative ROI analyses did not reveal any of significant main effects of SCD status or amyloid status. Moreover, no significant interaction effects between CSF amyloid status and SCD status were found (**Table 3.3**).

Table 3.3: Interaction effect of amyloid status factor (Aβ+/Aβ-) and group factor (HC, SCD) on the exploratory structural brain regions.

	HC- [mm^3]	HC+ [mm^3]	SCD- [mm^3]	SCD+ [mm^3]	Interaction Effect	Post-hoc comparison
Entorhinal Cortex	2888 ± 54	2806 ± 85	2851 ± 64	2685 ± 88	F (1,74) = 0.43; p = 0.52	ns
CA1-HIP	1623 ± 25	1577 ± 40	1593 ± 30	1547 ± 42	F (1,74) < 0.001; p = 0.995	ns
HIP	6450 ± 89	6407 ± 141	6398 ± 106	6291 ± 146	F (1,74) = 0.069; p = 0.79	ns
Caudate	2871 ± 78	2808 ± 123	2821 ± 92	2898 ± 127	F (1,74) = 0.45; p = 0.50	ns
BA25	5367 ± 65	5388 ± 103	5373 ± 78	5262 ± 107	F (1,74) = 0.56; p = 0.46	ns

Values are estimated marginal values after removing age, gender, years of education, APOE4 and MRI scanners. Displayed are mean ± standard error. ns: not significance; HIP: Hippocampus; BA: Brodmann area; HC-: amyloid negative HC; SCD-: amyloid negative SCD; HC+: amyloid positive HC; SCD+: amyloid positive SCD.

Exploratory analysis: Effects of amyloid status in MCI and HC on BF volume

60% (18 of 30) of the MCI were categorized Aβ+ (Aβ42/40 < 0.09). A significant main effect of MCI status on Ch4p and Ch4al subregions was found (Ch4p: $F_{1,64}$ = 10.61, p = 0.002; Ch4al: $F_{1,64}$ = 4.15, p = 0.046) **(Table 3.4**). There was no significant main effect of amyloid status observed for the total BF volume or the volumes of the other subnuclei. No significant interaction effects of amyloid status and MCI status were found for either total BF volume or the volumes of the other subnuclei (**Table 3.4**). Partial correlation analyses showed no significant correlations between the Aβ42/40 ratio and the Ch4p volume (r = - 0.15; p = 0.53) or between the Aβ42/40 ratio and the Ch4al volume (r = - 0.36; p = 0.11) in the MCI subsample with CSF measures. We only found a significant trend positive correlation between the Ch4p with MEM (r = 0.38; p = 0.09), whereas the correlation was not significant in other four cognitive factors (all p > 0.36). There is no significant partial correlation between Ch4al and any of the 5 cognitive factors in MCI subsample (all p > 0.49)

Table 3.4: Interaction effect of amyloid status factor (Aβ+/Aβ-) and group factor (HC, MCI) on BF regions

	HC- [mm^3]	HC+ [mm^3]	MCI- [mm^3]	MCI+ [mm^3]	Main Effect (Group)	Interaction Effect
BF	606 ± 9	600 ± 14	570 ± 16	583 ± 13	F (1,64) = 3.16; p = 0.08	F (1,64) = 0.48; p = 0.49
Ch1/2	85 ± 2	84 ± 2	83 ± 3	83 ± 2	F (1,64) = 0.40; p = 0.53	F (1,64) = 0.11; p = 0.74
Ch3	151 ± 3	151 ± 5	145 ± 5	152 ± 4	F (1,64) = 0.34; p = 0.57	F (1,64) = 0.81; p = 0.37
Ch4ai	144 ± 3	143 ± 5	142 ± 5	139 ± 4	F (1,64) = 0.45; p = 0.51	F (1,64) = 0.06; p = 0.81
Ch4al	116 ± 2	113 ± 4	104 ± 4	110 ± 3	F (1,64) = 4.15; **p = 0.046**	F (1,64) = 1.97; p = 0.17
Ch4p	102 ± 2	102 ± 2	90 ± 3	92 ± 3	F (1,64) = 10.61; **p = 0.002**	F (1,64) = 0.21; p = 0.65

Values are estimated marginal values after removing age, gender, years of education, APOE4 and MRI scanners. Displayed are with estimated marginal mean ± standard error. HIP: Hippocampus; BA: Brodmann area; HC-: amyloid negative HC; MCI-: amyloid negative MCI; HC+: amyloid positive HC; MCI+: amyloid positive MCI.

3.1.4 Discussion

This study compared BF volumes of HC, SCD, MCI and DAD patients based on a large multi-center dataset. A significant effect of diagnosis on BF total and subnuclei volumes was found, with the most pronounced effect in Ch4p. In patients with DAD, almost all BF subnuclei presented volume reductions, whereas in MCI patients, the volume reduction was confined to Ch4al and Ch4p. Moreover, a significant correlation between Ch4p volume and cognitive performance measures (MEM and LANG) was found in the MCI group. In the MCI subsample with CSF information, also a significant main effect of diagnosis on both the Ch4p and Ch4al was observed, but no significant interaction effects with amyloid status, neither for total BF volume nor the volumes of the other subnuclei. For the SCD group, a volume reduction was observed only after taking the amyloid status into account, as indicated by a significant interaction between diagnosis (SCD vs. HC) and CSF amyloid status: The Ch4p volume was reduced in amyloid-positive SCD compared to amyloid-positive HC and amyloid-negative SCD.

The Ch4p volume was also correlated with the Aβ42/40 ratio in the SCD subgroup, but not in HC subgroup.

The findings reported here are in good agreement with the literature. The BF volume reduction in DAD patients is consistent with *post mortem* studies and *in vivo* MRI morphometric studies (Whitehouse *et al.*, 1982; Vogels *et al.*, 1990; Grothe *et al.*, 2012; Kilimann *et al.*, 2014; Machado *et al.*, 2020). In addition, BF volume loss was most pronounced in the Ch4p subregion in DAD which is consistent with histopathological findings from DAD patients showing neuronal loss is most severe in Ch4p (Mesulam, 2004a). Previous histological studies in DAD patients suggest that the BF neuronal loss is most pronounced in the posterior NBM and less severe in the rostral parts of BF (Arendt *et al.*, 1985; Vogels *et al.*, 1990; Liu *et al.*, 2015). Several in vivo MRI studies in DAD also confirmed previous histological findings and found the strongest volume reduction located in the Ch4p region (Teipel *et al.*, 2005; Teipel *et al.*, 2011; Kilimann *et al.*, 2014). Confirming earlier *in vivo* MRI studies in MCI patients (Grothe *et al.*, 2010), volume reductions of Ch4p and Ch4al were also found in the MCI group, which may indicate that the atrophy of cholinergic BF subregions occurred sequentially during earlier stages of AD progression. The findings in AD and MCI, combined with previous results, showed the strongest and earliest effects located in the Ch4p region. The possible reason is that Ch4p mainly provides cholinergic innervation to the superior temporal gyrus and temporal pole, key targets of the cholinergic projections from Ch4p (Mesulam *et al.*, 1983; Mesulam and Geula, 1988), which correlates well with memory loss and language impairment (Liu *et al.*, 2015). This explanation is further supported by the significant positive correlations between the Ch4p volume and MEM as well as LANG for the MCI group. The associations between volume loss of Ch4p and decline in memory and language performance in MCI group is partially consistent with a previous study that found significant correlations between total BF volume with memory and executive test scores, respectively (Grothe *et al.*, 2016). However, interpolation should be cautious due to the uncorrected significance threshold. Moreover, there was no significant correlation between the BF volumes and any of the 5 cognitive factors in DAD patients. The lack of complementary correlations in DAD patients is not consistent with a recent study investigating DAD patients under cholinesterase inhibitor treatment, which found significant correlations between total BF volume and global cognition, as well as memory and executive functions (Teipel *et*

al., 2018a). A possible reason for this inconsistency is that current sample of AD patients (n = 34) was much smaller than that in Teipel's study(n = 124), limiting the statistical power of the present analyses.

Consistent with the idea that BF atrophy may already begin during the preclinical stage of AD, the present findings extend this BF atrophy pattern to SCD individuals with amyloid pathology. It was found that Ch4p was the only subregion showing volume reduction in SCD amyloid positive, which may suggest Ch4p appears to be most vulnerable to amyloid pathology. Two recent longitudinal studies in a large cohort of age-matched older adults ranging from cognitively normal to AD (Schmitz *et al.*, 2016a; Fernandez-Cabello *et al.*, 2020) found that NBM atrophy precedes and predicts greater neurodegeneration in entorhinal and perirhinal cortices, whereas entorhinal volumes predicted degeneration in the medial temporal cortex. These two studies suggest that BF atrophy is an upstream event of entorhinal and neocortical degeneration and a very early BF involvement in AD pathogenesis. The present findings further supported this view by showing that Ch4p volume reductions are present in amyloid-positive SCD, while no atrophic changes were detectable in the entorhinal (and also hippocampal) areas. It seems that no significant atrophic changes in hippocampal and entorhinal cortex were not consistent with the findings from several previous studies (van der Flier *et al.*, 2004; Jessen *et al.*, 2006; Scheef *et al.*, 2012; Perrotin *et al.*, 2015; Hu *et al.*, 2019; Scheef *et al.*, 2019). One possible explanation is that SCD in majority of previous studies corresponded to subjective decline in the memory function, which is SCD plus feature currently (Jessen *et al.*, 2014a). The other possible reason is that analytical method in our study is different (i.e. ROI vs voxel-wise analysis) with the study of Hu, Teunissen et al., (2019). More importantly, Ch4p volume reductions were only present in amyloid-positive SCD, while no atrophic changes were detectable in amyloid-positive HC or amyloid-negative SCD. Therefore, these results suggest that the simultaneous presence of SCD *plus* CSF amyloid pathology was linked with NBM atrophy. In contrast, SCD or CSF amyloid pathology alone were not associated with NBM atrophy. This interpretation is supported by Vogel *et al.* (2017) who assessed whether SCD and brain Aβ contribute unique information to cognitive decline and suggested that brain Aβ and SCD contribute to the prediction of cognitive decline in a complementary manner. This is also consistent with a previous study showing increased hippocampal atrophy and

lower cognitive performance in SCD with APOE4 genotype (Striepens *et al.*, 2011), even though APOE4 is a risk factor rather than a direct biomarker for amyloid pathology. Taken together with findings that Ch4p volume loss precedes entorhinal atrophy and mediates longitudinal memory loss (Schmitz *et al.*, 2016a), the findings may suggest that amyloid-positive SCD represent a very early clinical manifestation of an AD-related cholinergic BF atrophy. In this stage, amyloid positive SCD individuals cannot fully compensate downstream neurotoxic effects of amyloid aggregates anymore, therefore showing first symptoms of incipient cognitive decline.

Regarding linear associations between BF volume and amyloid pathology, a significant positive correlation between the Ch4p volume and Aβ42/40 ratio was found in the SCD subsample. Both animal models (Beach, 2008; Bohnen *et al.*, 2018) and post mortem studies in humans (Arendt *et al.*, 1985; Potter *et al.*, 2011) found correlations between cortical amyloid accumulation and cholinergic system. A recent study determined associations between BF volume from ante mortem MRI brain scans and post mortem assessment of neuropathological features and found that BF atrophy was associated with Thal amyloid phases instead of amyloid plaques or neurofibrillary tangles within itself (Teipel *et al.*, 2020). This finding suggests that the mechanism of BF atrophy was associated with cortical amyloid load, but not with amyloid plaque load in the BF itself (Teipel *et al.*, 2020). Therefore, the strong association between Ch4p atrophy and Aβ42/40 ratio in individuals with SCD in our study may reflect downstream neurotoxic effects of cortical amyloid aggregates (Bloom, 2014) and vulnerability of Ch4p cholinergic cells to amyloid-related neurodegeneration, which may trigger incipient functional impairments in innervated brain regions (Scheef *et al.*, 2019). This is compatible with previous findings showing that Ch4p volume reductions in SCD correlated with reduced glucose metabolism in the precuneus (Scheef *et al.*, 2019). Reduced precuneus glucose metabolism has previously been suggested to constitute a highly sensitive biomarker for AD (Minoshima *et al.*, 1997; Minoshima *et al.*, 1999), and in MCI, it is associated with a conversion rate toward DAD of more than 90% within two years (Chetelat *et al.*, 2003; Drzezga *et al.*, 2003). The other possible direction for this correlation between Ch4p volume and amyloid pathology is that BF degeneration may contribute to increased accumulation of amyloid pathology due to altered amyloid processing and clearance mechanisms subserved by cholinergic signalling (Kar *et al.*, 2004; Kolisnyk *et al.*, 2016; Kolisnyk *et al.*, 2017). Future

longitudinal in vivo studies investigating the respective biomarkers may help to understand the directionality of the interactions between cholinergic BF atrophy and amyloid pathology in the human brain. Regarding the correlation analysis between Ch4p volume and 5 cognitive factors in SCD subsample, we found no significant correlations. The non-significant correlations between Ch4p volumes and cognitive domain scores in HC and SCD groups is consistent with an earlier study in healthy elderly that observed no correlations with specific neuropsychological tests, except for a positive association with a global intelligence score (Wolf *et al.*, 2014; Grothe *et al.*, 2016).

The present findings are consistent with the formulated hypothesis that BF atrophy already starts in amyloid-positive SCD instead of in amyloid positive HC. Notably, the fact that amyloid-positive HC subjects did not show Ch4p atrophy compared to the amyloid-negative HC subjects is consistent with a recent study (Cantero *et al.*, 2020). Therefore, BF atrophy pattern preferentially starts in Ch4p and subsequently spreads across the whole brain with AD progression. Non-significant Ch4p atrophy in amyloid-positive HC individuals suggests that they represent an earlier AD disease stage (NIA-AA stage 1) and BF atrophy emerges only in a late preclinical stage (as represented by amyloid-positive SCD) where individuals already have the subjective experience of subtle cognitive decline (NIA-AA stage 2).

To have a systematic understanding the amyloid status effect on BF volume across the AD spectrum, its effect was also explored in the later stage of AD, i.e. MCI patients. Interestingly, we only observed reduced volumes of Ch4p and Ch4al in MCI compared to HC. There is no significant interaction between CSF amyloid status and MCI diagnosis, neither for the volume of Ch4p, nor for the other BF subnuclei. Although it seems surprising at first view,, a missing association between amyloid load and BF volumes in MCI was also reported by other groups (Kilimann *et al.*, 2017). Taken together the significant interaction findings of amyloid status and SCD diagnosis on Ch4p volume, non-significant interaction findings in MCI may suggest that the amyloid deposition is the driving force for the BF atrophy at the earlier SCD stadium, whereas at MCI stage, the atrophy is more likely driven by other factors than amyloid. However, future studies that include tau and other biomarkers would be needed to further prove our hypothesis.

3.2 Study 2: Distinct alterations of functional connectivity in the basal forebrain subregions in Subjective Cognitive Decline

3.2.1 Introduction

The BF is the primary source of cholinergic inputs to the entire cortex and is considered as a major neuromodulatory hub for brain regions supporting cognition due to its broad projections (Ballinger *et al.*, 2016; Bell and Shine, 2016; Gritton *et al.*, 2016; Markello *et al.*, 2018). Distinct projections of BF subregions have been revealed in nonhuman rodents and primates with Ch12 to the hippocampus (Swanson and Cowan, 1979; Hedreen *et al.*, 1984), Ch3 to the olfactory bulb and Ch4 to the cortex and amygdala (Mesulam *et al.*, 1983; Bloem *et al.*, 2014). While a plethora of publications on BF have demonstrated divisions in the neuromodulatory projections of BF using direct axonal tracing technique in rodents and primates available (Kim *et al.*, 2015; Golden *et al.*, 2016; Kim *et al.*, 2016; Kondo and Zaborszky, 2016; Li *et al.*, 2018), only very limited human data investigated how the BF may functionally differentiate given that direct axonal tracing studies are not feasible in humans. One method to study the interplay between the BF, cortical and subcortical structures in human data are FC analyses. Over the last years, FC analysis of rs-fMRI data has emerged as a powerful in vivo method to investigate interconnected neuronal systems and subcortical–cortical interactions in the human brain (Roy *et al.*, 2009; Englot *et al.*, 2017). This method has previously been used to characterize the FC profile of the NBM using a seed region derived from a cytoarchitectonically-defined stereotactic atlas of BF nuclei (Li *et al.*, 2017; Zaborszky *et al.*, 2018). More recently, FC differences between BF subdivisions were explored using rs-fMRI data from young adults (Markello *et al.*, 2018) and in an older population (Fritz *et al.*, 2019). The study in the older population found that BF is functionally organized into two subdivisions that largely follow anatomically defined boundaries of Ch1-3 and Ch4 (Fritz *et al.*, 2019). Moreover, decreased FC of Ch4 has been found in MCI compared to the healthy control group (Li *et al.*, 2017; Meng *et al.*, 2018), while increased FC of the NBM was found in patients with AD after treatment with a cholinesterase inhibitor. However, the question whether altered FC of the BF emerges already in SCD patients remains unclear.

This study investigated if any indicators for functional abnormalities of the BF can be found in SCD and examined the relationship between observed alterations and neuropsychological measures. Available CSF biomarker information for a substantial

subgroup of this sample allowed to explore the interplay between CSF amyloid status and BF FC in SCD and HC. The first hypothesis was that reductions of Ch4 FC and Ch1-3 FC can already be observed in SCD patients, as compared to HC. The second hypothesis was that Ch4 and Ch1-3 showed a distinct patterns of FC alterations in SCD when compared to HC.

3.2.2 Study specific materials and methods

Participants included in this study

Cross-sectional data of 194 individuals with SCD and 194 HC who had undergone structural MR imaging, neuropsychological testing, and APOE genotyping, were analyzed. Seventy-three individuals out of the 194 HC and 84 individuals out of 194 SCD also had information about CSF amyloid status available.

Preprocessing of resting-state fMRI data and seed-based FC

Refer to MRI Methods in 2.7.3 (page 40).

Neuropsychological tests

Refer to Materials and Methods in 2.3 (page 35).

Calculation of total intracranial volume, grey matter and Ch4/Ch1-3 volume

Previous studies suggested that FC results could potentially be influenced by structural grey matter differences among groups (Oakes *et al.*, 2007; Wang *et al.*, 2011). To check this possibility, it was explored whether there were total intracranial volume (TIV), grey matter (GM) and Ch4/Ch1-3 volume differences between HC and SCD groups. For the processing steps and volume calculations refer to 2.7.2 in general material and methods of the presented studies

Statistical analyses

Statistical analyses were performed with SPM12 (Wellcome Department of Cognitive Neurology, London) and SPSS 22.0 (IBM Corp.: Armonk, NY).

Demographic, clinical and neuropsychological characteristics

Group differences were assessed using independent two-sample t-test, Mann-Whitney U-test, or chi-squared test ($p<0.05$) for demographic and clinical characteristics of the sample. Univariate analyses of covariance (ANCOVA) were used to test significant differences of the NPT tests between the two groups, controlling for age, gender, education in years and APOE4 genotype.

Total intracranial volume, grey matter and Ch4/Ch1-3 volume

Group differences were assessed using independent two sample t-tests ($p<0.05$) for total intracranial volume, grey matter and Ch4/Ch1-3 volume, controlling for age, gender, education in years, dummy variables for the MRI scanners and APOE4 genotype.

Significant group differences on seed-based FC and relationships with NPT

To check potential confounding influences on Ch4-based FC and Ch1-3-based FC, additional covariates, including age, gender, years of education, APOE4 genotype, and MRI scanner (dummy coded) were entered into the regression model in SPM12. Covariates were considered to have significant influences on seed-based FC at $p< 0.1$, FWE-corrected at cluster level, based on a voxel-level threshold $p<0.01$. It was observed that all covariates in the regression model had significant influences on the Ch4-FC and Ch1-3 FC, except for APOE genotype. Therefore, controlling for covariates that had significant effects (including age, gender, years of education and MRI scanner), a second-level two-sample t-test was performed on the individual z maps of Ch1-3 FC and Ch4 FC between HC and SCD, respectively. The results were considered significant at $p<0.05$, FWE-corrected at cluster level, based on a voxel-level threshold $p<0.01$. To further explore linear relationships between the brain regions showing significant group differences on Ch4-FC/ Ch1-3-FC with the 5 cognitive factors, Pearson correlations were calculated between peak z-FC values in clusters showing significant groups differences and 5-cognitive factor scores in HC and SCD groups, respectively, with the same covariates as in the two-sample t-tests.

Effects of amyloid status in SCD and HC on seed-based FC

To investigate whether there are any main effects of group or amyloid status, or group $\times$ amyloid status interaction on Ch4-based FC and Ch1-3 based FC, the full-factorial 2-way (group and amyloid status) were used controlling for covariates above. The results were considered significant at $p<0.05$, FWE-corrected at cluster level, based on a voxel-level threshold $p<0.01$.

3.2.3 Results

Demographic, clinical and neuropsychological characteristics

Descriptive statistics of background characteristics for the HC and SCD samples are shown in **Table 3.5**. The two groups differed significantly in age, gender, APOE4

genotype, clinical measures including CDR-global, CDR-SOB, as well as the five cognitive factor scores derived from the NPT battery, including MEM, LANG and EXEC. The HC group (mean age ± standard deviation: 68.81 years ± 5.32) was significantly younger than the SCD group (mean age ± standard deviation: 70.98 years ± 5.80). APOE4 carriers were significantly less frequent in HC (41 APOE4 [21.6 %]) than in SCD (61 APOE4 [32.1 %]). Male proportion in SCD (103 males [53.1 %]) was significantly higher than in HC (80 males [41.2 %]). The CDR-SOB and the CDR-global score in SCD was significantly higher than in HC. Moreover, the scores of MEM, LANGE and EXEC in HC was significantly higher than in SCD, which indicate better cognitive performance in HC group compared to SCD.

Table 3.5: Demographic, clinical and neuropsychological tests characteristics

	HC (194)	**SCD (194)**	**Test Statistics**	**P value**
Age (yrs)	68.81 ± 5.32	70.98 ± 5.80	t (386) = -3.84	< 0.001
Gender (F/M)	114/80	91/103	χ^2 (1) = 5.47	0.02
APOE (ε4/non-4)	41/149[B]	61/129[B]	5.36	0.02
Education (yrs)	14.82 ± 2.78	14.80 ± 3.07[A]	t (385) = 0.05	0.96
MMSE	29.44 ± 0.85	29.26 ± 0.97	U (386) = 39693	0.05
CDR-global	0.00 ± 0.00	0.23 ± 0.25[C]	U (380) = 28660	< 0.001
CDR-SOB	0.04 ± 0.13[A]	0.39 ± 0.60[C]	U (380) = 28850	< 0.001
MEM	0.62 ± 0.38	0.35 ± 0.47	F (1, 363) = 21.05	< 0.001
LANG	0.53 ± 0.40	0.35 ± 0.49	F (1, 363) = 5.93	0.02
EXEC	0.53 ± 0.43	0.33 ± 0.54	F (1, 363) = 6.03	0.02
WME	0.40 ± 0.48	0.31± 0.61	F (1, 363) = 0.12	0.73
VIS	0.36 ± 0.41	0.28 ± 0.48	F (1, 363) = 0.55	0.46

Values are represented with mean ± standard deviation. Superscript capital letters denote number of missing values: A = 1 missing value; B = 4 missing values; C = 5 missing values. HC, Healthy Control; SCD, Subjective Cognitive Decline; MMSE, Mini-Mental State Examination; CDR: Clinical Dementia Ratings; CDR-SOB: CDR sum of boxes score; Factor scores: MEM for learning and memory); LANG for language abilities; EXEC for Executive function and processing speed; WM for working memory performance; VIS for visuospatial performance; The higher value of 5 cognitive scores indicate better cognitive performance.

Total intracranial volume, grey matter and Ch4/Ch1-3 volume

No significant differences were found on TIV, GM and Ch4/Ch1-3 volume between HC and SCD (**Table 3.6**).

Table 3.6: Grey matter, TIV and BF volume differences between HC and SCD groups

	HC (194)	SCD (194)	Test Statistics	P value
GM Volume	585.67 ± 50.02	587.86 ± 53.47	F (1,362) = 1.62	0.20
TIV	1494.42 ± 148.08	1529.35 ± 156.68	F (1,362) = 2.46	0.12
Ch1-3	186.38 ± 21.10	183.23 ± 22.41	F (1,362) = 0.36	0.55
Ch4	288.12 ± 29.67	279.46 ± 33.84	F (1, 362) = 0.89	0.35

GM= Grey Matter; TIV = Total intracranial Volume

Significant group differences on seed-based FC and relationships with NPT

Voxel-wise Ch4-FC analysis revealed three clusters in the SCD group that showed significantly decreased FC with Ch4 compared to HC (**Table 3.7, Figure 3.5**). The first cluster mainly includes the left dorsal precuneus and superior parietal gyrus; The second and third clusters include bilateral superior, middle occipital gyrus and left cuneus.

Table 3.7: Brain regions showing decreased Ch4-based FC in the SCD group

Clusters	Cluster Size	Brain Regions	peak MNI Coordinate			peak t-value
			x	y	z	
Cluster 1	484	Dorsal_precuneus_L	-14	-58	54	3.52
		Parietal_Sup_L	-30	-50	50	3.47
Cluster 2	916	Occipital_Mid_L	-18	-92	12	5.05
		Occipital_Sup_L	-20	-78	26	4.44
		Cuneus_L	-10	-90	28	3.96
Cluster 3	699	Occipital_Sup_R	26	-74	24	4.20
		Occipital_Mid_R	34	-88	8	3.78

Abbreviations: L: Left; R: Right; FC: Functional Connectivity; Sup: Superior; Mid: Middle.

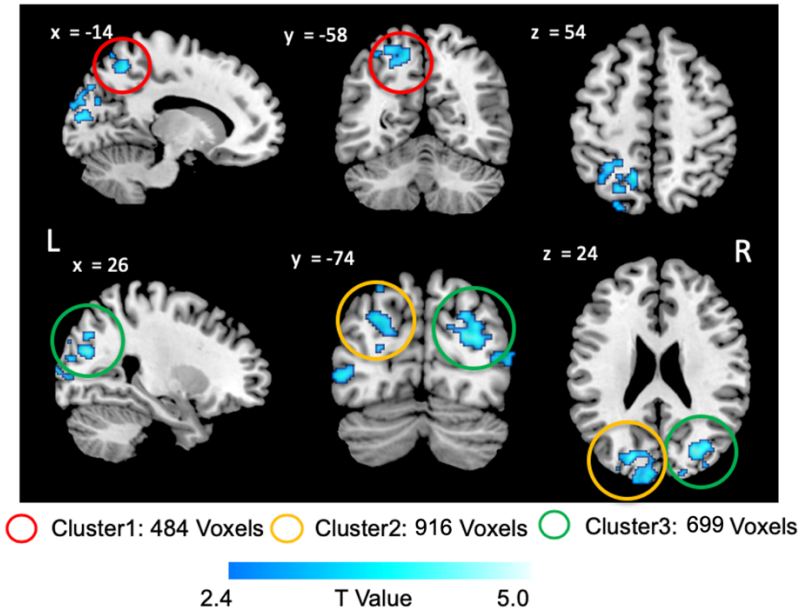

Figure 3.5: Brain regions showing decreased Ch4-based FC in the SCD.

The partial correlation analysis only revealed that the FC in the peak voxel (34 -88 8) of right middle occipital gyrus was significantly negatively correlated with the VIS score in SCD (r = - 0.19; p = 0.015) (**Figure 3.6**), but not in HC (r = -0.11; p = 0.15), without a significant difference between the correlation coefficients for the two groups (z = -0.8, p = 0.21). Moreover, there was a trend level negative correlation between the z-FC value in the peak voxel (-14 -58 54) of left precuneus and MEM score in SCD group (r = -0.13; p = 0.09), whereas the correlation in the HC group was not significant (r = -0.03; p = 0.68). The correlations coefficients for the two groups is not significant (z = -0.98; p = 0.16).

Voxel-wise FC of Ch1-3 analysis revealed no significant group differences. When a more liberal statistic criterial by increasing the voxel-level threshold from $p < 0.01$ to $p<0.05$ was used, three clusters showed significantly decreased FC with Ch1-3 in SCD (**Table 3.8, Figure 3.7**). The first cluster mainly includes the right ventral precuneus and lingual gyrus as well as left parahipocampal gyrus and hippocampus. The second cluster includes the left superior and middle temporal gyrus. The left superior frontal gyrus left medial superior frontal gyrus and left supplementary motor area were covered by the third cluster.

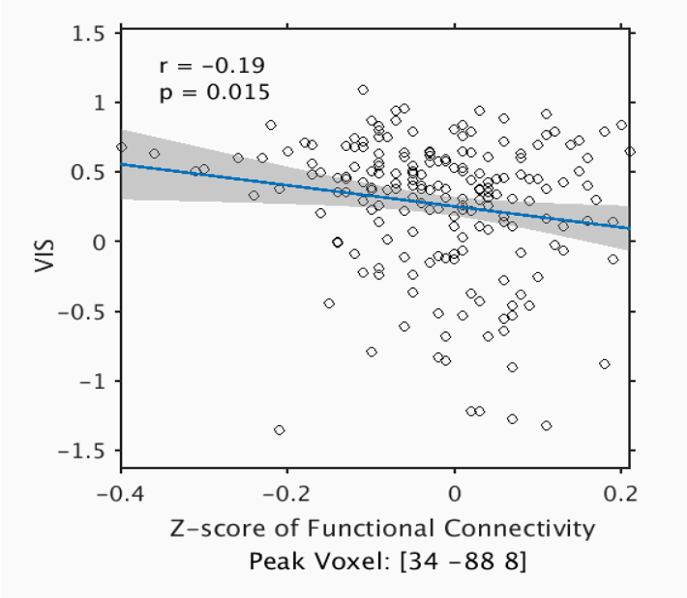

Figure 3.6: Partial correlations between VIS and z-score of functional connectivity in the peak voxel of right middle occipital gyrus in SCD group. VIS: factor score of visuospatial; The dotted area is the 95% confidential interval

Table 3.8: Brain regions showing a decreased Ch1-3 based FC in the SCD compared to HC

Clusters	Cluster Size	Brain Regions	Peak MNI Coordinate			Peak T Value
			x	y	z	
Cluster 1	1120	Ventral_Precuneus_R	12	-50	16	3.74
		Parahipocampal_L	-32	-38	-12	3.35
		Lingual_R	8	-48	4	3.14
Cluster 2	1890	Temporal_Mid_L	-60	-46	-10	3.67
		Tempral_Sup_L	-60	4	-16	3.65
Cluster 3	2162	Frontal_Sup_Medial_L	-10	34	34	4.50
		Supp_Motor_Area_L	-8	24	54	3.96
		Frontal_Sup_L	-16	54	32	3.77

Abbreviations: L: Left; R: Right; FC: Functional Connectivity; Sup: Superior; Mid: Middle.

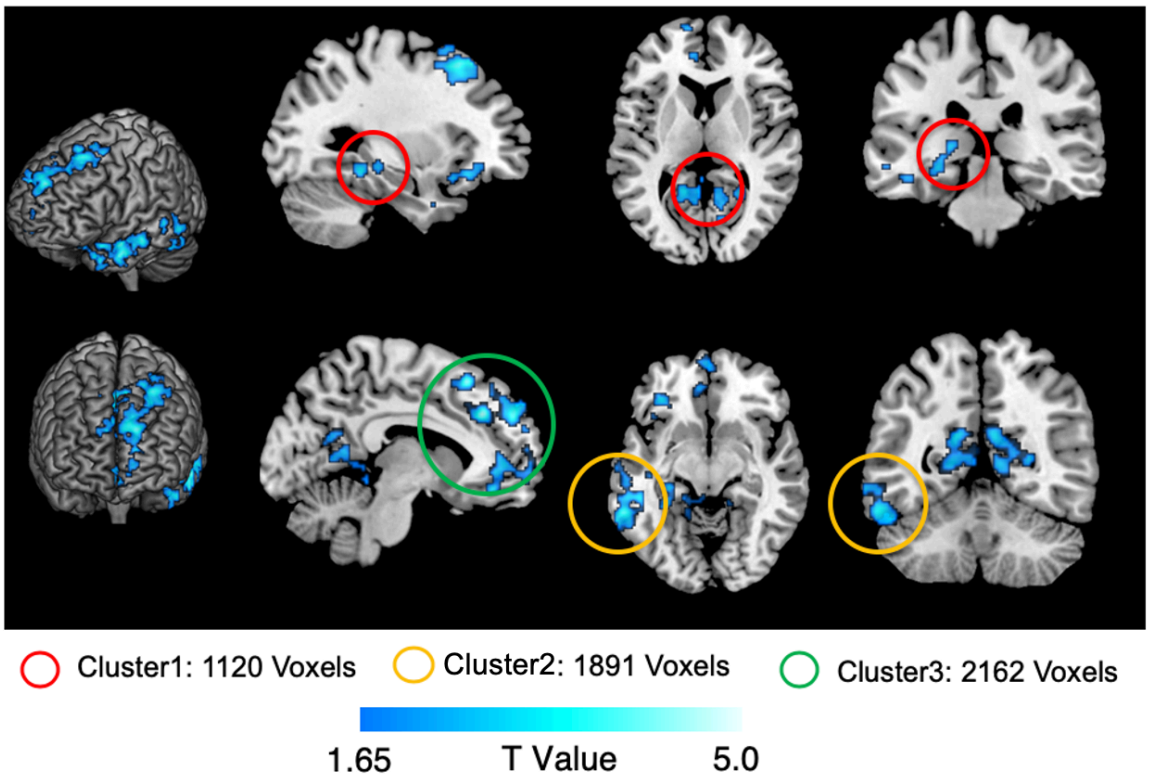

Figure 3.7: Brain regions showing a decreased FC with Ch1-3 in SCD.

Effects of amyloid status in SCD and HC on seed-based FC

All HC and SCD participants with rs-fMRI scans and CSF biomarker available were used for this analysis, including 73 individuals in HC group and 84 individuals in SCD group. There were 34% (25 of 73) HC and 41% (34 of 84) SCD being categorized as Aβ+ (Aβ42/40 < 0.09). Regarding the Ch4 FC, the full-factorial analysis revealed a significant main effect of groups. The pattern of brain regions showing decreased FC with Ch4 in SCD compared to HC in this analysis was similar to the above-mentioned finding based on the larger sample whole group comparison of HC and SCD (**Figure 3.8**). No significant amyloid status main effect and interaction between group × amyloid status was found in the full-factorial analysis.

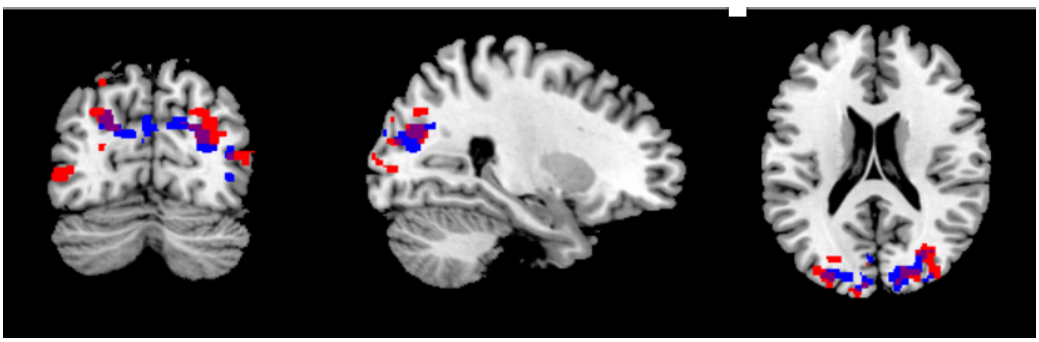

Figure 3.8: Overlay patterns of brain regions showing decreased FC with Ch4 in SCD compared to HC. Red color: brain regions showing reduced Ch4 FC in SCD from the large sample comparisons. Blue: brain regions showing reduced Ch4 FC in SCD from the factorial analysis.

Regarding the FC of Ch1-3, the full factorial analysis revealed no significant main effects of groups and amyloid status as well as no interaction effect between group × amyloid status at $p<0.05$, FWE-corrected at cluster level, based on a voxel-level threshold $p<0.01$. When a comparative liberal statistic criterial of $p<0.05$, FWE-corrected at cluster level, with a voxel-level threshold $p<0.05$ was used, the full factorial analysis revealed significant main effect of groups. The pattern of brain regions showing decreased FC with Ch1-3 in SCD compared to HC in this analysis was similar to above finding based on the larger whole group comparison of HC and SCD (**Figure 3.9**).

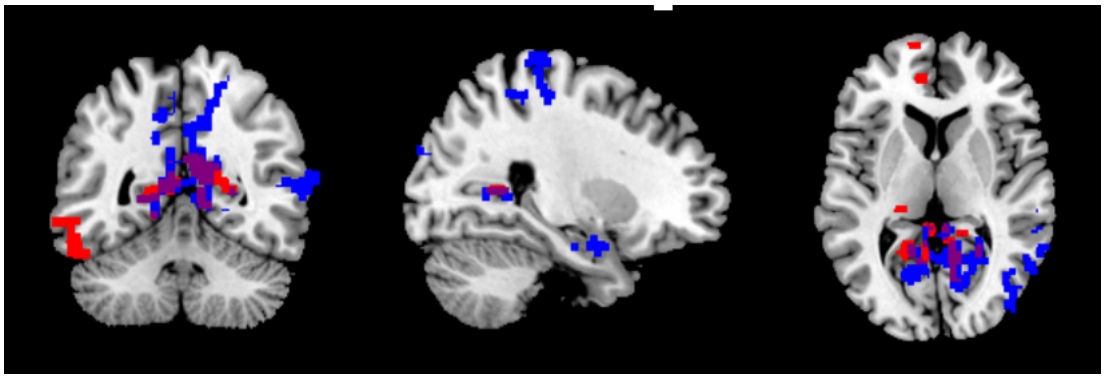

Figure 3.9: Overlay patterns of brain regions showing decreased FC with Ch1-3 in SCD compared to HC. Red color: brain regions showing reduced Ch1-3 FC in SCD from the large sample comparisons. Blue: brain regions showing reduced Ch1-3 FC in SCD from the factorial analysis.

3.2.4 Discussion

The study provided in vivo evidence for alterations of whole-brain FC of BF subregions in SCD individuals compared to HC group. The connectivity between Ch4 and the left dorsal precuneus, superior parietal gyrus and bilateral superior and medial occipital gyrus were reduced. The FC between Ch4 and middle occipital gyrus was negatively correlated with VIS score in the SCD group. Moreover, there was also a trend level correlation of the connectivity strength between Ch4 and the precuneus and the MEM score in SCD group. An exploratory analysis using Ch1-3 as seed region showed decreased connectivity with the parahippocampal gyrus, the hippocampus, the ventral

precuneus, the middle and inferior temporal gyrus as well as the medial superior frontal gyrus in the SCD group. The further full-factorial analysis including the amyloid status as a second grouping factor revealed a significant main effect of group, but neither a significant main effect for the amyloid status nor a significant group × amyloid interaction.

Severe atrophy of Ch4 and an ensuing reduction of cholinergic innervation of the cortex are considered to be a part of the pathophysiological cascade in progressive AD (Grothe *et al.*, 2012; Schmitz *et al.*, 2016a; Fernandez-Cabello *et al.*, 2020). Recent in vivo fMRI studies using seed-based FC analysis revealed decreased Ch4-FC in MCI patients (Li *et al.*, 2017; Meng *et al.*, 2018). The decreased Ch4-FC in MCI group was located in extensive brain regions, including bilateral occipital lobes, the limbic regions, bilateral superior and medial temporal gyri compared with healthy control participants (Meng *et al.*, 2018). Moreover, they found that decreased Ch4-FC in late MCI was mainly located in precuneus, parietal and occipital lobules compared with early MCI (Meng *et al.*, 2018). The pattern identified in MCI was in line with previous studies showing reduced acetylcholine activity in multiple brain regions by using PET imaging techniques (Kuhl *et al.*, 1999; Herholz *et al.*, 2004). The findings provide an important addition to the previous literature by showing decreased Ch4-FC in SCD compared to HC mainly in occipital lobule, dorsal precuneus, and superior parietal cortex. Taken together with the more extensive brain regions showing decreased Ch4-FC in MCI, the specific brain regions showing decreased Ch4-FC in SCD may support the progressive nature of cholinergic dysfunction. Previous animal studies have reported that the parietal cortex receives cholinergic innervation from subfields of Ch4 (Mesulam *et al.*, 1983). ChAT activity in the precuneus was lower in AD than in healthy controls (Ikonomovic *et al.*, 2011). Moreover, lower glucose precuneus metabolism has previously been reported to be a highly sensitive and early marker for the development of AD (Minoshima *et al.*, 1997), and correlated with volume reduction in the posterior part of Ch4 in SCD (Scheef *et al.*, 2019). This correlation may suggest that there is a close link between the reduced glucose metabolism of precuneus and reduced cholinergic innervation of Ch4. Therefore, in the present study, the findings of reduced Ch4-FC in superior parietal and precuneus in the SCD group may provide more direct evidence to support cholinergic denervation of Ch4 to parietal cortex in SCD individuals.

The superior/middle occipital gyrus, as parts of the visual cortex, is involved in visual spatial processing. The grey matter volume of atrophied visual cortices in AD and MCI subjects were found to be correlated to the deterioration of overall cognitive status and to object recognition functions (Derflinger *et al.*, 2011; Deng *et al.*, 2016). Cortical thinning in the occipital lobe was also reported in AD recently (Hartikainen *et al.*, 2012; Eskildsen *et al.*, 2013). In a resting-state fMRI study combined with ReHo method, AD patients were found to show significant decreases of regional spontaneous neuronal synchronization in the precuneus but increases neuronal synchronization in the occipital lobes compared with the healthy controls (He *et al.*, 2007). In addition, a previous study combined both regional gray matter volume and resting-state functional characteristics, to discriminate patients with AD from healthy controls. They found that occipital, default mode network and subcortical regions were the most discriminative features for classification of the AD and healthy controls. All the above-mentioned findings and visual spatial dysfunction in AD (Possin, 2010) may suggest the involvement of visual cortex during the progression of AD. Two previous FDG-PET studies have shown that the cholinesterase inhibitor treatment increased glucose metabolism in the middle occipital gyrus, precuneus and inferior parietal lobule in AD patients (Smith *et al.*, 2009; Tepmongkol *et al.*, 2019). These two studies suggest that middle occipital gyrus may be an important brain region involving neurochemical pathways of acetylcholine innervation in cholinesterase inhibitor treatment of AD (Smith *et al.*, 2009; Tepmongkol *et al.*, 2019). Acetylcholine, which is released in the visual cortex predominantly by cholinergic projections from the Ch4, is an important neurotransmitter for the regulation of visual attention (Herrero *et al.*, 2008). An early study (Hodges *et al.*, 1991) demonstrated that lesioned BF rats do not process visuospatial information relevant to the solution of a radial arm maze task. In this study, FC between Ch4 and middle occipital cortex was significantly correlated with VIS score in SCD, which indicates that functional synchronization between Ch4 and occipital gyrus associates with visual spatial ability in SCD individuals. Interestingly, the direction of the above-mentioned correlation was negative in the current study. A possible explanation for this negative correlation is that functional synchronization between Ch4 and the occipital gyrus is increased to overcome the cholinergic denervation from Ch4 to occipital gyrus in order to keep visual spatial ability normal in SCD individuals.

Even though the initial analysis did not reveal an alteration of the Ch1-3 connectivity, by lowering the statistical threshold slightly, a reduced connectivity of the BF with key structures was observed. In the SCD group the BF-connectivity was reduced for the hippocampus, the middle and inferior temporal gyrus, the ventral precuneus, as well as the medial superior frontal gyrus. Especially the findings in the medial temporal lobe fit very well with animal research and recent human data. In rodents and nonhuman primates, Ch1 and Ch2 have the major cholinergic projections to the hippocampus (Mesulam *et al.*, 1983; Hedreen *et al.*, 1984). In humans, recent studies supported these findings, proving this connectivity between BF and the hippocampus using fMRI (Fritz *et al.*, 2019; Yuan *et al.*, 2019). Although reduced FC between Ch1-3 and hippocampus showed up in SCD compared to HC, the present study showed no significant correlation of the FC between Ch1-3 and hippocampus and MEM in SCD. Although Ch1-3 provides the main cholinergic innervation for the hippocampus, a brain structure which is considered to be a core structure for episodic memory, previous findings of correlation between volume of Ch12 and memory were inconsistent (Butler *et al.*, 2012; Wolf *et al.*, 2014; Scheef *et al.*, 2019). Butler et al., showed the volume of this region is predictive for memory performance in healthy adults (age range: 21-62 years) (Butler *et al.*, 2012).Wolf et al. showed a stronger correlation between Ch2 volume and memory task performance than other BF subregions in healthy adults (age range: 60-85), but the correlation is not significant (Wolf *et al.*, 2014). Scheef et al. could also not replicate the previously reported correlations between Ch12 volume and memory decline in SCD individuals (Scheef *et al.*, 2019). Interestingly, Scheef et al., found it was Ch4p, instead of Ch12, that showed a significant correlation with reduced glucose metabolism in the precuneus for the SCD group (Scheef *et al.*, 2019). These findings suggest that Ch12 atrophy does not fit well with AD-related neurodegeneration processes. Therefore, the lack of correlation between FC of Ch1-3 and hippocampus with memory is partially supported by previous findings. A possible explanation is that the FC of Ch4 in SCD ($r = -0.13$; $p = 0.09$) is more closely related to memory than FC of Ch1-3 and hippocampus. Previous animal studies have reported that precuneus received cholinergic innervation mainly from anterior parts of the BF (Mesulam, 2004b; Parvizi *et al.*, 2006) and spontaneous activity of the anterior parts of the BF was positively associated with several cortical regions, including ventral precuneus, posterior cingulate cortex, parahippocampal, the superior and middle temporal gyrus, the middle and inferior frontal gyrus (Yuan *et al.*, 2019). Therefore,

the decreased FC pattern of Ch1-3 in SCD group in the current study appeared to follow well-established cholinergic projections and functional networks, which indicates that FC alterations of Ch1-3 in SCD reflect early dysfunction of cholinergic projections of Ch1-3.

The main effect of amyloid status and the interaction of amyloid × group were not significant, neither in Ch4-FC nor in Ch1-3 FC in the current study. A recent study evaluated the association between the global fibrillary amyloid pathology using PET measurements and the BF-FC at rest in subject memory complaints. They found no significant correlations between the FC of the anterior BF and global SUVR values, whereas these global SUVR values were found to be negatively correlated with FC between posterior of BF and the hippocampus and the thalamus (Chiesa *et al.*, 2019). The non-significant interaction between amyloid × group on FC of Ch1-3 was supported by this study (Chiesa *et al.*, 2019). However, the finding regarding Ch4-FC is inconsistent. One possible reason for the inconsistency is that the search space for the voxelwise analyses in Chiesa's study were only restricted to the significant positive FC of BF maps. However, the statistical analyses in our analysis is based on whole brain voxel wise analyses. The other possible reason for the inconsistency is that the current sample of SCD patients (n = 84) was much smaller than that in Chiesa's study(n = 276), limiting the statistical power of the present analyses. Therefore, the decreased FC pattern in Ch4/Ch1-3 in SCD individuals in the present study is independent from amyloid effects and may be related to cholinergic neurochemical dysfunction. Previous studies have shown that cholinergic system could regulate APP metabolism (Nitsch *et al.*, 1992; Pittel *et al.*, 1996; Kar *et al.*, 2004). Therefore, these FC alterations may indicate cholinergic pathway of BF might be impaired at SCD stage. The conclusions here need to be proven by further large sample size.

3.3 Study 3: Aberrant precuneus functional connectivity in subjective cognitive decline depending on cerebral amyloid status

3.3.1 Introduction

Disruption of FC within the DMN is a key feature in AD which is likely due to amyloid-beta plaque-associated neuronal toxicity or vice versa (Buckner *et al.*, 2005; Myers *et al.*, 2014; Badhwar *et al.*, 2017). Previous studies have shown that Aβ accumulation preferentially starts in the precuneus, along with the medial orbitofrontal, and posterior cingulate cortex (Palmqvist *et al.*, 2017; Mattsson *et al.*, 2019). Moreover, dysfunction of FC in the DMN was also found in cognitively normal elderly subjects with amyloid burden (Hedden *et al.*, 2009; Sperling *et al.*, 2009; Mormino *et al.*, 2011). ReHo, as a local FC metric, could complement the disruptions of large-scale FC networks from the functional segregation view (Lv *et al.*, 2018). Previous studies in MCI and AD patients have found decreased ReHo mainly in DMN brain regions, even though parallel increases in the occipital and frontal regions were also observed (He *et al.*, 2007; Bai *et al.*, 2008; Zhang *et al.*, 2012; Long *et al.*, 2016; Yuan *et al.*, 2016). However, the impact of amyloid depositions on precuneus FC is not well understood in SCD. Based on amyloid PET and rs-fMRI, this study specifically addressed the question how amyloid pathology relates to precuneus FC and regional functional synchronization in SCD patients. In this study, precuneus-based FC and ReHo were compared among 24 amyloid-positive SCD ($SCD_{A\beta+)}$ and 24 age- and sex-matched amyloid-negative SCD ($SCD_{A\beta-}$) participants based on the visual ratings from amyloid PET examinations (Li *et al.*, 2020). The hypothesis is that $SCD_{A\beta+}$ group exhibits alterations of both precuneus-based FC and ReHo compared to $SCD_{A\beta-}$. However, the direction of these functional alterations was not estimated due to the equivocal results in the previous SCD literature. In addition, it was explored whether the observed functional alterations correlated with the quantitative global and regional precuneus Aβ load, and whether they were correlated with the global level of cognitive function in these patients, which may help to interpret whether these FC changes reflect incipient decay or, alternatively, its functional compensation.

3.3.2 Study-specific materials and methods

All participants in this study were based on the PET sub-cohort of the DELCODE study (Li *et al.*, 2020). Twenty-four $SCD_{A\beta+}$ subjects with significant cerebral amyloid

depositions and valid rs-fMRI data, as well as 24 age- and sex-matched $SCD_{Aβ-}$ participants without significant cerebral amyloid depositions were selected.

Neuropsychological tests

Refer to Materials and Methods in 2.3 (page 35).

[18F]-Florbetaben PET acquisition and analyses

Refer to PET Methods in 2.6 (page 36)

Rs-fMRI data preprocessing

Refer to preprocessing steps for rs-fMRI data in 2.7.3 (page 40).

ReHo and precuneus-based FC calculation

Refer to Seed-based functional connectivity and ReHo in 2.7.3 (page 40).

Statistical analyses

SPM12 (Wellcome Department of Cognitive Neurology, London) and SPSS 22.0 (IBM Corp.: Armonk, NY) were used for the statistical analyses. Group differences were assessed using independent sample t-, Mann-Whitney U-, or chi-squared tests for background characteristics of the sample. The statistical significance threshold was set to $p<0.05$. For the imaging data, two-sample t-tests comparing $SCD_{Aβ+}$ and $SCD_{Aβ-}$ were performed on the individual FC and ReHo maps in a voxel-by-voxel manner. The results were considered significant at $p < 0.05$, FWE-corrected at cluster level, after thresholding on a voxel level at $p < 0.01$. Based on these results, the mean FC value was extracted from significant clusters, and partially correlated with (i) the mean $SUVR_{FBB}$ of the precuneus and (ii) the global $SUVR_{FBB}$, respectively.

Finally, analogous partial correlations with performance of MMSE and ADAS-Cog were calculated in order to explore the potential functional relevance of FC group differences in these clusters.

3.3.3 Results

Sample characteristics and amyloid SUVRs

Both groups, $SCD_{Aβ+}$ and $SCD_{Aβ-}$ did not differ statistically in any background variable except for the fact that a higher proportion of APOE4carriers was found in the $SCD_{Aβ+}$ group (**Table 3.9**). The regional precuneus $SUVR_{FBB}$ and global $SUVR_{FBB}$ in the $SCD_{Aβ-}$ group was significantly lower compared to $SCD_{Aβ+}$. Yet, the global SUVR values of several participants in both $SCD_{Aβ+}$ and $SCD_{Aβ-}$ groups were borderline to

FBB SUVR cut-off definitions for amyloid positivity in the study of Barthel et al (Barthel *et al.*, 2011a). N=5 $SCD_{Aβ-}$ would be grouped into amyloid-positive, while only N=1 $SCD_{Aβ+}$ would be classified amyloid-negative when we used $SUVR_{global}$ = 1.39 from Barthel et al. (Barthel *et al.*, 2011a). This result indicates moderate consistency of amyloid status classifications (>80%) when using global SUVR cut-offs compared with visual reading since several patients are located near the cut-off point.

Table 3.9: Sample characteristics and regional amyloid tracer uptake for the amyloid-positive and -negative subgroups.

	$SCD_{Aβ+}$	**$SCD_{Aβ-}$**	**Test Statistics**	**P value**
Age (yrs)	74.54 ± 4.40	74.04 ± 4.13	t (46) = 0.41	0.69
Gender (F/M)	9/15	9/15	χ^2 (1) = 0.00	1
Education (yrs)	14.42 ± 2.78	14.96 ± 3.36	t (46) = 0.61	0.55
MMSE	29.13 ± 0.90*	29.00 ± 1.44*	U (46) = 247.50	0.69
ADAS-cog13	8.38 ± 3.68	7.25 ± 3.27	t (46) = 1.12	0.27
APOE(*ε4/non-4*)	17/6*	6/17*	χ^2 (1) = 10.52	0.001
Global $SUVR_{FBB}$	1.79 ± 0.25	1.32 ± 0.10	t (46) = 8.38	<0.001
Precuneus $SUVR_{FBB}$	1.92 ± 0.31	1.29 ± 0.07	t (46) = 9.74	<0.001

*: Denotes 1 missing value. Abbreviations: $SCD_{Aß+}$ = Amyloid-positive subjective cognitive decline group, $SCD_{Aß-}$ = amyloid-negative subjective cognitive decline group; U= Whitney U value; MMSE Mini-Mental -State Examination; ADAS-cog13 Alzheimer's Disease Assessment Scale—cognitive part; APOE: Apolipoprotein; SUVR=Standard Uptake Value Ratio with cerebellar cortex as reference region; FBB= [18F]-Florbetaben. Continuous data are presented as means ± standard deviations.

Group comparison: ReHo and precuneus-based FC

In $SCD_{Aβ+}$ significantly greater ReHo values were found in the bilateral precuneus and the adjacent superior parietal lobule when compared to the $SCD_{Aβ-}$ group (**Table 3.10, Figure 3.10**).

Table 3.10: Brain regions showing increased regional homogeneity in amyloid-positive compared to amyloid-negative SCD participants.

Cluster Size	p value (FWE)	Brain Regions	Peak MNI Coordinate			Peak T Value
			x	y	z	
270	0.034	Right precuneus	6	-54	69	4.34
		Left superior parietal lobule	-18	-54	72	3.75
		Right superior parietal lobule	15	-63	66	3.63

Abbreviations: FWE – Family-wise error. MNI – Montreal Neurological Institute.

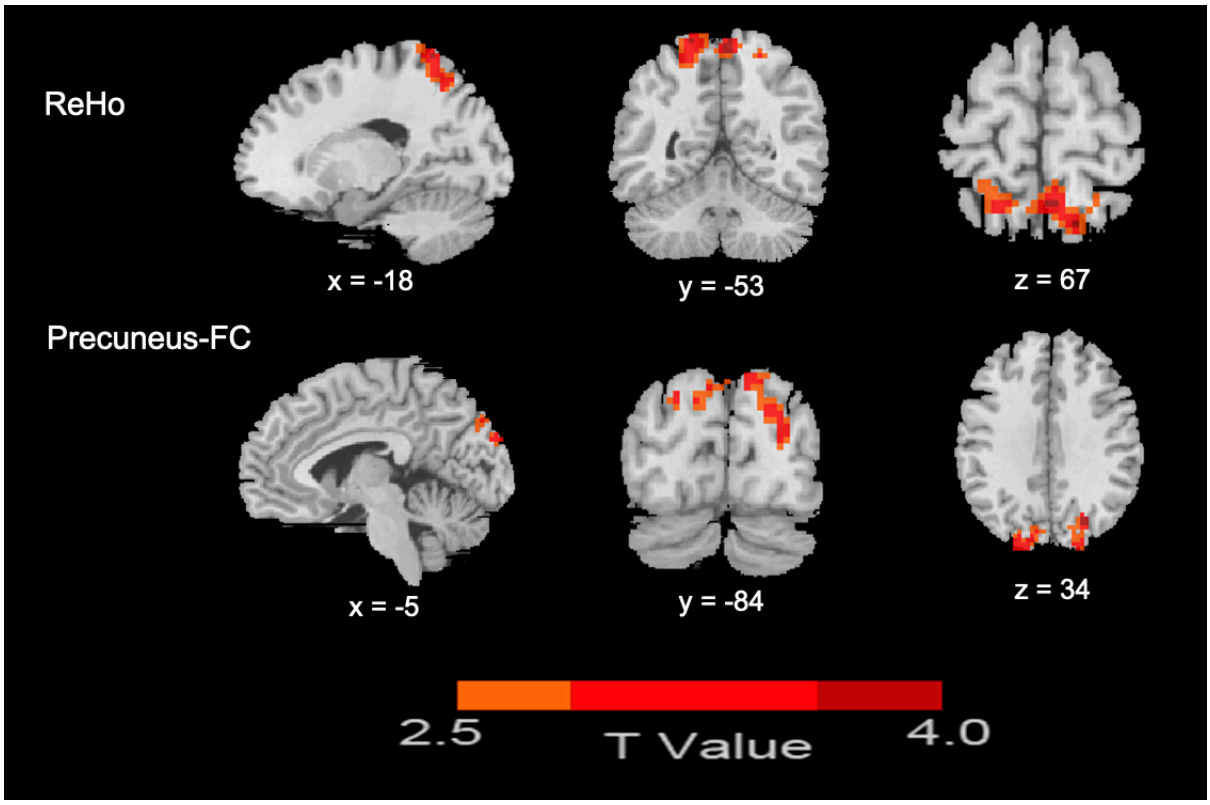

Figure 3.10: Brain regions showing increased ReHo and precuneus-based FC in $SCD_{A\beta+}$ compared to $SCD_{A\beta-}$. The upper panel shows the regions with significant increased ReHo value in $SCD_{A\beta+}$ compared to $SCD_{A\beta-}$ ($p < 0.05$, FWE cluster-level). The lower panel shows increased voxel-wise FC of the precuneus seed region with the cuneus and superior/middle occipital regions in the $SCD_{A\beta+}$ group ($p < 0.05$, FWE cluster-level). Abbreviations: ReHo: Regional Homogeneity; FC: Functional Connectivity; The color bar represents the heights of suprathreshold t-values.

Voxel-wise FC analysis revealed that the $SCD_{A\beta+}$ group showed higher FC between the precuneus mean time course and occipital regions, including the superior occipital gyrus and the bilateral cuneus (**Table 3.11, Figure 3.10**).

Table 3.11: Brain regions showing increased precuneus-based functional connectivity in amyloid-positive compared to amyloid-negative SCD participants.

Cluster Size	p value (FWE)	Brain Regions	Peak MNI Coordinate			Peak T Value
			x	y	z	
296	< 0.001	Right middle occipital gyrus	27	-75	30	3.95
		Right cuneus	12	-87	42	3.62
		Right superior occipital gyrus	27	-84	21	3.17

Abbreviations: FWE – Family-wise error. MNI – Montreal Neurological Institute.

Analysis of nuisance variables on the ReHo and precuneus-based FC findings

In order to test for possible effects of different MR scanners and the differences in APOE genotype on both ReHo and precuneus-based FC, second-level two-sample t-tests with APOE status (ε4+/ε4-) and MR scanners (dummy-coded) as covariates were performed. Regarding the ReHo result, the additional second-level two-sample t-tests with both MRI scanner and APOE status as covariates showed slightly weaker findings, which might be due to the reduced degrees of freedom. The left-sided group differences of ReHo between the two groups were still significant (**Figure 3.11**), which suggest that group differences of ReHo were not primarily influenced by APOE status or MRI scanner effects.

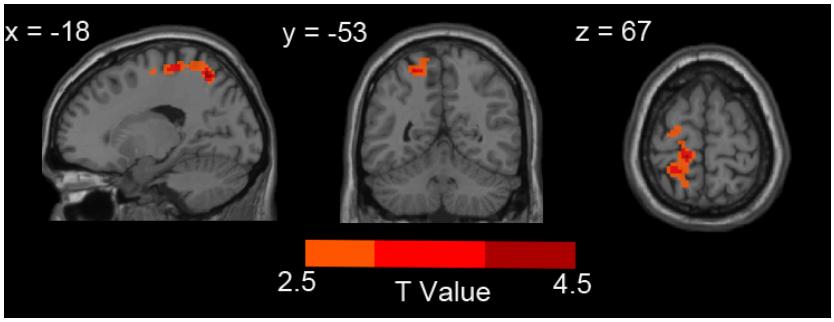

Figure 3.11: Brain regions showing increased ReHo in $SCD_{A\beta+}$ compared to $SCD_{A\beta-}$ with MR scanners and APOE status as additional covariates.

As for the precuneus-FC findings, we found no significant group differences with the additional second-level two-sample t-tests with both MRI scanner and APOE status as covariates. Since the significant group differences of precuneus-FC were still evident in a separate two-sample t-tests model controlling for MR scanners only (**Figure 3.12**), the nonsignificant findings indicate that confounding influence of APOE genotype cannot be excluded.

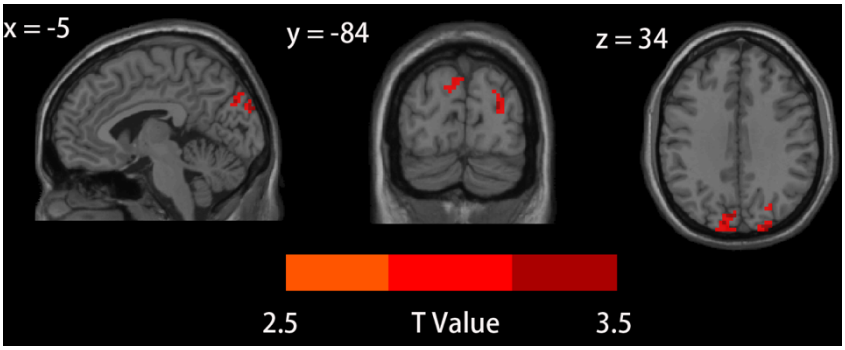

Figure 3.12: Brain regions showing increased precuneus-based FC in $SCD_{A\beta+}$ compared to $SCD_{A\beta-}$ based on voxel-wise FC, with MRI scanner covariates only.

Correlations between FC differences and quantitative amyloid load

Given the above-mentioned observations, the correlation analyses between amyloid SUVR values and FC metrics in the significant clusters additionally controlled for APOE status and MR scanners. There were no significant associations between the global and/or local precuneus $SUVR_{FBB}$ and the mean z-score of the ReHo extracted from the precuneus cluster in the $SCD_{A\beta+}$ group (global $SUVR_{FBB}$: $r_{A\beta+}$ = -0.14, p=0.60; precuneus $SUVR_{FBB}$: $r_{A\beta+}$ = 0.05, p=0.85). Similarly, no significant associations were found in the $SCD_{A\beta-}$ group (global $SUVR_{FBB}$: -0.04, p=0.89; precuneus $SUVR_{FBB}$: $r_{A\beta+}$ = 0.05, p=0.86). Regarding the global SUVR, there was positive partial correlation ($r_{A\beta+}$ =0.49, p=0.03) between the mean z-score of the FC extracted from the superior occipital gyrus and bilateral cuneus with global SUVR, but not in the $SCD_{A\beta-}$ ($r_{A\beta-}$= 0.20, p=0.48) group. Moreover, there was a significant difference between the correlation coefficients for the two groups (z = 1.05, p = 0.15). As for the regional precuneus $SUVR_{FBB}$, positive partial correlations between regional precuneus $SUVR_{FBB}$ and the mean z-score of the FC extracted from the superior occipital gyrus and the bilateral cuneus emerged in both $SCD_{A\beta+}$ ($r_{A\beta+}$= 0.45, p=0.05) and $SCD_{A\beta-}$ ($r_{A\beta-}$= 0.49, p=0.03)

group. However, the correlation coefficients for the two groups were not significantly different (z = 0.16, p = 0.44). The scatterplots of the above-mentioned significant correlations (for the raw values) are shown in **Figure 3.13**, which additionally visualizes the APOE status of the participants.

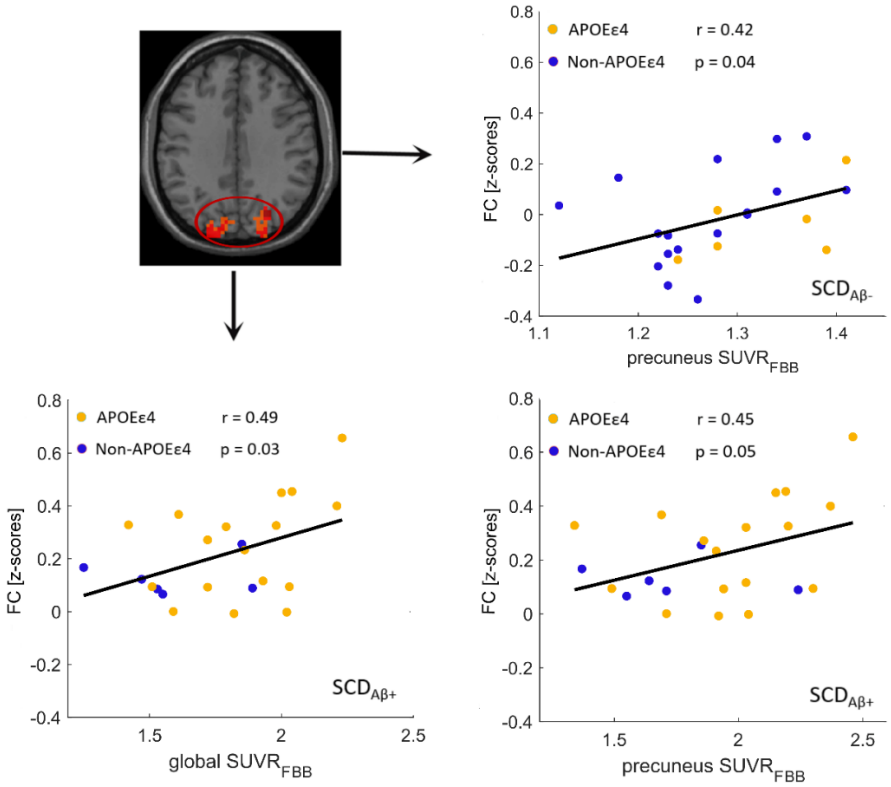

Figure 3.13: Positive correlations between precuneus-occipital FC and global $SUVR_{FBB}$ and precuneus $SUVR_{FBB}$. The mean Z-Score of the FC was extracted from significant cluster within the red circles. The scatterplots show raw data, additionally coded by APOE4 genotype to allow for visual inspection. Correlation coefficients represent partial correlations after controlling for APOE status and MR scanners. There are 23 datapoints in each group since one individual in each group lacked APOE information. The grey regions are 95% confidential intervals. Abbreviations: FC: Functional Connectivity; $SCD_{Aβ+}$ - amyloid-positive SCD; $SCD_{Aβ-}$ - amyloid-negative SCD; SUVR=Standard Uptake Value Ratio (with cerebellar cortex as reference region).

Correlations between FC differences and cognitive performance

There were negative correlations between the zReHo values in the $SCD_{Aβ-}$ group and MMSE ($r_{Aβ-}$= -0.74, p = 0.003). A moderate, but non-significant negative correlation was found between the zReHo values in the $SCD_{Aβ-}$ group and ADAS-Cog-13 scores ($r_{Aβ-}$= 0.41, p = 0.13). As for the precuneus-occipital zFC, we only found weak and nonsignificant partial correlations (r < 0.25, p > 0.4) in $SCD_{Aβ-}$ group. For both ReHo and precuneus-FC, the partial correlations for the $SCD_{Aβ+}$ group were weak and non-

significant ($r_{A\beta-} \leq |0.1|$, $p \geq 0.7$). Yet, we found a moderate, but nonsignificant partial correlation between precuneus-occipital zFC and MMSE (r=-0.37, p=0.18).

3.3.4 Discussion

This study explored precuneus-based whole-brain FC and ReHo changes in two age- and gender- matched SCD groups that varied in their amyloid positivity status and tried to find a relationship between the rs-fMRI measures and global/ precuneus Aβ load. One key finding was an increased ReHo in the bilateral precuneus and adjacent superior parietal gyrus in the $SCD_{A\beta+}$ as compared to the amyloid negative group $SCD_{A\beta-}$ group. Moreover, $SCD_{A\beta+}$ patients were characterized by an increased FC of the precuneus with occipital regions. As for the associations of precuneus-based FC and amyloid load, it was found that precuneus and occipital areas showed positive linear associations with global ($SCD_{A\beta+}$) as well as local precuneus amyloid load ($SCD_{A\beta+ \text{ and }} SCD_{A\beta-}$). These correlations indicate that FC changes in SCD were related to incipient accumulation of amyloid pathology, while APOE genotype influences on these group differences cannot be excluded.

As far as known, previous studies investigating ReHo alterations in SCD populations are lacking. Thus, it is novel that this study found higher ReHo in precuneus and superior parietal areas in $SCD_{A\beta+}$ as compared to $SCD_{A\beta-}$. The finding of higher ReHo in amyloid-positive SCD individuals indicates that this local FC marker is associated with amyloid deposition. However, this is not converging with the only study that investigated cognitively normal, i.e. asymptomatic, individuals depending on amyloid status (Kang *et al.*, 2017a). In the study of Kang et al., they found that, compared to amyloid negative cognitively normal individuals, ReHo decreases in the left precuneus, and increases in the left fusiform gyrus in amyloid positive cognitively normal individuals (Kang *et al.*, 2017b), which would represent the asymptomatic stage 1 of the NIA-AA clinical AD continuum. However, a possible reason for the inconsistent findings between the present and the previous study is that the control group was different, i.e. the reference for identifying potential functional alterations. While the present study recruited treatment-seeking SCD individuals from memory clinics with amyloid negative biomarker for AD, Kang et al. examined a cognitively normal group without reported subjective impairments (Kang *et al.*, 2017b). It cannot be excluded that the $SCD_{A\beta-}$ group in the present study is not completely comparable with the amyloid negative cognitively normal control subjects of the previous study. Therefore,

ReHo alterations in the $SCD_{Aβ-}$ group due to other (i.e. non-amyloid) clinical factors may disguise latent impairments in the $SCD_{Aβ+}$ group, but this cannot be tested due to the lack of an amyloid-negative healthy control group. Moreover, the individuals in the current study were older, included less female subjects, and had a higher educational level compared with those in the study of Kang et al., (2017b). All of the factors showing differences between the studies may influence resilience mechanisms against amyloidosis to some extent. Given these discrepancies, future studies on local ReHo alterations in biomarker stratified SCD samples are needed.

The present results revealed greater FC of the bilateral precuneus seed with adjacent occipital areas in $SCD_{Aβ+}$, which is partially consistent with a study (Sheline *et al.*, 2010b) observing stronger precuneus-occipital connectivity in Aβ+ (as compared to Aβ-) cognitively normal participants. Moreover, using independent component analysis with dual regression, another study observed higher FC within the DMN and the medial visual network in patients with subjective memory complaints, as compared to healthy elderly without SCD symptoms (Hafkemeijer *et al.*, 2013). However, in this study the group comparison was not informed by amyloid biomarker information. In a recent paper focusing on individuals with a family history of AD, an increased FC of the posterior DMN (PCC) with the medial temporal memory system was found in participants complaining about SCD compared to non-complainers (Verfaillie *et al.*, 2018). However, the SCD classification was only based on a single questionnaire item examining subjective worsening of memory, and AD biomarkers were again not available. In this context, it is noteworthy that this study has the amyloid pathology biomarker and found evidence for relationship with amyloid burden, drawing a closer link with AD pathology than previous SCD-related studies.

The observed higher connectivity of the precuneus with the occipital gyrus significantly correlated positively with regional precuneus Aβ load. Interestingly, the positive correlation between precuneus-occipital FC and global $SUVR_{FBB}$ values was only found in the $SCD_{Aβ+}$ subgroup, while a positive correlation with the precuneus $SUVR_{FBB}$ also observed in the $SCD_{Aβ-}$ subgroup. This result may indicate that these FC alterations are mainly due to incipient local amyloid accumulations, which are masked in the global composites scores. This explanation is also supported by a previous study (Palmqvist *et al.*, 2017), which found that a positive correlation between the dynamic whole-brain connectivity measures and SUVR values in early Aβ

deposition regions, including the PCC and precuneus in the cognitively normal elderly (consisting of healthy controls and SCD) with negative amyloid PET. These relationships were not found between the SUVR values from entire DMN or global cortical mask with the dynamic FC.

The observed higher FC in $SCD_{A\beta+}$ together with precuneal ReHo may correspond to a compensatory upregulation in preclinical AD (Mormino *et al.*, 2011; Hafkemeijer *et al.*, 2013; Verfaillie *et al.*, 2018). This finding may indicate that the hyperconnectivity represents an indicator for a compensational process at preclinical stage of AD. This would fit very well to the existing literature showing elevated compensation in preclinical AD, where extra neuronal processing is needed to balance the brain workload, thereby, keeping normal cognitive functioning under the influence of increasing amyloid deposition (Mormino *et al.*, 2011; Hafkemeijer *et al.*, 2013; Verfaillie *et al.*, 2018). The increased FC may indeed reflect a local compensatory mechanism at an early pathophysiological stage that helps to maintain normal behavioral performance in $SCD_{A\beta+}$. However, cautious is needed with this interpretation. The reason is that the only robust negative correlations with cognitive performance were observed in the amyloid-negative (not: -positive) group and would indicate that higher connectivity was associated with worse performance and, thus, favor a *dysfunctional* upregulation. SCD might be the first indication that the losses cannot be compensated any more. This would also be compatible with an alternative interpretation that assumes reverse causality. In a mechanistic sense, Aβ pathology may also be accelerated by increased metabolism and elevated intrinsic activity / connectivity (Greicius *et al.*, 2004; Bero *et al.*, 2011; Drzezga *et al.*, 2011). Laboratory evidence exists that neuronal activity directly increases production of Aβ peptides (Cirrito *et al.*, 2005). Considering that the precuneus is a prominent ‘hub’ in DMN and is metabolically highly active (Leech and Sharp, 2014), our finding of relatively higher connectivity and ReHo within this region might be also interpreted as being triggered by an increased (or amplified) Aβ production in $SCD_{A\beta+}$.

One further aspect has to be discussed here, the higher rate of APOE4 carriers in the amyloid-positive group. This difference was not unexpected given the frequently observed association between APOE genotype and amyloidosis (Morris *et al.*, 2010). It is not easy to differentiate the relative contributions of amyloid positivity *per se* and APOE genotype to FC group differences. The available small sample size in the

current study precluded further stratifications according to APOE status. While APOE genotype was shown to have independent effects on FC measures, even in individuals whose amyloid PET was negative (Sheline *et al.*, 2010a; Hafkemeijer *et al.*, 2012; Jones *et al.*, 2016), its influence may also be indirectly mediated by its effect on amyloid accumulation. Future studies are needed to investigate independent effect of APOE genotype by examining whether these FC alterations are already present in the amyloid negative APOE4 carriers.

4 Discussion

4.1 Aims and main findings

The main research objective of this thesis was to investigate SCD using different MRI-techniques as well as Amyloid-PET to find earliest structural and functional changes in biomarker positive controls and SCD that might help to further elucidate the progression from stage 1 (asymptomatic) to stage 2 (transitional cognitive impairment) of the clinical Alzheimer's continuum (Jack *et al.*, 2018). Therefore, this thesis was focused on early AD-related structural and functional MRI markers, including cholinergic BF volume, resting-state FC of the BF, and precuneus resting-state FC in patients with clinical SCD symptomatology. Despite earlier studies, CSF biomarkers for AD pathology were available for a part of the cohort. To this end, three studies were conducted, based on datasets from the DELCODE project. The aim of the first presented study was to examine if cholinergic BF volume alterations in SCD patients could be found, and if so, how they could be related the CSF AD biomarker status. The most important finding was the interaction between diagnosis (SCD vs. Healthy control), CSF amyloid status and Ch4p volume reductions. A Ch4p atrophy was only emerging in amyloid-positive SCD, neither in amyloid-positive HC nor in amyloid-negative SCD. In addition, the Ch4p volume was linearly correlated with amyloid burden assessed by the CSF-Aβ42/40 ratio. This effect was found in the SCD subgroup only, not in the controls.

Considering BF plays an important neuromodulatory role in brain regions supporting cognition due to its broad cholinergic projections (Ballinger *et al.*, 2016; Bell and Shine, 2016; Markello *et al.*, 2018), one of the aims of the presented second study was to examine whether altered resting-state FC for different BF subregions could be identified in SCD patients as compared to HC, and whether these patterns relate to

CSF amyloid pathology (Chapter 3.2). Decreased Ch4-FC in the left dorsal precuneus, superior parietal gyrus, and occipital gyrus was observed. The exploratory results showed a decreased FC of Ch1-3 with parahippocampal gyrus, hippocampus, ventral precuneus, middle and inferior temporal gyrus as well as medial superior frontal gyrus in SCD group compared with HC group. However, these FC alterations were independent from underlying CSF amyloid pathology.

The aim of the third presented study was to investigate alterations of precuneus seed-based FC and ReHo in SCD with proven cerebral amyloid pathology (Chapter 3.3). In this study, two groups of age- and gender-matched $SCD_{A\beta+}$ and $SCD_{A\beta-}$ patients were selected according to visual [18F]-FBB-PET readings. We found that ReHo was significantly higher in the bilateral precuneus for the $SCD_{A\beta+}$ group. Moreover, relatively higher precuneus-based FC with occipital areas was observed in the $SCD_{A\beta+}$ group. In the latter regions, FC value between precuneus and occipital areas showed positive linear associations with both global ($SCD_{A\beta+}$) and local precuneus amyloid load ($SCD_{A\beta+}$ and $SCD_{A\beta-}$).

4.2 Contributions of the studies to the field

The presented three studies in this thesis provide additional neuroimaging evidence for SCD plus proven AD pathology as an advanced preclinical stage of the Alzheimer's continuum, as it is now proposed in the NIA-AA research framework (Jack *et al.*, 2018). Accumulative neuroimaging evidence supports that SCD patients show atrophy in established brain regions showing early AD-related neurodegeneration, including hippocampal and CA1-subfield and entorhinal cortex (Jessen *et al.*, 2006; Perrotin *et al.*, 2015; Hu *et al.*, 2019; Scheef *et al.*, 2019). An earlier study was able to show that the volume of the posterior part of the Ch4p was already reduced in a population of SCD patients, as compared to HC, and that the volume loss was significant correlated with a reduced glucose metabolism as measured by FDG-PET (Scheef *et al.*, 2019). Even though the results were suggestive for a close relationship between structural damage of the cholinergic system and AD pathology (Scheef *et al.*, 2019), however the study was lacking any biomarker based evidence for AD. Based on the DELCODE cohort, the present study 1 extended the investigation of the cholinergic system by stratifying the examined sample with respect to CSF-based AD biomarkers. We also could replicae to a large extent the findings reported in the literature with respect to MCI and AD. Previous *post mortem* and in *vivo* MRI studies showed a BF volume

reductions in AD (Whitehouse *et al.*, 1982; Vogels *et al.*, 1990; Grothe *et al.*, 2012; Kilimann *et al.*, 2014; Machado *et al.*, 2020), with the most significant neuronal loss in Ch4p (Arendt *et al.*, 1985; Vogels *et al.*, 1990; Liu *et al.*, 2015). Moreover, volume reductions of BF were already shown in MCI based on the in vivo MRI studies (Grothe *et al.*, 2010; Teipel *et al.*, 2014). Study 1 first found almost all BF subnuclei presented volume reductions in AD, whereas in MCI patients, the volume reduction was confined to Ch4al and Ch4p, which confirmed the earlier findings (Grothe *et al.*, 2010; Teipel *et al.*, 2014). Study 1 extended the previous findings with regard to SCD and found that Ch4p atrophy already emerged in SCD with positive AD biomarkers at an early stage of AD pathogenesis, which was not found in the SCD subgroup with a negative biomarker status. This finding consists well with the assumption that incipient BF atrophy already begins in individuals with preclinical AD pathology (Schmitz *et al.*, 2016a; Fernandez-Cabello *et al.*, 2020) and indicates BF atrophy preferentially starts in Ch4p and subsequently spreads to other BF nucleus with progressing disease. The role of Ch4p in an early stage of AD was further supported by the finding that the Ch4p volume reductions was only found in amyloid-positive SCD, but not in amyloid-positive HC or amyloid-negative SCD. This result suggests that simultaneous presence of both SCD and CSF amyloid pathology associated with NBM. Even though it cannot be proven given the available data, the finding is highly suggestive for that the Ch4p atrophy may associate with the cognitive problems experienced by the participants. However, at least one can state that SCD and AD related-CSF pathology are highly associated with a beginning NBM degeneration. The notion is supported by Vogel *et al.* (2017) who found that brain Aβ and SCD contribute to the prediction of cognitive decline in a complementary manner. In the context of the recent NIA-AA Research Framework (Jack *et al.*, 2018), the atrophy of cholinergic BF in amyloid-positive SCD and the absence of any volume reductions in the Aβ-positive HC suggests that these 'subjective cognitive decline' symptoms reflect progression from stage 1 (asymptomatic) to stage 2 (transitional cognitive impairment) of the Alzheimer's continuum, indicating that a BF neurodegeneration might cannot be fully compensated any more. Therefore, SCD with CSF amyloid pathology seem to be a more promising target population for AD prevention/intervention trials than 'pure' amyloid-positive populations or SCD populations alone. The last but not least, a linear positive correlation was found with Aβ42/40 ratio in the SCD subgroup, but not in the HC. This finding is supported by AD-animal models (Beach, 2008; Bohnen *et al.*, 2018)

and post mortem studies in humans (Arendt *et al.*, 1985; Potter *et al.*, 2011) showing correlations between cortical amyloid accumulation and cholinergic system. Combined with previous studies (Arendt *et al.*, 1985; Potter *et al.*, 2011), this finding suggests that the mechanism of BF atrophy was associated closely with the neurotoxic effects of amyloid aggregation.

The second study focused on the functional consequences of the disturbance of the cholinergic system. Although the plethora of projections of the different BF subregions into different cortical and subcortical regions have been identified using direct axonal tracing technique in rodents and primates available (Kim *et al.*, 2015; Ballinger *et al.*, 2016; Golden *et al.*, 2016; Kim *et al.*, 2016; Kondo and Zaborszky, 2016; Li *et al.*, 2018), very limited studies using rs-fMRI have investigated in human data how the BF may functionally differentiate since direct axonal tracing studies are not applicable in humans (Markello *et al.*, 2018; Fritz *et al.*, 2019). In MCI, a previous studies found a decreased FC of Ch4 compared to HC group (Li *et al.*, 2017; Meng *et al.*, 2018). However, it remains unclear whether FC alterations of BF subregions (Ch4 and Ch1-3) already emerge in SCD compared to HC. Study 2 focused on this question. Moreover, CSF biomarker information for a substantial subgroup of this sample allowed to explore the interplay between CSF amyloid status and FC of BF changes in SCD and HC. Based on the DELCODE cohort, study 2 first found a decreased FC and a distinct pattern of FC alteration of Ch1-3/Ch4 connectivity in SCD individuals compared to HC. The brain regions with a reduced Ch4 connectivity were mainly located in left dorsal precuneus, superior parietal gyrus and bilateral superior and medial occipital gyrus. A previous study found more extensive brain regions showing decreased Ch4-FC in MCI (Meng *et al.*, 2018). The latter fits well to PET data showing reduced acetylcholine activity in these regions in MCI (Kuhl *et al.*, 1999; Herholz *et al.*, 2004). Study 2 extends these findings by showing that decreased Ch4-FC has already started in SCD. In addition, the found reduced FC between Ch4 and superior parietal gyrus fits well to the finding that the parietal cortex receives cholinergic input from Ch4 subfields (Mesulam *et al.*, 1983). It is also known that ChAT activity in the precuneus is reduced in AD (Ikonomovic *et al.*, 2011). Taking these points together, it appears to be reasonable to assume that the found reduced connectivity is likely to reflect the functional consequences of a cholinergic denervation in SCD. Even though the observed connectivity reduction of the cholinergic forebrain nuclei (except NBM) to

mainly temporal lobe regions was found only on an exploratory level, it fits well to known cholinergic projections of these nuclei (Mesulam *et al.*, 1983; Hedreen *et al.*, 1984; Fritz *et al.*, 2019; Yuan *et al.*, 2019). Even though the findings of study 2 fit well to the literature, it has to be noted that the reported FC alterations were not linked to the underlying CSF amyloid status. However, considering the inherently low statistical power of FC measures one cannot exclude that it may exists. But of course, before this has been explicitly shown, these findings have to be considered with caution.

One of the most interesting regions in SCD related AD-research is the precuneus. The precuneus is one of the earliest brain regions harboring amyloid deposition and is a key hub region of the DMN. Abnormal connectivity in the DMN is thought to be linked to amyloid-beta plaque-associated neuronal toxicity (Buckner *et al.*, 2005; Badhwar *et al.*, 2017). However, the links between cerebral Aβ accumulation and precuneus-based FC in SCD were rarely investigated so far. Therefore, study 3 focused on the question how cortical amyloid pathology relates to precuneus FC on a large as well as on a regional scale. Study 3 revealed that ReHo was significantly higher in the bilateral precuneus for the $SCD_{A\beta+}$ group compared to $SCD_{A\beta-}$ group. This result suggests that amyloid deposition in the brain in this stage is already associated with the alterations of this local connectivity marker. On the large-scale analysis, it was found that the functional connectivity of the precuneus with the occipital cortex was increased in $SCD_{A\beta+}$ group, and positively associated with the cortical Aβ load. This finding is in line with a study (Sheline *et al.*, 2010b) showing stronger precuneus-occipital connectivity in Aβ+ cognitively normal participants compared to Aβ-. An increased connectivity was also found in other SCD-cohorts – but unfortunately the cohorts reported on were not stratified with respect to AD biomarker status (Verfaillie *et al.*, 2018; Viviano *et al.*, 2019). Taken together with the increased ReHo in precuneus, the observed hyperconnectivity of the precuneus may reflect a local compensatory mechanism that helps to maintain normal behavioral performance under the influence of increasing amyloid burden in $SCD_{A\beta+}$ patients (Mormino *et al.*, 2011; Hafkemeijer *et al.*, 2013; Verfaillie *et al.*, 2018). However, this interpretation is needed to be cautious since we only found higher FC with worse cognitive performance in $SCD_{A\beta-}$ group. In summary, these findings in study 3 may indicate early alterations of precuneal neural activity in the SCD stage with positive biomarker evidence for amyloid pathology (NIA-AA stage 2 of the clinical AD continuum) and suggests resting-state FC to be a useful

neuroimaging biomarker for highlighting early brain functional consequences of AD pathology in SCD stage.

4.3 Methodological limitations and future prospects

Considering the small size of the BF nuclei, one methodological limitation is the limited spatial resolution of our imaging methods. In addition, the atlas used, is based on *post mortem* data from one single subject. However, the locations of the BF nuclei derived from this atlas are in good agreement with a cytoarchitectonical probability map derived from ten subjects (Zaborszky *et al.*, 2008; Grothe *et al.*, 2010; Kilimann *et al.*, 2014). The morphometric measures derived from MR seems to be robust enough to assess BF-alterations. In a pre-work, not shown here, I was able to show that the BF-volumes reported in the literature using a similar processing stream are largely reproducible across cohorts and scanners. In addition, morphological changes were found in those subnuclei which were proposed by the literature – without taking this prior knowledge into account when extraction the information from the data. Testing "nearby regions" (like the caudate nucleus or BA25) also supported that the observed changes were specific to the BF, and not based on global effects.

When analyzing volumetry data derived from standard MR one has to keep in mind that this method is not suited to distinguish between cell death, glial or neural loss or reduction of extracellular space. The words 'atrophy' or 'volume loss' are not used as histological or histo-pathological sense. MR-volumetry catches any structural changes altering the MR signal in a voxel. These can be changes on a microscopic or macroscopic level and are not specific of any tissue changes. Therefore, the wordings 'atrophy' or 'volume' loss are only descriptive terms in this context. They describe the observation of a locally reduced probability to attribute a certain voxel to belong to the GM partition. This can be caused by any process that alters local signal intensity as well as morphological changes. However, considering the findings using this voxel based morphometry method across diseases reported throughout the literature, the findings are in good agreement with histological data, indirectly justifying using these terms. However, one always has to keep in mind that these terms ('atrophy', 'volume loss') are used as abbreviations and include already an interpretation for MRI signal changes but are not based on histological evidence.

With regard to the reported PET-data, one has to note that the classification between visual reading and application of previously established global SUVR cut-offs was not

perfectly consistent. However, it is known that the consistency between visual reading and classification with global SUVR cut-offs is high (>85%), but not perfect (Bullich *et al.*, 2017). Unfortunately, the number of cases showing these inconsistencies was too low to further investigate if these ambiguous cases share any AD-related feature leading to these inconsistencies. An additional draw back of the PET substudy is the lack of a proven AD-biomarker negative healthy control group. Therefore, it remains speculative if the observed hyperconnectivity of FC in $SCD_{A\beta+}$ reflects a true hyperconnectivity. However, for ethical and radiation protective reasons, the healthy control group did not undergo the PET procedure.

There are two general limitations, one refers to the group sizes and one to the overall design. One important aspect of SCD research is the (sub)group stratification according to AD-biomarker. In the presented studies this leads to drastically reduces group sizes and -as a consequence – a reduction in statistical power. Even though the DELCODE cohort is large and this information is collected in a high percentage, only a limited number of probes were available, when the MR-analysis were conducted. For this reason, it was not possible to investigate the different roles of amyloid and tau in SCD. Even though information on CSF-tau was available, it was not further taking into account because it would have led to further split up the groups into very small groups (n<10). Therefore, a further subgroup analysis according to both amyloid and tau pathology was precluded. With respect to the overall design, it is a drawback of this study that only cross-sectional data were available. It would be very interesting to follow BF volume alterations and cognitive changes over time and try to associate these with certain aspect of the AD trajectory. However, this has to be explored in future studies, as the collection of follow-up data in DELCODE is still ongoing.

4.4 Conclusion

This thesis comprises three investigations of structural and functional MRI markers in individuals with SCD taking proven AD-biomarkers into account. The presented studies are based on the DELCODE project, but differ with respect to target brain regions, analysis techniques and research objectives. Taking the CSF-amyloid status into account a Ch4p volume reduction could be directly linked to AD pathology and SCD. These results clearly show that neither the existence of amyloid alone explains SCD nor that SCD is necessarily connected with AD. SCD in general is not a stage of preclinical AD by its own. But the presented data clearly show, that within the AD

continuum, SCD appears to be a hallmark on the AD-trajectory marking the point when neurodegenerative process begins to exceed a level that can't be functionally compensated. It seems that SCD in amyloid positive individuals reflects the progression from stage 1 (asymptomatic) to stage 2 (transitional cognitive impairment) of the Alzheimer's continuum. The cholinergic system, especially the posterior part of the NBM (Ch4p) seems to play a key role in this process – which affects not only memory processes but has also a " long range effect". The decreased Ch4-FC with left dorsal precuneus, superior parietal gyrus and bilateral occipital gyrus -even though independent of amyloid pathology- may directly reflect the functional consequences of the BF cholinergic denervation. The changes observed in the DMN connectivity related to cortical amyloid deposition further consolidated this "decompensation" hypothesis – however also raises the question if these changes might be not caused by a cortical amyloidosis but causing the accumulation of amyloid. Analyzing longitudinal changes and taking tau into account, might help to answer this question in the future.

5 Abstract

Subjective Cognitive Decline (SCD) is increasingly recognized as an efficient concept to study in an early preclinical stage of Alzheimer's disease (AD). It is marked by a perceived subjective worsening of cognitive function compared to the earlier performance level without noticeable impairments in standard neuro-psychological testing. Even though SCD individuals do not necessarily share the same underlying AD pathology, a variety of studies have identified an increased AD biomarker positivity and risk to develop clinical AD. SCD also show atrophy in regions that are known to be vulnerable to AD-pathology (i.e. hippocampus, entorhinal cortex, precuneus). Recent studies suggest that cholinergic basal forebrain (BF) volume loss even precedes degeneration of the entorhinal cortex.

This thesis focusses on the question how BF-atrophy relates to amyloid pathology in SCD and healthy controls and tried to further investigate the functional consequences as assessable by resting state functional MRI. The three conducted studies are based on German Center for Neurodegenerative Diseases Longitudinal Cognitive Impairment and Dementia Study (DELCODE) project. Study 1 examined cholinergic BF volume alterations in SCD. A significant interaction between diagnosis (SCD vs. Healthy control [HC]) and CSF amyloid status was found, with posterior of NBM volume reductions only in amyloid-positive SCD. The observed volume reduction of the cholinergic BF in amyloid-positive SCD and the absence of any volume reductions in the amyloid-positive HC suggests that SCD plus amyloid pathology reflects an advanced stage of preclinical AD, revealing the beginning neurodegeneration on a macroscopic level. The second study revealed that the degeneration of the BF alters the functional connectivity to certain cortical brain regions. More or less the overall trend observed was a reduced connectivity. Based on a group stratification with respect to cortical amyloid deposition, the alteration of the functional connectivity of the precuneus was investigated in Study 3. Compared to amyloid-negative SCD, significantly higher regional homogeneity within the precuneus was found for amyloid-positive SCD as well as a higher FC to occipital areas.

Taking everything together, the presented data indicate that the cholinergic system, especially the posterior part of the NBM (Ch4p) seems to play a key role in the very early stage of AD. It affects not only memory processes but has also a 'long range effect' leading to decreased FC. SCD appears to be a hallmark on the AD-trajectory

marking the point when neurodegenerative process begins to exceed a level that can't be functionally compensated, and therefore amyloid-positive SCD might reflect the progression from an asymptomatic stage (stage 1) to stage 2 of the Alzheimer's continuum, where cognitive functions start to impairment.

6 List of figures

7 List of tables

8 References

Abdulrab K, Heun R. Subjective Memory Impairment. A review of its definitions indicates the need for a comprehensive set of standardised and validated criteria. Eur Psychiatry 2008; 23(5): 321-30.

Aizenstein HJ, Nebes RD, Saxton JA, Price JC, Mathis CA, Tsopelas ND*, et al.* Frequent amyloid deposition without significant cognitive impairment among the elderly. Arch Neurol 2008; 65(11): 1509-17.

Albert MS, DeKosky ST, Dickson D, Dubois B, Feldman HH, Fox NC*, et al.* The diagnosis of mild cognitive impairment due to Alzheimer's disease: recommendations from the National Institute on Aging-Alzheimer's Association workgroups on diagnostic guidelines for Alzheimer's disease. Alzheimers Dement 2011; 7(3): 270-9.

Alzheimer's Association. 2020 Alzheimer's disease facts and figures. Alzheimers Dement 2020.

Alzheimer A, Stelzmann RA, Schnitzlein HN, Murtagh FR. An English translation of Alzheimer's 1907 paper, "Uber eine eigenartige Erkankung der Hirnrinde". Clin Anat 1995; 8(6): 429-31.

Amariglio RE, Becker JA, Carmasin J, Wadsworth LP, Lorius N, Sullivan C*, et al.* Subjective cognitive complaints and amyloid burden in cognitively normal older individuals. Neuropsychologia 2012; 50(12): 2880-6.

Anstey KJ, Cherbuin N, Budge M, Young J. Body mass index in midlife and late-life as a risk factor for dementia: a meta-analysis of prospective studies. Obes Rev 2011; 12(5): e426-37.

Arendt T, Bigl V, Tennstedt A, Arendt A. Neuronal loss in different parts of the nucleus basalis is related to neuritic plaque formation in cortical target areas in Alzheimer's disease. Neuroscience 1985; 14(1): 1-14.

Ashburner J. A fast diffeomorphic image registration algorithm. Neuroimage 2007; 38(1): 95-113.

Ashburner J, Friston KJ. Unified segmentation. Neuroimage 2005; 26(3): 839-51.

Auerbach JM, Segal M. A novel cholinergic induction of long-term potentiation in rat hippocampus. J Neurophysiol 1994; 72(4): 2034-40.

Badhwar A, Tam A, Dansereau C, Orban P, Hoffstaedter F, Bellec P. Resting-state network dysfunction in Alzheimer's disease: A systematic review and meta-analysis. Alzheimers Dement (Amst) 2017; 8: 73-85.

Bai F, Zhang Z, Yu H, Shi Y, Yuan Y, Zhu W*, et al.* Default-mode network activity distinguishes amnestic type mild cognitive impairment from healthy aging: a combined structural and resting-state functional MRI study. Neurosci Lett 2008; 438(1): 111-5.

Ballinger EC, Ananth M, Talmage DA, Role LW. Basal Forebrain Cholinergic Circuits and Signaling in Cognition and Cognitive Decline. Neuron 2016; 91(6): 1199-218.

Barthel H, Gertz HJ, Dresel S, Peters O, Bartenstein P, Buerger K*, et al.* Cerebral amyloid-beta PET with florbetaben (18F) in patients with Alzheimer's disease and healthy controls: a multicentre phase 2 diagnostic study. Lancet Neurol 2011a; 10(5): 424-35.

Barthel H, Luthardt J, Becker G, Patt M, Hammerstein E, Hartwig K*, et al.* Individualized quantification of brain beta-amyloid burden: results of a proof of mechanism phase 0 florbetaben PET trial in patients with Alzheimer's disease and healthy controls. Eur J Nucl Med Mol Imaging 2011b; 38(9): 1702-14.

Bateman RJ, Xiong C, Benzinger TL, Fagan AM, Goate A, Fox NC*, et al.* Clinical and biomarker changes in dominantly inherited Alzheimer's disease. N Engl J Med 2012; 367(9): 795-804.

Beach TG. Physiologic origins of age-related beta-amyloid deposition. Neurodegener Dis 2008; 5(3-4): 143-5.

Beach TG, Honer WG, Hughes LH. Cholinergic fibre loss associated with diffuse plaques in the non-demented elderly: the preclinical stage of Alzheimer's disease? Acta Neuropathol 1997; 93(2): 146-53.

Beach TG, McGeer EG. Senile plaques, amyloid beta-protein, and acetylcholinesterase fibres: laminar distributions in Alzheimer's disease striate cortex. Acta Neuropathol 1992; 83(3): 292-9.

Bell PT, Shine JM. Subcortical contributions to large-scale network communication. Neurosci Biobehav Rev 2016; 71: 313-22.

Benzinger TL, Blazey T, Jack CR, Jr., Koeppe RA, Su Y, Xiong C*, et al.* Regional variability of imaging biomarkers in autosomal dominant Alzheimer's disease. Proc Natl Acad Sci U S A 2013; 110(47): E4502-9.

Berger-Sweeney J, Heckers S, Mesulam MM, Wiley RG, Lappi DA, Sharma M. Differential effects on spatial navigation of immunotoxin-induced cholinergic lesions of the medial septal area and nucleus basalis magnocellularis. J Neurosci 1994; 14(7): 4507-19.

Bero AW, Yan P, Roh JH, Cirrito JR, Stewart FR, Raichle ME*, et al.* Neuronal activity regulates the regional vulnerability to amyloid-beta deposition. Nat Neurosci 2011; 14(6): 750-6.

Bickel H, Kurz A. Education, occupation, and dementia: the Bavarian school sisters study. Dement Geriatr Cogn Disord 2009; 27(6): 548-56.

Bird TD. Early-Onset Familial Alzheimer Disease - ARCHIVED CHAPTER, FOR HISTORICAL REFERENCE ONLY. In: Adam MP, Ardinger HH, Pagon RA, Wallace SE, Bean LJH, Stephens K*, et al.*, editors. GeneReviews((R)). Seattle (WA); 1993.

Biswal B, Hudetz AG, Yetkin FZ, Haughton VM, Hyde JS. Hypercapnia reversibly suppresses low-frequency fluctuations in the human motor cortex during rest using echo-planar MRI. J Cereb Blood Flow Metab 1997; 17(3): 301-8.

Biswal B, Yetkin FZ, Haughton VM, Hyde JS. Functional connectivity in the motor cortex of resting human brain using echo-planar MRI. Magn Reson Med 1995; 34(4): 537-41.

Bloem B, Poorthuis RB, Mansvelder HD. Cholinergic modulation of the medial prefrontal cortex: the role of nicotinic receptors in attention and regulation of neuronal activity. Front Neural Circuits 2014; 8: 17.

Bloom GS. Amyloid-beta and tau: the trigger and bullet in Alzheimer disease pathogenesis. JAMA Neurol 2014; 71(4): 505-8.

Bohnen NI, Grothe MJ, Ray NJ, Muller M, Teipel SJ. Recent advances in cholinergic imaging and cognitive decline-Revisiting the cholinergic hypothesis of dementia. Curr Geriatr Rep 2018; 7(1): 1-11.

Braak H, Braak E. Neuropathological stageing of Alzheimer-related changes. Acta Neuropathol 1991; 82(4): 239-59.

Bryan KJ, Lee H, Perry G, Smith MA, Casadesus G. Transgenic Mouse Models of Alzheimer's Disease: Behavioral Testing and Considerations. In: nd, Buccafusco JJ, editors. Methods of Behavior Analysis in Neuroscience. Boca Raton (FL); 2009.

Bu G. Apolipoprotein E and its receptors in Alzheimer's disease: pathways, pathogenesis and therapy. Nat Rev Neurosci 2009; 10(5): 333-44.

Buckley RF, Maruff P, Ames D, Bourgeat P, Martins RN, Masters CL*, et al.* Subjective memory decline predicts greater rates of clinical progression in preclinical Alzheimer's disease. Alzheimers Dement 2016; 12(7): 796-804.

Buckner RL, Snyder AZ, Shannon BJ, LaRossa G, Sachs R, Fotenos AF*, et al.* Molecular, structural, and functional characterization of Alzheimer's disease: evidence for a relationship between default activity, amyloid, and memory. J Neurosci 2005; 25(34): 7709-17.

Buerger K, Ewers M, Pirttila T, Zinkowski R, Alafuzoff I, Teipel SJ*, et al.* CSF phosphorylated tau protein correlates with neocortical neurofibrillary pathology in Alzheimer's disease. Brain 2006; 129(Pt 11): 3035-41.

Bullich S, Seibyl J, Catafau AM, Jovalekic A, Koglin N, Barthel H*, et al.* Optimized classification of 18F-Florbetaben PET scans as positive and negative using an SUVR quantitative approach and comparison to visual assessment. NeuroImage: Clinical 2017; 15: 325-32.

Burns A, Iliffe S. Alzheimer's disease. BMJ 2009; 338: b158.

Butler T, Blackmon K, Zaborszky L, Wang X, DuBois J, Carlson C*, et al.* Volume of the human septal forebrain region is a predictor of source memory accuracy. J Int Neuropsychol Soc 2012; 18(1): 157-61.

Cantero JL, Atienza M, Lage C, Zaborszky L, Vilaplana E, Lopez-Garcia S*, et al.* Atrophy of Basal Forebrain Initiates with Tau Pathology in Individuals at Risk for Alzheimer's Disease. Cereb Cortex 2020; 30(4): 2083-98.

Caselli RJ, Dueck AC, Osborne D, Sabbagh MN, Connor DJ, Ahern GL*, et al.* Longitudinal modeling of age-related memory decline and the APOE epsilon4 effect. N Engl J Med 2009; 361(3): 255-63.

Chen GF, Xu TH, Yan Y, Zhou YR, Jiang Y, Melcher K*, et al.* Amyloid beta: structure, biology and structure-based therapeutic development. Acta Pharmacol Sin 2017; 38(9): 1205-35.

Chetelat G, Desgranges B, de la Sayette V, Viader F, Eustache F, Baron JC. Mild cognitive impairment: Can FDG-PET predict who is to rapidly convert to Alzheimer's disease? Neurology 2003; 60(8): 1374-7.

Chiesa PA, Cavedo E, Grothe MJ, Houot M, Teipel SJ, Potier MC*, et al.* Relationship between Basal Forebrain Resting-State Functional Connectivity and Brain Amyloid-beta Deposition in Cognitively Intact Older Adults with Subjective Memory Complaints. Radiology 2019; 290(1): 167-76.

Cirrito JR, Yamada KA, Finn MB, Sloviter RS, Bales KR, May PC*, et al.* Synaptic activity regulates interstitial fluid amyloid-beta levels in vivo. Neuron 2005; 48(6): 913-22.

Citron M. Alzheimer's disease: strategies for disease modification. Nat Rev Drug Discov 2010; 9(5): 387-98.

Corder EH, Saunders AM, Strittmatter WJ, Schmechel DE, Gaskell PC, Small GW*, et al.* Gene dose of apolipoprotein E type 4 allele and the risk of Alzheimer's disease in late onset families. Science 1993; 261(5123): 921-3.

Damoiseaux JS, Rombouts SA, Barkhof F, Scheltens P, Stam CJ, Smith SM*, et al.* Consistent resting-state networks across healthy subjects. Proc Natl Acad Sci U S A 2006; 103(37): 13848-53.

De Santi S, de Leon MJ, Rusinek H, Convit A, Tarshish CY, Roche A*, et al.* Hippocampal formation glucose metabolism and volume losses in MCI and AD. Neurobiol Aging 2001; 22(4): 529-39.

Deng Y, Shi L, Lei Y, Liang P, Li K, Chu WC*, et al.* Mapping the "What" and "Where" Visual Cortices and Their Atrophy in Alzheimer's Disease: Combined Activation Likelihood Estimation with Voxel-Based Morphometry. Front Hum Neurosci 2016; 10: 333.

Derflinger S, Sorg C, Gaser C, Myers N, Arsic M, Kurz A*, et al.* Grey-matter atrophy in Alzheimer's disease is asymmetric but not lateralized. J Alzheimers Dis 2011; 25(2): 347-57.

Deutsch JA. The cholinergic synapse and the site of memory. Science 1971; 174(4011): 788-94.

Dickerson BC, Goncharova I, Sullivan MP, Forchetti C, Wilson RS, Bennett DA*, et al.* MRI-derived entorhinal and hippocampal atrophy in incipient and very mild Alzheimer's disease. Neurobiol Aging 2001; 22(5): 747-54.

Dillen KNH, Jacobs HIL, Kukolja J, Richter N, von Reutern B, Onur OA*, et al.* Functional Disintegration of the Default Mode Network in Prodromal Alzheimer's Disease. J Alzheimers Dis 2017; 59(1): 169-87.

Donovan NJ, Amariglio RE, Zoller AS, Rudel RK, Gomez-Isla T, Blacker D*, et al.* Subjective cognitive concerns and neuropsychiatric predictors of progression to the early clinical stages of Alzheimer disease. Am J Geriatr Psychiatry 2014; 22(12): 1642-51.

Drachman DA. Memory and cognitive function in man: does the cholinergic system have a specific role? Neurology 1977; 27(8): 783-90.

Drachman DA, Leavitt J. Human memory and the cholinergic system. A relationship to aging? Arch Neurol 1974; 30(2): 113-21.

Drzezga A, Becker JA, Van Dijk KR, Sreenivasan A, Talukdar T, Sullivan C*, et al.* Neuronal dysfunction and disconnection of cortical hubs in non-demented subjects with elevated amyloid burden. Brain 2011; 134(Pt 6): 1635-46.

Drzezga A, Lautenschlager N, Siebner H, Riemenschneider M, Willoch F, Minoshima S*, et al.* Cerebral metabolic changes accompanying conversion of mild cognitive impairment into Alzheimer's disease: a PET follow-up study. Eur J Nucl Med Mol Imaging 2003; 30(8): 1104-13.

Dufouil C, Fuhrer R, Alperovitch A. Subjective cognitive complaints and cognitive decline: consequence or predictor? The epidemiology of vascular aging study. J Am Geriatr Soc 2005; 53(4): 616-21.

Eickhoff SB, Stephan KE, Mohlberg H, Grefkes C, Fink GR, Amunts K*, et al.* A new SPM toolbox for combining probabilistic cytoarchitectonic maps and functional imaging data. Neuroimage 2005; 25(4): 1325-35.

Ellis JM. Cholinesterase inhibitors in the treatment of dementia. J Am Osteopath Assoc 2005; 105(3): 145-58.

Englot DJ, D'Haese PF, Konrad PE, Jacobs ML, Gore JC, Abou-Khalil BW*, et al.* Functional connectivity disturbances of the ascending reticular activating system in temporal lobe epilepsy. J Neurol Neurosurg Psychiatry 2017; 88(11): 925-32.

Eskildsen SF, Coupe P, Garcia-Lorenzo D, Fonov V, Pruessner JC, Collins DL*, et al.* Prediction of Alzheimer's disease in subjects with mild cognitive impairment from the ADNI cohort using patterns of cortical thinning. Neuroimage 2013; 65: 511-21.

Fernandez-Cabello S, Kronbichler M, Van Dijk KRA, Goodman JA, Spreng RN, Schmitz TW*, et al.* Basal forebrain volume reliably predicts the cortical spread of Alzheimer's degeneration. Brain 2020; 143(3): 993-1009.

Fleisher AS, Chen K, Quiroz YT, Jakimovich LJ, Gutierrez Gomez M, Langois CM*, et al.* Associations between biomarkers and age in the presenilin 1 E280A autosomal dominant Alzheimer disease kindred: a cross-sectional study. JAMA Neurol 2015; 72(3): 316-24.

Foster NL, Chase TN, Fedio P, Patronas NJ, Brooks RA, Di Chiro G. Alzheimer's disease: focal cortical changes shown by positron emission tomography. Neurology 1983; 33(8): 961-5.

Friston KJ, Williams S, Howard R, Frackowiak RS, Turner R. Movement-related effects in fMRI time-series. Magn Reson Med 1996; 35(3): 346-55.

Fritz HJ, Ray N, Dyrba M, Sorg C, Teipel S, Grothe MJ. The corticotopic organization of the human basal forebrain as revealed by regionally selective functional connectivity profiles. Hum Brain Mapp 2019; 40(3): 868-78.

Galani R, Lehmann O, Bolmont T, Aloy E, Bertrand F, Lazarus C*, et al.* Selective immunolesions of CH4 cholinergic neurons do not disrupt spatial memory in rats. Physiol Behav 2002; 76(1): 75-90.

Geula C, Mesulam MM. Cortical cholinergic fibers in aging and Alzheimer's disease: a morphometric study. Neuroscience 1989; 33(3): 469-81.

Geula C, Mesulam MM. Systematic regional variations in the loss of cortical cholinergic fibers in Alzheimer's disease. Cereb Cortex 1996; 6(2): 165-77.

Geula C, Nagykery N, Nicholas A, Wu CK. Cholinergic neuronal and axonal abnormalities are present early in aging and in Alzheimer disease. J Neuropathol Exp Neurol 2008; 67(4): 309-18.

Gifford KA, Liu D, Lu Z, Tripodis Y, Cantwell NG, Palmisano J*, et al.* The source of cognitive complaints predicts diagnostic conversion differentially among nondemented older adults. Alzheimers Dement 2014; 10(3): 319-27.

Glenner GG, Wong CW. Alzheimer's disease: initial report of the purification and characterization of a novel cerebrovascular amyloid protein. Biochem Biophys Res Commun 1984; 120(3): 885-90.

Goedert M, Wischik CM, Crowther RA, Walker JE, Klug A. Cloning and sequencing of the cDNA encoding a core protein of the paired helical filament of Alzheimer disease: identification as the microtubule-associated protein tau. Proc Natl Acad Sci U S A 1988; 85(11): 4051-5.

Golden SA, Heshmati M, Flanigan M, Christoffel DJ, Guise K, Pfau ML*, et al.* Basal forebrain projections to the lateral habenula modulate aggression reward. Nature 2016; 534(7609): 688-92.

Goldman JS, Hahn SE, Catania JW, LaRusse-Eckert S, Butson MB, Rumbaugh M*, et al.* Genetic counseling and testing for Alzheimer disease: joint practice

guidelines of the American College of Medical Genetics and the National Society of Genetic Counselors. Genet Med 2011; 13(6): 597-605.

Good CD, Johnsrude IS, Ashburner J, Henson RN, Friston KJ, Frackowiak RS. A voxel-based morphometric study of ageing in 465 normal adult human brains. Neuroimage 2001; 14(1 Pt 1): 21-36.

Gravina SA, Ho L, Eckman CB, Long KE, Otvos L, Jr., Younkin LH*, et al.* Amyloid beta protein (A beta) in Alzheimer's disease brain. Biochemical and immunocytochemical analysis with antibodies specific for forms ending at A beta 40 or A beta 42(43). J Biol Chem 1995; 270(13): 7013-6.

Greicius MD, Srivastava G, Reiss AL, Menon V. Default-mode network activity distinguishes Alzheimer's disease from healthy aging: evidence from functional MRI. Proc Natl Acad Sci U S A 2004; 101(13): 4637-42.

Gritton HJ, Howe WM, Mallory CS, Hetrick VL, Berke JD, Sarter M. Cortical cholinergic signaling controls the detection of cues. Proc Natl Acad Sci U S A 2016; 113(8): E1089-97.

Grothe M, Heinsen H, Teipel SJ. Atrophy of the cholinergic Basal forebrain over the adult age range and in early stages of Alzheimer's disease. Biol Psychiatry 2012; 71(9): 805-13.

Grothe M, Zaborszky L, Atienza M, Gil-Neciga E, Rodriguez-Romero R, Teipel SJ*, et al.* Reduction of basal forebrain cholinergic system parallels cognitive impairment in patients at high risk of developing Alzheimer's disease. Cereb Cortex 2010; 20(7): 1685-95.

Grothe MJ, Ewers M, Krause B, Heinsen H, Teipel SJ, Alzheimer's Disease Neuroimaging I. Basal forebrain atrophy and cortical amyloid deposition in nondemented elderly subjects. Alzheimers Dement 2014; 10(5 Suppl): S344-53.

Grothe MJ, Heinsen H, Amaro E, Jr., Grinberg LT, Teipel SJ. Cognitive Correlates of Basal Forebrain Atrophy and Associated Cortical Hypometabolism in Mild Cognitive Impairment. Cereb Cortex 2016; 26(6): 2411-26.

Gu L, Guo Z. Alzheimer's Abeta42 and Abeta40 peptides form interlaced amyloid fibrils. J Neurochem 2013; 126(3): 305-11.

Gyure KA, Durham R, Stewart WF, Smialek JE, Troncoso JC. Intraneuronal abeta-amyloid precedes development of amyloid plaques in Down syndrome. Arch Pathol Lab Med 2001; 125(4): 489-92.

Haass C, Lemere CA, Capell A, Citron M, Seubert P, Schenk D*, et al.* The Swedish mutation causes early-onset Alzheimer's disease by beta-secretase cleavage within the secretory pathway. Nat Med 1995; 1(12): 1291-6.

Hafkemeijer A, Altmann-Schneider I, Oleksik AM, van de Wiel L, Middelkoop HA, van Buchem MA*, et al.* Increased functional connectivity and brain atrophy in elderly with subjective memory complaints. Brain Connect 2013; 3(4): 353-62.

Hafkemeijer A, van der Grond J, Rombouts SA. Imaging the default mode network in aging and dementia. Biochim Biophys Acta 2012; 1822(3): 431-41.

Hansson O, Zetterberg H, Buchhave P, Andreasson U, Londos E, Minthon L*, et al.* Prediction of Alzheimer's disease using the CSF Abeta42/Abeta40 ratio in patients with mild cognitive impairment. Dement Geriatr Cogn Disord 2007; 23(5): 316-20.

Hardy J, Selkoe DJ. The amyloid hypothesis of Alzheimer's disease: progress and problems on the road to therapeutics. Science 2002; 297(5580): 353-6.

Hardy JA, Higgins GA. Alzheimer's disease: the amyloid cascade hypothesis. Science 1992; 256(5054): 184-5.

Hartikainen P, Rasanen J, Julkunen V, Niskanen E, Hallikainen M, Kivipelto M*, et al.* Cortical thickness in frontotemporal dementia, mild cognitive impairment, and Alzheimer's disease. J Alzheimers Dis 2012; 30(4): 857-74.

He Y, Wang L, Zang Y, Tian L, Zhang X, Li K*, et al.* Regional coherence changes in the early stages of Alzheimer's disease: a combined structural and resting-state functional MRI study. Neuroimage 2007; 35(2): 488-500.

Hebert LE, Weuve J, Scherr PA, Evans DA. Alzheimer disease in the United States (2010-2050) estimated using the 2010 census. Neurology 2013; 80(19): 1778-83.

Hedden T, Van Dijk KR, Becker JA, Mehta A, Sperling RA, Johnson KA*, et al.* Disruption of functional connectivity in clinically normal older adults harboring amyloid burden. J Neurosci 2009; 29(40): 12686-94.

Hedreen JC, Struble RG, Whitehouse PJ, Price DL. Topography of the magnocellular basal forebrain system in human brain. J Neuropathol Exp Neurol 1984; 43(1): 1-21.

Heneka MT, Carson MJ, El Khoury J, Landreth GE, Brosseron F, Feinstein DL*, et al.* Neuroinflammation in Alzheimer's disease. Lancet Neurol 2015; 14(4): 388-405.

Henneman WJ, Sluimer JD, Barnes J, van der Flier WM, Sluimer IC, Fox NC*, et al.* Hippocampal atrophy rates in Alzheimer disease: added value over whole brain volume measures. Neurology 2009; 72(11): 999-1007.

Herholz K, Weisenbach S, Zundorf G, Lenz O, Schroder H, Bauer B*, et al.* In vivo study of acetylcholine esterase in basal forebrain, amygdala, and cortex in mild to moderate Alzheimer disease. Neuroimage 2004; 21(1): 136-43.

Herrero JL, Roberts MJ, Delicato LS, Gieselmann MA, Dayan P, Thiele A. Acetylcholine contributes through muscarinic receptors to attentional modulation in V1. Nature 2008; 454(7208): 1110-4.

Hippius H, Neundorfer G. The discovery of Alzheimer's disease. Dialogues Clin Neurosci 2003; 5(1): 101-8.

Hodges H, Allen Y, Kershaw T, Lantos PL, Gray JA, Sinden J. Effects of cholinergic-rich neural grafts on radial maze performance of rats after excitotoxic lesions of the forebrain cholinergic projection system--I. Amelioration of cognitive deficits by transplants into cortex and hippocampus but not into basal forebrain. Neuroscience 1991; 45(3): 587-607.

Hu X, Teunissen CE, Spottke A, Heneka MT, Duzel E, Peters O*, et al.* Smaller medial temporal lobe volumes in individuals with subjective cognitive decline and biomarker evidence of Alzheimer's disease-Data from three memory clinic studies. Alzheimers Dement 2019; 15(2): 185-93.

Huang Y, Mahley RW. Apolipoprotein E: structure and function in lipid metabolism, neurobiology, and Alzheimer's diseases. Neurobiol Dis 2014; 72 Pt A: 3-12.

Huang Y, Weisgraber KH, Mucke L, Mahley RW. Apolipoprotein E: diversity of cellular origins, structural and biophysical properties, and effects in Alzheimer's disease. J Mol Neurosci 2004; 23(3): 189-204.

Ikonomovic MD, Klunk WE, Abrahamson EE, Wuu J, Mathis CA, Scheff SW*, et al.* Precuneus amyloid burden is associated with reduced cholinergic activity in Alzheimer disease. Neurology 2011; 77(1): 39-47.

Inestrosa NC, Alvarez A, Perez CA, Moreno RD, Vicente M, Linker C*, et al.* Acetylcholinesterase accelerates assembly of amyloid-beta-peptides into Alzheimer's fibrils: possible role of the peripheral site of the enzyme. Neuron 1996; 16(4): 881-91.

Iwatsubo T, Odaka A, Suzuki N, Mizusawa H, Nukina N, Ihara Y. Visualization of A beta 42(43) and A beta 40 in senile plaques with end-specific A beta monoclonals: evidence that an initially deposited species is A beta 42(43). Neuron 1994; 13(1): 45-53.

Jack CR, Jr., Albert MS, Knopman DS, McKhann GM, Sperling RA, Carrillo MC*, et al.* Introduction to the recommendations from the National Institute on Aging-Alzheimer's Association workgroups on diagnostic guidelines for Alzheimer's disease. Alzheimers Dement 2011; 7(3): 257-62.

Jack CR, Jr., Bennett DA, Blennow K, Carrillo MC, Dunn B, Haeberlein SB*, et al.* NIA-AA Research Framework: Toward a biological definition of Alzheimer's disease. Alzheimers Dement 2018; 14(4): 535-62.

Jack CR, Jr., Knopman DS, Chetelat G, Dickson D, Fagan AM, Frisoni GB*, et al.* Suspected non-Alzheimer disease pathophysiology--concept and controversy. Nat Rev Neurol 2016; 12(2): 117-24.

Jack CR, Jr., Knopman DS, Jagust WJ, Shaw LM, Aisen PS, Weiner MW*, et al.* Hypothetical model of dynamic biomarkers of the Alzheimer's pathological cascade. Lancet Neurol 2010; 9(1): 119-28.

Jagust W, Reed B, Mungas D, Ellis W, Decarli C. What does fluorodeoxyglucose PET imaging add to a clinical diagnosis of dementia? Neurology 2007; 69(9): 871-7.

Janelidze S, Zetterberg H, Mattsson N, Palmqvist S, Vanderstichele H, Lindberg O*, et al.* CSF Abeta42/Abeta40 and Abeta42/Abeta38 ratios: better diagnostic markers of Alzheimer disease. Ann Clin Transl Neurol 2016; 3(3): 154-65.

Jansen WJ, Ossenkoppele R, Knol DL, Tijms BM, Scheltens P, Verhey FR*, et al.* Prevalence of cerebral amyloid pathology in persons without dementia: a meta-analysis. JAMA 2015; 313(19): 1924-38.

Jessen F, Amariglio RE, van Boxtel M, Breteler M, Ceccaldi M, Chetelat G*, et al.* A conceptual framework for research on subjective cognitive decline in preclinical Alzheimer's disease. Alzheimers Dement 2014a; 10(6): 844-52.

Jessen F, Feyen L, Freymann K, Tepest R, Maier W, Heun R*, et al.* Volume reduction of the entorhinal cortex in subjective memory impairment. Neurobiol Aging 2006; 27(12): 1751-6.

Jessen F, Spottke A, Boecker H, Brosseron F, Buerger K, Catak C*, et al.* Design and first baseline data of the DZNE multicenter observational study on predementia Alzheimer's disease (DELCODE). Alzheimers Res Ther 2018; 10(1): 15.

Jessen F, Wiese B, Bachmann C, Eifflaender-Gorfer S, Haller F, Kolsch H*, et al.* Prediction of dementia by subjective memory impairment: effects of severity and temporal association with cognitive impairment. Arch Gen Psychiatry 2010; 67(4): 414-22.

Jessen F, Wolfsgruber S, Wiese B, Bickel H, Mosch E, Kaduszkiewicz H*, et al.* AD dementia risk in late MCI, in early MCI, and in subjective memory impairment. Alzheimers Dement 2014b; 10(1): 76-83.

Jones DT, Knopman DS, Gunter JL, Graff-Radford J, Vemuri P, Boeve BF*, et al.* Cascading network failure across the Alzheimer's disease spectrum. Brain 2016; 139(2): 547-62.

Juva K, Verkkoniemi A, Viramo P, Polvikoski T, Kainulainen K, Kontula K*, et al.* Apolipoprotein E, cognitive function, and dementia in a general population aged 85 years and over. Int Psychogeriatr 2000; 12(3): 379-87.

Kang DW, Choi WH, Jung WS, Um YH, Lee CU, Lim HK. Impact of Amyloid Burden on Regional Functional Synchronization in the Cognitively Normal Older Adults. Scientific Reports 2017a; 7(1): 14690.

Kang DW, Choi WH, Jung WS, Um YH, Lee CU, Lim HK. Impact of Amyloid Burden on Regional Functional Synchronization in the Cognitively Normal Older Adults. Sci Rep 2017b; 7(1): 14690.

Kang J, Lemaire HG, Unterbeck A, Salbaum JM, Masters CL, Grzeschik KH*, et al.* The precursor of Alzheimer's disease amyloid A4 protein resembles a cell-surface receptor. Nature 1987; 325(6106): 733-6.

Kar S, Slowikowski SP, Westaway D, Mount HT. Interactions between beta-amyloid and central cholinergic neurons: implications for Alzheimer's disease. J Psychiatry Neurosci 2004; 29(6): 427-41.

Kepp KP. Ten Challenges of the Amyloid Hypothesis of Alzheimer's Disease. J Alzheimers Dis 2017; 55(2): 447-57.

Kilimann I, Grothe M, Heinsen H, Alho EJ, Grinberg L, Amaro E, Jr.*, et al.* Subregional basal forebrain atrophy in Alzheimer's disease: a multicenter study. J Alzheimers Dis 2014; 40(3): 687-700.

Kilimann I, Hausner L, Fellgiebel A, Filippi M, Wurdemann TJ, Heinsen H*, et al.* Parallel Atrophy of Cortex and Basal Forebrain Cholinergic System in Mild Cognitive Impairment. Cereb Cortex 2017; 27(3): 1841-8.

Killiany RJ, Hyman BT, Gomez-Isla T, Moss MB, Kikinis R, Jolesz F*, et al.* MRI measures of entorhinal cortex vs hippocampus in preclinical AD. Neurology 2002; 58(8): 1188-96.

Kim J, Basak JM, Holtzman DM. The role of apolipoprotein E in Alzheimer's disease. Neuron 2009; 63(3): 287-303.

Kim JH, Jung AH, Jeong D, Choi I, Kim K, Shin S*, et al.* Selectivity of Neuromodulatory Projections from the Basal Forebrain and Locus Ceruleus to Primary Sensory Cortices. J Neurosci 2016; 36(19): 5314-27.

Kim T, Thankachan S, McKenna JT, McNally JM, Yang C, Choi JH*, et al.* Cortically projecting basal forebrain parvalbumin neurons regulate cortical gamma band oscillations. Proc Natl Acad Sci U S A 2015; 112(11): 3535-40.

Kivipelto M, Helkala EL, Laakso MP, Hanninen T, Hallikainen M, Alhainen K*, et al.* Apolipoprotein E epsilon4 allele, elevated midlife total cholesterol level, and high midlife systolic blood pressure are independent risk factors for late-life Alzheimer disease. Ann Intern Med 2002; 137(3): 149-55.

Kivipelto M, Helkala EL, Laakso MP, Hanninen T, Hallikainen M, Alhainen K*, et al.* Midlife vascular risk factors and Alzheimer's disease in later life: longitudinal, population based study. BMJ 2001; 322(7300): 1447-51.

Klunk WE, Engler H, Nordberg A, Wang Y, Blomqvist G, Holt DP*, et al.* Imaging brain amyloid in Alzheimer's disease with Pittsburgh Compound-B. Ann Neurol 2004; 55(3): 306-19.

Klunk WE, Koeppe RA, Price JC, Benzinger TL, Devous MD, Sr., Jagust WJ*, et al.* The Centiloid Project: standardizing quantitative amyloid plaque estimation by PET. Alzheimers Dement 2015; 11(1): 1-15 e1-4.

Koch W, Teipel S, Mueller S, Benninghoff J, Wagner M, Bokde AL*, et al.* Diagnostic power of default mode network resting state fMRI in the detection of Alzheimer's disease. Neurobiol Aging 2012; 33(3): 466-78.

Kolisnyk B, Al-Onaizi M, Soreq L, Barbash S, Bekenstein U, Haberman N*, et al.* Cholinergic Surveillance over Hippocampal RNA Metabolism and Alzheimer's-Like Pathology. Cereb Cortex 2017; 27(7): 3553-67.

Kolisnyk B, Al-Onaizi MA, Xu J, Parfitt GM, Ostapchenko VG, Hanin G*, et al.* Cholinergic Regulation of hnRNPA2/B1 Translation by M1 Muscarinic Receptors. J Neurosci 2016; 36(23): 6287-96.

Kondo H, Zaborszky L. Topographic organization of the basal forebrain projections to the perirhinal, postrhinal, and entorhinal cortex in rats. J Comp Neurol 2016; 524(12): 2503-15.

Kosik KS, Joachim CL, Selkoe DJ. Microtubule-associated protein tau (tau) is a major antigenic component of paired helical filaments in Alzheimer disease. Proc Natl Acad Sci U S A 1986; 83(11): 4044-8.

Kuhl DE, Koeppe RA, Minoshima S, Snyder SE, Ficaro EP, Foster NL*, et al.* In vivo mapping of cerebral acetylcholinesterase activity in aging and Alzheimer's disease. Neurology 1999; 52(4): 691-9.

Kwong KK, Belliveau JW, Chesler DA, Goldberg IE, Weisskoff RM, Poncelet BP*, et al.* Dynamic magnetic resonance imaging of human brain activity during primary sensory stimulation. Proc Natl Acad Sci U S A 1992; 89(12): 5675-9.

LaFerla FM, Green KN, Oddo S. Intracellular amyloid-beta in Alzheimer's disease. Nat Rev Neurosci 2007; 8(7): 499-509.

Ledig C, Schuh A, Guerrero R, Heckemann RA, Rueckert D. Structural brain imaging in Alzheimer's disease and mild cognitive impairment: biomarker analysis and shared morphometry database. Sci Rep 2018; 8(1): 11258.

Leech R, Sharp DJ. The role of the posterior cingulate cortex in cognition and disease. Brain 2014; 137(Pt 1): 12-32.

Levy-Lahad E, Wasco W, Poorkaj P, Romano DM, Oshima J, Pettingell WH*, et al.* Candidate gene for the chromosome 1 familial Alzheimer's disease locus. Science 1995; 269(5226): 973-7.

Lewczuk P, Matzen A, Blennow K, Parnetti L, Molinuevo JL, Eusebi P*, et al.* Cerebrospinal Fluid Abeta42/40 Corresponds Better than Abeta42 to Amyloid PET in Alzheimer's Disease. J Alzheimers Dis 2017; 55(2): 813-22.

Li H, Jia X, Qi Z, Fan X, Ma T, Ni H*, et al.* Altered Functional Connectivity of the Basal Nucleus of Meynert in Mild Cognitive Impairment: A Resting-State fMRI Study. Front Aging Neurosci 2017; 9: 127.

Li S, Daamen M, Scheef L, Gaertner CF, Buchert R, Buchmann M*, et al.* Abnormal Regional and Global Connectivity Measures in Subjective Cognitive Decline Depending on Cerebral Amyloid Status. Journal of Alzheimer's Disease 2020; DOI 10.3233/JAD-200472.

Li SJ, Biswal B, Li Z, Risinger R, Rainey C, Cho JK*, et al.* Cocaine administration decreases functional connectivity in human primary visual and motor cortex as detected by functional MRI. Magn Reson Med 2000; 43(1): 45-51.

Li X, Yu B, Sun Q, Zhang Y, Ren M, Zhang X*, et al.* Generation of a whole-brain atlas for the cholinergic system and mesoscopic projectome analysis of basal forebrain cholinergic neurons. Proc Natl Acad Sci U S A 2018; 115(2): 415-20.

Liu AK, Chang RC, Pearce RK, Gentleman SM. Nucleus basalis of Meynert revisited: anatomy, history and differential involvement in Alzheimer's and Parkinson's disease. Acta Neuropathol 2015; 129(4): 527-40.

Liu Y, Wang K, Yu C, He Y, Zhou Y, Liang M*, et al.* Regional homogeneity, functional connectivity and imaging markers of Alzheimer's disease: a review of resting-state fMRI studies. Neuropsychologia 2008; 46(6): 1648-56.

Liu Z, Wei W, Bai L, Dai R, You Y, Chen S*, et al.* Exploring the patterns of acupuncture on mild cognitive impairment patients using regional homogeneity. PLoS One 2014; 9(6): e99335.

Long Z, Jing B, Yan H, Dong J, Liu H, Mo X*, et al.* A support vector machine-based method to identify mild cognitive impairment with multi-level characteristics of magnetic resonance imaging. Neuroscience 2016; 331: 169-76.

Lv H, Wang Z, Tong E, Williams LM, Zaharchuk G, Zeineh M*, et al.* Resting-State Functional MRI: Everything That Nonexperts Have Always Wanted to Know. AJNR Am J Neuroradiol 2018; 39(8): 1390-9.

Machado A, Ferreira D, Grothe MJ, Eyjolfsdottir H, Almqvist PM, Cavallin L*, et al.* The cholinergic system in subtypes of Alzheimer's disease: an in vivo longitudinal MRI study. Alzheimers Res Ther 2020; 12(1): 51.

Mahley RW, Rall SC, Jr. Apolipoprotein E: far more than a lipid transport protein. Annu Rev Genomics Hum Genet 2000; 1: 507-37.

Mak K, Yang F, Vinters HV, Frautschy SA, Cole GM. Polyclonals to beta-amyloid(1-42) identify most plaque and vascular deposits in Alzheimer cortex, but not striatum. Brain Res 1994; 667(1): 138-42.

Makris N, Goldstein JM, Kennedy D, Hodge SM, Caviness VS, Faraone SV*, et al.* Decreased volume of left and total anterior insular lobule in schizophrenia. Schizophr Res 2006; 83(2-3): 155-71.

Malone IB, Leung KK, Clegg S, Barnes J, Whitwell JL, Ashburner J*, et al.* Accurate automatic estimation of total intracranial volume: a nuisance variable with less nuisance. Neuroimage 2015; 104: 366-72.

Mann DM, Yates PO, Marcyniuk B. Changes in nerve cells of the nucleus basalis of Meynert in Alzheimer's disease and their relationship to ageing and to the accumulation of lipofuscin pigment. Mech Ageing Dev 1984; 25(1-2): 189-204.

Marchitelli R, Aiello M, Cachia A, Quarantelli M, Cavaliere C, Postiglione A*, et al.* Simultaneous resting-state FDG-PET/fMRI in Alzheimer Disease: Relationship between glucose metabolism and intrinsic activity. Neuroimage 2018; 176: 246-58.

Markello RD, Spreng RN, Luh WM, Anderson AK, De Rosa E. Segregation of the human basal forebrain using resting state functional MRI. Neuroimage 2018; 173: 287-97.

Marquez F, Yassa MA. Neuroimaging Biomarkers for Alzheimer's Disease. Mol Neurodegener 2019; 14(1): 21.

Masters CL, Simms G, Weinman NA, Multhaup G, McDonald BL, Beyreuther K. Amyloid plaque core protein in Alzheimer disease and Down syndrome. Proc Natl Acad Sci U S A 1985; 82(12): 4245-9.

Matsuda H, Shigemoto Y, Sato N. Neuroimaging of Alzheimer's disease: focus on amyloid and tau PET. Jpn J Radiol 2019; 37(11): 735-49.

Mattsson N, Palmqvist S, Stomrud E, Vogel J, Hansson O. Staging beta-Amyloid Pathology With Amyloid Positron Emission Tomography. JAMA Neurol 2019.

Mauch DH, Nagler K, Schumacher S, Goritz C, Muller EC, Otto A*, et al.* CNS synaptogenesis promoted by glia-derived cholesterol. Science 2001; 294(5545): 1354-7.

McKhann G, Drachman D, Folstein M, Katzman R, Price D, Stadlan EM. Clinical diagnosis of Alzheimer's disease: report of the NINCDS-ADRDA Work Group under the auspices of Department of Health and Human Services Task Force on Alzheimer's Disease. Neurology 1984; 34(7): 939-44.

McKhann GM, Knopman DS, Chertkow H, Hyman BT, Jack CR, Jr., Kawas CH*, et al.* The diagnosis of dementia due to Alzheimer's disease: recommendations from the National Institute on Aging-Alzheimer's Association workgroups on diagnostic guidelines for Alzheimer's disease. Alzheimers Dement 2011; 7(3): 263-9.

Meng D, Li X, Bauer M, Taylor JP, Auer DP, Alzheimer's Disease Neuroimaging I. Altered Nucleus Basalis Connectivity Predicts Treatment Response in Mild Cognitive Impairment. Radiology 2018; 289(3): 775-85.

Meng X, D'Arcy C. Education and dementia in the context of the cognitive reserve hypothesis: a systematic review with meta-analyses and qualitative analyses. PLoS One 2012; 7(6): e38268.

Mesulam M. The cholinergic lesion of Alzheimer's disease: pivotal factor or side show? Learn Mem 2004a; 11(1): 43-9.

Mesulam MM. The cholinergic innervation of the human cerebral cortex. Prog Brain Res 2004b; 145: 67-78.

Mesulam MM, Geula C. Nucleus basalis (Ch4) and cortical cholinergic innervation in the human brain: observations based on the distribution of acetylcholinesterase and choline acetyltransferase. J Comp Neurol 1988; 275(2): 216-40.

Mesulam MM, Mufson EJ, Levey AI, Wainer BH. Cholinergic innervation of cortex by the basal forebrain: cytochemistry and cortical connections of the septal area, diagonal band nuclei, nucleus basalis (substantia innominata), and hypothalamus in the rhesus monkey. J Comp Neurol 1983; 214(2): 170-97.

Mesulam MM, Mufson EJ, Wainer BH. Three-dimensional representation and cortical projection topography of the nucleus basalis (Ch4) in the macaque: concurrent demonstration of choline acetyltransferase and retrograde transport with a stabilized tetramethylbenzidine method for horseradish peroxidase. Brain Res 1986; 367(1-2): 301-8.

Mikl M, Marecek R, Hlustik P, Pavlicova M, Drastich A, Chlebus P*, et al.* Effects of spatial smoothing on fMRI group inferences. Magn Reson Imaging 2008; 26(4): 490-503.

Minoshima S, Cross DJ, Foster NL, Henry TR, Kuhl DE. Discordance between traditional pathologic and energy metabolic changes in very early Alzheimer's disease. Pathophysiological implications. Ann N Y Acad Sci 1999; 893: 350-2.

Minoshima S, Giordani B, Berent S, Frey KA, Foster NL, Kuhl DE. Metabolic reduction in the posterior cingulate cortex in very early Alzheimer's disease. Ann Neurol 1997; 42(1): 85-94.

Mintun MA, Larossa GN, Sheline YI, Dence CS, Lee SY, Mach RH*, et al.* [11C]PIB in a nondemented population: potential antecedent marker of Alzheimer disease. Neurology 2006; 67(3): 446-52.

Mitchell AJ, Beaumont H, Ferguson D, Yadegarfar M, Stubbs B. Risk of dementia and mild cognitive impairment in older people with subjective memory complaints: meta-analysis. Acta Psychiatr Scand 2014; 130(6): 439-51.

Moller HJ, Graeber MB. The case described by Alois Alzheimer in 1911. Historical and conceptual perspectives based on the clinical record and neurohistological sections. Eur Arch Psychiatry Clin Neurosci 1998; 248(3): 111-22.

Monsell SE, Mock C, Hassenstab J, Roe CM, Cairns NJ, Morris JC*, et al.* Neuropsychological changes in asymptomatic persons with Alzheimer disease neuropathology. Neurology 2014; 83(5): 434-40.

Mormino EC, Smiljic A, Hayenga AO, Onami SH, Greicius MD, Rabinovici GD*, et al.* Relationships between beta-amyloid and functional connectivity in different components of the default mode network in aging. Cereb Cortex 2011; 21(10): 2399-407.

Morris JC, Roe CM, Xiong C, Fagan AM, Goate AM, Holtzman DM*, et al.* APOE predicts amyloid-beta but not tau Alzheimer pathology in cognitively normal aging. Annals of Neurology 2010; 67(1): 122-31.

Mosconi L, De Santi S, Brys M, Tsui WH, Pirraglia E, Glodzik-Sobanska L*, et al.* Hypometabolism and altered cerebrospinal fluid markers in normal apolipoprotein E E4 carriers with subjective memory complaints. Biol Psychiatry 2008; 63(6): 609-18.

Murphy K, Fox MD. Towards a consensus regarding global signal regression for resting state functional connectivity MRI. Neuroimage 2017; 154: 169-73.

Murphy MP, LeVine H, 3rd. Alzheimer's disease and the amyloid-beta peptide. J Alzheimers Dis 2010; 19(1): 311-23.

Myers N, Pasquini L, Gottler J, Grimmer T, Koch K, Ortner M*, et al.* Within-patient correspondence of amyloid-beta and intrinsic network connectivity in Alzheimer's disease. Brain 2014; 137(Pt 7): 2052-64.

Nelissen N, Van Laere K, Thurfjell L, Owenius R, Vandenbulcke M, Koole M*, et al.* Phase 1 study of the Pittsburgh compound B derivative 18F-flutemetamol in healthy volunteers and patients with probable Alzheimer disease. J Nucl Med 2009; 50(8): 1251-9.

Nelson PT, Alafuzoff I, Bigio EH, Bouras C, Braak H, Cairns NJ*, et al.* Correlation of Alzheimer disease neuropathologic changes with cognitive status: a review of the literature. J Neuropathol Exp Neurol 2012; 71(5): 362-81.

Nelson PT, Head E, Schmitt FA, Davis PR, Neltner JH, Jicha GA*, et al.* Alzheimer's disease is not "brain aging": neuropathological, genetic, and epidemiological human studies. Acta Neuropathol 2011; 121(5): 571-87.

Ni L, Liu R, Yin Z, Zhao H, Nedelska Z, Hort J*, et al.* Aberrant Spontaneous Brain Activity in Patients with Mild Cognitive Impairment and concomitant Lacunar Infarction: A Resting-State Functional MRI Study. J Alzheimers Dis 2016; 50(4): 1243-54.

Nitsch RM, Slack BE, Wurtman RJ, Growdon JH. Release of Alzheimer amyloid precursor derivatives stimulated by activation of muscarinic acetylcholine receptors. Science 1992; 258(5080): 304-7.

Oakes TR, Fox AS, Johnstone T, Chung MK, Kalin N, Davidson RJ. Integrating VBM into the General Linear Model with voxelwise anatomical covariates. Neuroimage 2007; 34(2): 500-8.

Ogawa S, Lee TM, Nayak AS, Glynn P. Oxygenation-sensitive contrast in magnetic resonance image of rodent brain at high magnetic fields. Magn Reson Med 1990; 14(1): 68-78.

Pajula J, Tohka J. Effects of spatial smoothing on inter-subject correlation based analysis of FMRI. Magn Reson Imaging 2014; 32(9): 1114-24.

Palmqvist S, Scholl M, Strandberg O, Mattsson N, Stomrud E, Zetterberg H*, et al.* Earliest accumulation of beta-amyloid occurs within the default-mode network and concurrently affects brain connectivity. Nat Commun 2017; 8(1): 1214.

Papassotiropoulos A, Fountoulakis M, Dunckley T, Stephan DA, Reiman EM. Genetics, transcriptomics, and proteomics of Alzheimer's disease. J Clin Psychiatry 2006; 67(4): 652-70.

Parvizi J, Van Hoesen GW, Buckwalter J, Damasio A. Neural connections of the posteromedial cortex in the macaque. Proc Natl Acad Sci U S A 2006; 103(5): 1563-8.

Perrotin A, de Flores R, Lamberton F, Poisnel G, La Joie R, de la Sayette V*, et al.* Hippocampal Subfield Volumetry and 3D Surface Mapping in Subjective Cognitive Decline. J Alzheimers Dis 2015; 48 Suppl 1: S141-50.

Perry EK, Blessed G, Tomlinson BE, Perry RH, Crow TJ, Cross AJ*, et al.* Neurochemical activities in human temporal lobe related to aging and Alzheimer-type changes. Neurobiol Aging 1981; 2(4): 251-6.

Perry EK, Tomlinson BE, Blessed G, Bergmann K, Gibson PH, Perry RH. Correlation of cholinergic abnormalities with senile plaques and mental test scores in senile dementia. Br Med J 1978; 2(6150): 1457-9.

Philip NS, Kuras YI, Valentine TR, Sweet LH, Tyrka AR, Price LH*, et al.* Regional homogeneity and resting state functional connectivity: associations with exposure to early life stress. Psychiatry Res 2013; 214(3): 247-53.

Piaceri I, Nacmias B, Sorbi S. Genetics of familial and sporadic Alzheimer's disease. Front Biosci (Elite Ed) 2013; 5: 167-77.

Pike KE, Savage G, Villemagne VL, Ng S, Moss SA, Maruff P*, et al.* Beta-amyloid imaging and memory in non-demented individuals: evidence for preclinical Alzheimer's disease. Brain 2007; 130(Pt 11): 2837-44.

Pittel Z, Heldman E, Barg J, Haring R, Fisher A. Muscarinic control of amyloid precursor protein secretion in rat cerebral cortex and cerebellum. Brain Res 1996; 742(1-2): 299-304.

Possin KL. Visual spatial cognition in neurodegenerative disease. Neurocase 2010; 16(6): 466-87.

Potter PE, Rauschkolb PK, Pandya Y, Sue LI, Sabbagh MN, Walker DG*, et al.* Pre- and post-synaptic cortical cholinergic deficits are proportional to amyloid plaque presence and density at preclinical stages of Alzheimer's disease. Acta Neuropathol 2011; 122(1): 49-60.

Power JD, Barnes KA, Snyder AZ, Schlaggar BL, Petersen SE. Spurious but systematic correlations in functional connectivity MRI networks arise from subject motion. Neuroimage 2012; 59(3): 2142-54.

Querfurth HW, LaFerla FM. Alzheimer's disease. N Engl J Med 2010; 362(4): 329-44.

Raichle ME. The brain's default mode network. Annu Rev Neurosci 2015; 38: 433-47.

Rebeck GW, Kindy M, LaDu MJ. Apolipoprotein E and Alzheimer's disease: the protective effects of ApoE2 and E3. J Alzheimers Dis 2002; 4(3): 145-54.

Reiman EM, Caselli RJ, Yun LS, Chen K, Bandy D, Minoshima S*, et al.* Preclinical evidence of Alzheimer's disease in persons homozygous for the epsilon 4 allele for apolipoprotein E. N Engl J Med 1996; 334(12): 752-8.

Reisberg B, Ferris SH, de Leon MJ, Crook T. The Global Deterioration Scale for assessment of primary degenerative dementia. Am J Psychiatry 1982; 139(9): 1136-9.

Reisberg B, Gauthier S. Current evidence for subjective cognitive impairment (SCI) as the pre-mild cognitive impairment (MCI) stage of subsequently manifest Alzheimer's disease. Int Psychogeriatr 2008; 20(1): 1-16.

Reisberg B, Shulman MB, Torossian C, Leng L, Zhu W. Outcome over seven years of healthy adults with and without subjective cognitive impairment. Alzheimers Dement 2010; 6(1): 11-24.

Resnick SM, Sojkova J, Zhou Y, An Y, Ye W, Holt DP*, et al.* Longitudinal cognitive decline is associated with fibrillar amyloid-beta measured by [11C]PiB. Neurology 2010; 74(10): 807-15.

Ridley RM, Murray TK, Johnson JA, Baker HF. Learning impairment following lesion of the basal nucleus of Meynert in the marmoset: modification by cholinergic drugs. Brain Res 1986; 376(1): 108-16.

Rombouts SA, Barkhof F, Goekoop R, Stam CJ, Scheltens P. Altered resting state networks in mild cognitive impairment and mild Alzheimer's disease: an fMRI study. Hum Brain Mapp 2005; 26(4): 231-9.

Rombouts SA, Damoiseaux JS, Goekoop R, Barkhof F, Scheltens P, Smith SM*, et al.* Model-free group analysis shows altered BOLD FMRI networks in dementia. Hum Brain Mapp 2009; 30(1): 256-66.

Ronnlund M, Sundstrom A, Adolfsson R, Nilsson LG. Subjective memory impairment in older adults predicts future dementia independent of baseline memory performance: Evidence from the Betula prospective cohort study. Alzheimers Dement 2015; 11(11): 1385-92.

Roses AD. Apolipoprotein E alleles as risk factors in Alzheimer's disease. Annu Rev Med 1996; 47: 387-400.

Roy AK, Shehzad Z, Margulies DS, Kelly AM, Uddin LQ, Gotimer K*, et al.* Functional connectivity of the human amygdala using resting state fMRI. Neuroimage 2009; 45(2): 614-26.

Sabri O, Sabbagh MN, Seibyl J, Barthel H, Akatsu H, Ouchi Y*, et al.* Florbetaben PET imaging to detect amyloid beta plaques in Alzheimer's disease: phase 3 study. Alzheimers Dement 2015; 11(8): 964-74.

Sando SB, Melquist S, Cannon A, Hutton M, Sletvold O, Saltvedt I*, et al.* Risk-reducing effect of education in Alzheimer's disease. Int J Geriatr Psychiatry 2008; 23(11): 1156-62.

Sassin I, Schultz C, Thal DR, Rub U, Arai K, Braak E*, et al.* Evolution of Alzheimer's disease-related cytoskeletal changes in the basal nucleus of Meynert. Acta Neuropathol 2000; 100(3): 259-69.

Scheef L, Grothe MJ, Koppara A, Daamen M, Boecker H, Biersack H*, et al.* Subregional volume reduction of the cholinergic forebrain in subjective cognitive decline (SCD). Neuroimage Clin 2019; 21: 101612.

Scheef L, Spottke A, Daerr M, Joe A, Striepens N, Kolsch H*, et al.* Glucose metabolism, gray matter structure, and memory decline in subjective memory impairment. Neurology 2012; 79(13): 1332-9.

Scheuner D, Eckman C, Jensen M, Song X, Citron M, Suzuki N*, et al.* Secreted amyloid beta-protein similar to that in the senile plaques of Alzheimer's disease is increased in vivo by the presenilin 1 and 2 and APP mutations linked to familial Alzheimer's disease. Nat Med 1996; 2(8): 864-70.

Schliebs R, Arendt T. The significance of the cholinergic system in the brain during aging and in Alzheimer's disease. J Neural Transm (Vienna) 2006; 113(11): 1625-44.

Schmand B, Jonker C, Geerlings MI, Lindeboom J. Subjective memory complaints in the elderly: depressive symptoms and future dementia. Br J Psychiatry 1997; 171: 373-6.

Schmitz TW, Nathan Spreng R, Alzheimer's Disease Neuroimaging I. Basal forebrain degeneration precedes and predicts the cortical spread of Alzheimer's pathology. Nat Commun 2016a; 7: 13249.

Schmitz TW, Spreng RN, Alzheimer's Disease Neuroimaging I. Basal forebrain degeneration precedes and predicts the cortical spread of Alzheimer's pathology. Nat Commun 2016b; 7: 13249.

Schultz AP, Chhatwal JP, Hedden T, Mormino EC, Hanseeuw BJ, Sepulcre J*, et al.* Phases of Hyperconnectivity and Hypoconnectivity in the Default Mode and

Salience Networks Track with Amyloid and Tau in Clinically Normal Individuals. J Neurosci 2017; 37(16): 4323-31.

Schwartz WJ, Smith CB, Davidsen L, Savaki H, Sokoloff L, Mata M*, et al.* Metabolic mapping of functional activity in the hypothalamo-neurohypophysial system of the rat. Science 1979; 205(4407): 723-5.

Seibyl J, Catafau AM, Barthel H, Ishii K, Rowe CC, Leverenz JB*, et al.* Impact of Training Method on the Robustness of the Visual Assessment of 18F-Florbetaben PET Scans: Results from a Phase-3 Study. J Nucl Med 2016; 57(6): 900-6.

Selkoe DJ. Toward a comprehensive theory for Alzheimer's disease. Hypothesis: Alzheimer's disease is caused by the cerebral accumulation and cytotoxicity of amyloid beta-protein. Ann N Y Acad Sci 2000; 924: 17-25.

Sheline YI, Morris JC, Snyder AZ, Price JL, Yan Z, D'Angelo G*, et al.* APOE4 allele disrupts resting state fMRI connectivity in the absence of amyloid plaques or decreased CSF Abeta42. J Neurosci 2010a; 30(50): 17035-40.

Sheline YI, Raichle ME. Resting state functional connectivity in preclinical Alzheimer's disease. Biol Psychiatry 2013; 74(5): 340-7.

Sheline YI, Raichle ME, Snyder AZ, Morris JC, Head D, Wang S*, et al.* Amyloid plaques disrupt resting state default mode network connectivity in cognitively normal elderly. Biol Psychiatry 2010b; 67(6): 584-7.

Sherrington R, Rogaev EI, Liang Y, Rogaeva EA, Levesque G, Ikeda M*, et al.* Cloning of a gene bearing missense mutations in early-onset familial Alzheimer's disease. Nature 1995; 375(6534): 754-60.

Slot RER, Sikkes SAM, Berkhof J, Brodaty H, Buckley R, Cavedo E*, et al.* Subjective cognitive decline and rates of incident Alzheimer's disease and non-Alzheimer's disease dementia. Alzheimers Dement 2019; 15(3): 465-76.

Smith GS, Kramer E, Ma Y, Hermann CR, Dhawan V, Chaly T*, et al.* Cholinergic modulation of the cerebral metabolic response to citalopram in Alzheimer's disease. Brain 2009; 132(Pt 2): 392-401.

Sorg C, Riedl V, Muhlau M, Calhoun VD, Eichele T, Laer L*, et al.* Selective changes of resting-state networks in individuals at risk for Alzheimer's disease. Proc Natl Acad Sci U S A 2007; 104(47): 18760-5.

Sperling RA, Aisen PS, Beckett LA, Bennett DA, Craft S, Fagan AM*, et al.* Toward defining the preclinical stages of Alzheimer's disease: recommendations from the National Institute on Aging-Alzheimer's Association workgroups on

diagnostic guidelines for Alzheimer's disease. Alzheimers Dement 2011; 7(3): 280-92.

Sperling RA, Laviolette PS, O'Keefe K, O'Brien J, Rentz DM, Pihlajamaki M*, et al.* Amyloid deposition is associated with impaired default network function in older persons without dementia. Neuron 2009; 63(2): 178-88.

St George-Hyslop PH, Petit A. Molecular biology and genetics of Alzheimer's disease. C R Biol 2005; 328(2): 119-30.

Stern Y. Cognitive reserve in ageing and Alzheimer's disease. Lancet Neurol 2012; 11(11): 1006-12.

Stewart R. Subjective cognitive impairment. Curr Opin Psychiatry 2012; 25(6): 445-50.

Stewart R, Godin O, Crivello F, Maillard P, Mazoyer B, Tzourio C*, et al.* Longitudinal neuroimaging correlates of subjective memory impairment: 4-year prospective community study. Br J Psychiatry 2011; 198(3): 199-205.

Striepens N, Scheef L, Wind A, Meiberth D, Popp J, Spottke A*, et al.* Interaction effects of subjective memory impairment and ApoE4 genotype on episodic memory and hippocampal volume. Psychol Med 2011; 41(9): 1997-2006.

Strittmatter WJ, Roses AD. Apolipoprotein E and Alzheimer's disease. Annu Rev Neurosci 1996; 19: 53-77.

Studart AN, Nitrini R. Subjective cognitive decline: The first clinical manifestation of Alzheimer's disease? Dement Neuropsychol 2016; 10(3): 170-7.

Sulkava R, Kainulainen K, Verkkoniemi A, Niinisto L, Sobel E, Davanipour Z*, et al.* APOE alleles in Alzheimer's disease and vascular dementia in a population aged 85+. Neurobiol Aging 1996; 17(3): 373-6.

Summers WK, Majovski LV, Marsh GM, Tachiki K, Kling A. Oral tetrahydroaminoacridine in long-term treatment of senile dementia, Alzheimer type. N Engl J Med 1986; 315(20): 1241-5.

Swanson LW, Cowan WM. The connections of the septal region in the rat. J Comp Neurol 1979; 186(4): 621-55.

Tai LM, Bilousova T, Jungbauer L, Roeske SK, Youmans KL, Yu C*, et al.* Levels of soluble apolipoprotein E/amyloid-beta (Abeta) complex are reduced and oligomeric Abeta increased with APOE4 and Alzheimer disease in a transgenic mouse model and human samples. J Biol Chem 2013; 288(8): 5914-26.

Tanaka Y, Sakurai M, Hayashi S. Effect of scopolamine and HP 029, a cholinesterase inhibitor, on long-term potentiation in hippocampal slices of the guinea pig. Neurosci Lett 1989; 98(2): 179-83.

Teipel S, Heinsen H, Amaro E, Jr., Grinberg LT, Krause B, Grothe M*, et al.* Cholinergic basal forebrain atrophy predicts amyloid burden in Alzheimer's disease. Neurobiol Aging 2014; 35(3): 482-91.

Teipel SJ, Cavedo E, Hampel H, Grothe MJ, Alzheimer's Disease Neuroimaging I, Alzheimer Precision Medicine I. Basal Forebrain Volume, but Not Hippocampal Volume, Is a Predictor of Global Cognitive Decline in Patients With Alzheimer's Disease Treated With Cholinesterase Inhibitors. Front Neurol 2018a; 9: 642.

Teipel SJ, Cavedo E, Lista S, Habert MO, Potier MC, Grothe MJ*, et al.* Effect of Alzheimer's disease risk and protective factors on cognitive trajectories in subjective memory complainers: An INSIGHT-preAD study. Alzheimers Dement 2018b; 14(9): 1126-36.

Teipel SJ, Flatz WH, Heinsen H, Bokde AL, Schoenberg SO, Stockel S*, et al.* Measurement of basal forebrain atrophy in Alzheimer's disease using MRI. Brain 2005; 128(Pt 11): 2626-44.

Teipel SJ, Fritz HC, Grothe MJ, Alzheimer s Disease Neuroimaging I. Neuropathological features associated with basal forebrain atrophy in Alzheimer's disease. Neurology 2020.

Teipel SJ, Meindl T, Grinberg L, Grothe M, Cantero JL, Reiser MF*, et al.* The cholinergic system in mild cognitive impairment and Alzheimer's disease: an in vivo MRI and DTI study. Hum Brain Mapp 2011; 32(9): 1349-62.

Tepmongkol S, Hemrungrojn S, Dupont P, Tunvirachaisakul C, Aniwattanapong D, Likitjareon Y*, et al.* Early prediction of donepezil cognitive response in Alzheimer's disease by brain perfusion single photon emission tomography. Brain Imaging Behav 2019; 13(6): 1665-73.

Timmers T, Ossenkoppele R, Verfaillie SCJ, van der Weijden CWJ, Slot RER, Wesselman LMP*, et al.* Amyloid PET and cognitive decline in cognitively normal individuals: the SCIENCe project. Neurobiol Aging 2019; 79: 50-8.

Todd S, Barr S, Roberts M, Passmore AP. Survival in dementia and predictors of mortality: a review. Int J Geriatr Psychiatry 2013; 28(11): 1109-24.

Triantafyllou C, Hoge RD, Wald LL. Effect of spatial smoothing on physiological noise in high-resolution fMRI. Neuroimage 2006; 32(2): 551-7.

Turchi J, Chang C, Ye FQ, Russ BE, Yu DK, Cortes CR*, et al.* The Basal Forebrain Regulates Global Resting-State fMRI Fluctuations. Neuron 2018; 97(4): 940-52 e4.

Tzourio-Mazoyer N, Landeau B, Papathanassiou D, Crivello F, Etard O, Delcroix N*, et al.* Automated anatomical labeling of activations in SPM using a macroscopic anatomical parcellation of the MNI MRI single-subject brain. Neuroimage 2002; 15(1): 273-89.

van der Flier WM, van Buchem MA, Weverling-Rijnsburger AW, Mutsaers ER, Bollen EL, Admiraal-Behloul F*, et al.* Memory complaints in patients with normal cognition are associated with smaller hippocampal volumes. J Neurol 2004; 251(6): 671-5.

van Harten AC, Mielke MM, Swenson-Dravis DM, Hagen CE, Edwards KK, Roberts RO*, et al.* Subjective cognitive decline and risk of MCI: The Mayo Clinic Study of Aging. Neurology 2018; 91(4): e300-e12.

van Harten AC, Visser PJ, Pijnenburg YA, Teunissen CE, Blankenstein MA, Scheltens P*, et al.* Cerebrospinal fluid Abeta42 is the best predictor of clinical progression in patients with subjective complaints. Alzheimers Dement 2013; 9(5): 481-7.

Verfaillie SCJ, Pichet Binette A, Vachon-Presseau E, Tabrizi S, Savard M, Bellec P*, et al.* Subjective Cognitive Decline Is Associated With Altered Default Mode Network Connectivity in Individuals With a Family History of Alzheimer's Disease. Biol Psychiatry Cogn Neurosci Neuroimaging 2018; 3(5): 463-72.

Verlinden VJA, van der Geest JN, de Bruijn R, Hofman A, Koudstaal PJ, Ikram MA. Trajectories of decline in cognition and daily functioning in preclinical dementia. Alzheimers Dement 2016; 12(2): 144-53.

Villemagne VL, Burnham S, Bourgeat P, Brown B, Ellis KA, Salvado O*, et al.* Amyloid beta deposition, neurodegeneration, and cognitive decline in sporadic Alzheimer's disease: a prospective cohort study. Lancet Neurol 2013; 12(4): 357-67.

Villemagne VL, Pike KE, Chetelat G, Ellis KA, Mulligan RS, Bourgeat P*, et al.* Longitudinal assessment of Abeta and cognition in aging and Alzheimer disease. Ann Neurol 2011; 69(1): 181-92.

Visser PJ, Verhey F, Knol DL, Scheltens P, Wahlund LO, Freund-Levi Y*, et al.* Prevalence and prognostic value of CSF markers of Alzheimer's disease pathology

in patients with subjective cognitive impairment or mild cognitive impairment in the DESCRIPA study: a prospective cohort study. Lancet Neurol 2009; 8(7): 619-27.

Viviano RP, Hayes JM, Pruitt PJ, Fernandez ZJ, van Rooden S, van der Grond J*, et al.* Aberrant memory system connectivity and working memory performance in subjective cognitive decline. Neuroimage 2019; 185: 556-64.

Voevodskaya O, Simmons A, Nordenskjold R, Kullberg J, Ahlstrom H, Lind L*, et al.* The effects of intracranial volume adjustment approaches on multiple regional MRI volumes in healthy aging and Alzheimer's disease. Front Aging Neurosci 2014; 6: 264.

Vogel JW, Varga Dolezalova M, La Joie R, Marks SM, Schwimmer HD, Landau SM*, et al.* Subjective cognitive decline and beta-amyloid burden predict cognitive change in healthy elderly. Neurology 2017; 89(19): 2002-9.

Vogels OJ, Broere CA, ter Laak HJ, ten Donkelaar HJ, Nieuwenhuys R, Schulte BP. Cell loss and shrinkage in the nucleus basalis Meynert complex in Alzheimer's disease. Neurobiol Aging 1990; 11(1): 3-13.

Voytko ML, Olton DS, Richardson RT, Gorman LK, Tobin JR, Price DL. Basal forebrain lesions in monkeys disrupt attention but not learning and memory. J Neurosci 1994; 14(1): 167-86.

Wang J, Wang X, Xia M, Liao X, Evans A, He Y. Corrigendum: GRETNA: a graph theoretical network analysis toolbox for imaging connectomics. Front Hum Neurosci 2015a; 9: 458.

Wang Y, Risacher SL, West JD, McDonald BC, Magee TR, Farlow MR*, et al.* Altered default mode network connectivity in older adults with cognitive complaints and amnestic mild cognitive impairment. J Alzheimers Dis 2013; 35(4): 751-60.

Wang Y, Zhao X, Xu S, Yu L, Wang L, Song M*, et al.* Using regional homogeneity to reveal altered spontaneous activity in patients with mild cognitive impairment. Biomed Res Int 2015b; 2015: 807093.

Wang Z, Yan C, Zhao C, Qi Z, Zhou W, Lu J*, et al.* Spatial patterns of intrinsic brain activity in mild cognitive impairment and Alzheimer's disease: a resting-state functional MRI study. Hum Brain Mapp 2011; 32(10): 1720-40.

Ward A, Crean S, Mercaldi CJ, Collins JM, Boyd D, Cook MN*, et al.* Prevalence of apolipoprotein E4 genotype and homozygotes (APOE e4/4) among patients diagnosed with Alzheimer's disease: a systematic review and meta-analysis. Neuroepidemiology 2012; 38(1): 1-17.

Wenk GL, Stoehr JD, Quintana G, Mobley S, Wiley RG. Behavioral, biochemical, histological, and electrophysiological effects of 192 IgG-saporin injections into the basal forebrain of rats. J Neurosci 1994; 14(10): 5986-95.

Whitehouse PJ, Price DL, Clark AW, Coyle JT, DeLong MR. Alzheimer disease: evidence for selective loss of cholinergic neurons in the nucleus basalis. Ann Neurol 1981; 10(2): 122-6.

Whitehouse PJ, Price DL, Struble RG, Clark AW, Coyle JT, Delon MR. Alzheimer's disease and senile dementia: loss of neurons in the basal forebrain. Science 1982; 215(4537): 1237-9.

Whitmer RA, Gunderson EP, Barrett-Connor E, Quesenberry CP, Jr., Yaffe K. Obesity in middle age and future risk of dementia: a 27 year longitudinal population based study. BMJ 2005; 330(7504): 1360.

Wilson RS, Leurgans SE, Boyle PA, Schneider JA, Bennett DA. Neurodegenerative basis of age-related cognitive decline. Neurology 2010; 75(12): 1070-8.

Wolf D, Grothe M, Fischer FU, Heinsen H, Kilimann I, Teipel S*, et al.* Association of basal forebrain volumes and cognition in normal aging. Neuropsychologia 2014; 53: 54-63.

Wolfsgruber S, Kleineidam L, Guski J, Polcher A, Frommann I, Roeske S*, et al.* Minor neuropsychological deficits in patients with subjective cognitive decline. Neurology 2020; 95(9): e1134-e43.

Wong DF, Rosenberg PB, Zhou Y, Kumar A, Raymont V, Ravert HT*, et al.* In vivo imaging of amyloid deposition in Alzheimer disease using the radioligand 18F-AV-45 (florbetapir [corrected] F 18). J Nucl Med 2010; 51(6): 913-20.

Wu C, Zhou D, Wen C, Zhang L, Como P, Qiao Y. Relationship between blood pressure and Alzheimer's disease in Linxian County, China. Life Sci 2003; 72(10): 1125-33.

Wu X, Li R, Fleisher AS, Reiman EM, Guan X, Zhang Y*, et al.* Altered default mode network connectivity in Alzheimer's disease--a resting functional MRI and Bayesian network study. Hum Brain Mapp 2011; 32(11): 1868-81.

Yan CG, Craddock RC, He Y, Milham MP. Addressing head motion dependencies for small-world topologies in functional connectomics. Front Hum Neurosci 2013; 7: 910.

Yan CG, Wang XD, Zuo XN, Zang YF. DPABI: Data Processing & Analysis for (Resting-State) Brain Imaging. Neuroinformatics 2016; 14(3): 339-51.

Yasuno F, Kazui H, Yamamoto A, Morita N, Kajimoto K, Ihara M*, et al.* Resting-state synchrony between the retrosplenial cortex and anterior medial cortical structures relates to memory complaints in subjective cognitive impairment. Neurobiol Aging 2015; 36(6): 2145-52.

Yuan R, Biswal BB, Zaborszky L. Functional Subdivisions of Magnocellular Cell Groups in Human Basal Forebrain: Test-Retest Resting-State Study at Ultra-high Field, and Meta-analysis. Cereb Cortex 2019; 29(7): 2844-58.

Yuan X, Han Y, Wei Y, Xia M, Sheng C, Jia J*, et al.* Regional homogeneity changes in amnestic mild cognitive impairment patients. Neurosci Lett 2016; 629: 1-8.

Zaborszky L, Gombkoto P, Varsanyi P, Gielow MR, Poe G, Role LW*, et al.* Specific Basal Forebrain-Cortical Cholinergic Circuits Coordinate Cognitive Operations. J Neurosci 2018; 38(44): 9446-58.

Zaborszky L, Hoemke L, Mohlberg H, Schleicher A, Amunts K, Zilles K. Stereotaxic probabilistic maps of the magnocellular cell groups in human basal forebrain. Neuroimage 2008; 42(3): 1127-41.

Zang Y, Jiang T, Lu Y, He Y, Tian L. Regional homogeneity approach to fMRI data analysis. Neuroimage 2004; 22(1): 394-400.

Zhang B, Gaiteri C, Bodea LG, Wang Z, McElwee J, Podtelezhnikov AA*, et al.* Integrated systems approach identifies genetic nodes and networks in late-onset Alzheimer's disease. Cell 2013; 153(3): 707-20.

Zhang J, Su J, Wang M, Zhao Y, Yao Q, Zhang Q*, et al.* Increased default mode network connectivity and increased regional homogeneity in migraineurs without aura. J Headache Pain 2016; 17(1): 98.

Zhang Z, Liu Y, Jiang T, Zhou B, An N, Dai H*, et al.* Altered spontaneous activity in Alzheimer's disease and mild cognitive impairment revealed by Regional Homogeneity. Neuroimage 2012; 59(2): 1429-40.

Zhen D, Xia W, Yi ZQ, Zhao PW, Zhong JG, Shi HC*, et al.* Alterations of brain local functional connectivity in amnestic mild cognitive impairment. Transl Neurodegener 2018; 7: 26.

Zheng H, Koo EH. Biology and pathophysiology of the amyloid precursor protein. Mol Neurodegener 2011; 6(1): 27.

Zhou Y, Sun Y, Ma QH, Liu Y. Alzheimer's disease: amyloid-based pathogenesis and potential therapies. Cell Stress 2018; 2(7): 150-61.

Zou QH, Zhu CZ, Yang Y, Zuo XN, Long XY, Cao QJ*, et al.* An improved approach to detection of amplitude of low-frequency fluctuation (ALFF) for resting-state fMRI: fractional ALFF. J Neurosci Methods 2008; 172(1): 137-41.

9 Acknowledgement

First of all, I would like to express my special appreciation and thanks to my supervisor Prof. Dr. Lukas Scheef for his guidance and advice in all the time of my research and for his great support during my PhD study. I appreciate him for giving me the opportunity to pursue my PhD at the German Center for Neurodegenerative Diseases (DZNE). The abroad experiences during my PhD are precious and will benefit my careers in terms of both life and research.
I am also very grateful to Prof. Henning Boecker, Prof. Michael Wagner and Prof. Michael Heneka as my PhD committee members. They always took time out of there busy schedule to attend my PhD project progress meetings and they provided many insightful discussions and constructive suggestions during these meetings. Their positive comments during the PhD project meetings encourage me to keep going with my PhD research and finally finish my PhD study. They are always very kind and supportive, so I really appreciate to have them as my PhD committee members.

I am also grateful to my collogue, Dr. Marcel Daamen, for always being there when I encountered scientific, computer, or printer problems. I appreciate him for polishing my manuscripts, staying up all night, together with Lukas to meet the deadline for resubmitting the revised version of my manuscript. I'll never forget the time we were working together even if we had scientific argument sometimes. I'm also grateful to my collogue, Yilmaz Sagik, to encourage and support me when I'm frustrated during my PhD study. And I'm very lucky to have, Dr. Neeraj Upadhyay, as my college, who is always funny and kind and make my PhD study more relax. I am also grateful to my college, Dr. Hweeling Lee, who has always organized our Chinese friends hanging out together. The last but not least, I'm also very grateful to have my office colleagues, Xueyan Jiang and Sichu Wu, as companions during my PhD study. Having both of you make my PhD study have more happy memories. Moreover, I also would like to thank Hartmut Voelkel for driving me home after Christmas party of the clinical research group every year. I am also grateful Silke Greuel, Daniel Hoffmann, Roy, Nina for their help in getting the data and answering my questions regarding my project. I also would like to thank all my co-authors for their reading and giving me feedback for my manuscripts.

On a personal side of life, I would like to give all my special thanks to my family. Their care and wishes in the distant homeland for me were what supported me so far. At the end, I would like to express my appreciate to my beloved husband, Dr. Bin Wang, who is very supportive of me both in the life and work. It is my husband, who gave me supports and suggestions when I encountered problems in my study; It is my husband, who had prepared the tasty food for me after the work; It is my husband, who waited almost the whole night in the car to drive me home when I need to burn the midnight oil to submit the paper. I can’t imagine my life in Germany without you.

I dedicate this thesis to my family, my husband and all my beloved friends in Germany and China for their constant care and support.